

**A STUDY ON STRENGTH AND DURABILITY OF CEMENT  
MORTARS CONTAINING MARBLE POWDER**

**Ph.D. THESIS**

**Syed Ahmed Kabeer K. I.**

**2014RCE9549**



**DEPARTMENT OF CIVIL ENGINEERING  
MALAVIYA NATIONAL INSTITUTE OF TECHNOLOGY**

**JAIPUR - 302017**

**MARCH 2019**



**A STUDY ON STRENGTH AND DURABILITY OF CEMENT  
MORTARS CONTAINING MARBLE POWDER**

*Submitted in*

*fulfilment of the requirements for the degree of*

**Doctor of Philosophy**

By

**Syed Ahmed Kabeer K. I.**

**ID: 2014RCE9549**

Under the supervision of

**Prof. Ashok Kumar Vyas**



**DEPARTMENT OF CIVIL ENGINEERING**

**MALAVIYA NATIONAL INSTITUTE OF TECHNOLOGY**

**JAIPUR - 302017**

**MARCH 2019**



**© Malaviya National Institute of Technology, Jaipur - 2019**

**All Rights Reserved**



*This thesis is dedicated to*

*My Niece*

***Sakinah,***

*Cousins*

***Saif, Fatema and Adnan***

*And*

***My students at CSA***







**MALAVIYA NATIONAL INSTITUTE OF TECHNOLOGY**  
**JAIPUR, INDIA-302017**

**DECLARATION**

**I K. I. Syed Ahmed Kabeer**, declare that this thesis titled, “**A Study on Strength and Durability of Cement Mortars Containing Marble Powder**” and the work presented in it, are my own. I confirm that:

- This work was done wholly or mainly while in candidature for a research degree at this university.
- Where any part of this thesis has previously been submitted for a degree or any other qualification at this university or any other institution, this been clearly stated.
- Where I have consulted the published work of others, this is always clearly attributed.
- Where I have quoted from the work of others, the source is always given. With the exception of such quotations, this thesis is entirely my own work.
- I have acknowledged all main source of help.
- Where the thesis is based on work done by myself, jointly with others, I have made clear exactly what was done by other and what I have contributed myself.

**Date:**

**(Syed Ahmed Kabeer K. I.)**

ID No: 2014RCE9549





**MALAVIYA NATIONAL INSTITUTE OF TECHNOLOGY  
JAIPUR, INDIA-302017**

**CERTIFICATE**

This is to certify that the thesis entitled '**A Study on Strength and Durability of Cement Mortars Containing Marble Powder**' being submitted by **Syed Ahmed Kabeer K. I. (2014RCE9549)** is a bonafide research work carried out under my supervision and guidance in fulfilment of the requirement for the award of the degree of Doctor of Philosophy in the Department of Civil Engineering, Malaviya National Institute of Technology, Jaipur, India. The matter embodied in this thesis is original and has not been submitted to any other University or Institute for the award of any other degree.

**Dr. Ashok Kumar Vyas**  
Professor,  
Department of Civil Engineering,  
MNIT, Jaipur



## ACKNOWLEDGEMENT

I express my sincere gratitude to my supervisor Dr. Ashok Kumar Vyas, Professor of Department of Civil Engineering, MNIT for his unflinching support, valuable guidance, motivation and consistent encouragement throughout my research work. He will always remain a source of inspiration for me.

I take this opportunity to offer my thanks to Dr. A. B. Gupta, Professor, Department of Civil Engineering, MNIT for painstakingly identifying the areas where I can grow and achieve my goals with greater ease.

I also offer my thanks to Dr. Mahesh Kumar Jat, Professor and Head of the Department of Civil Engineering, MNIT; along with Prof. Sudhir Kumar and Prof. Gunwant Sharma, former Heads of the Department of Civil Engineering, MNIT, for maintaining a conducive environment for all the research scholars and students so that we can pursue our academic and research goals without any hindrances.

I am grateful to my esteemed DREC members Prof. Ravindra Nagar, Dr. Sandeep Shrivastava and Dr. Pawan Kalla and the DPGC convenor Prof. Urmila Brighu for providing me with valuable feedback at every opportunity presented to them. I am also thankful to Prof. Sandeep Chaudhary and Dr. Rajib Sarkar for their unrelenting belief in me that I could achieve anything at all. I would also acknowledge the guidance of Prof. Raj Kumar Vyas and Dr. Sumanta Kumar Meher in helping me prepare the necessary chemical solutions for various tests. I am thankful to Prof. Khaleequr Rehman Niazi for helping me setup the environmental chamber to conduct the rapid freezing and thawing test. My understanding of cement composites has been very significantly influenced by the book written on concrete by Dr. P. K. Mehta and Dr. P. J. M. Monteiro. So I am indebted to Mr. Ravi Jain for introducing me to this book. I am also thankful to my teachers Dr. Vidjeapriya R. (CEG, Anna University, Chennai) and Dr. Chitra G. (TCE, Madurai, Tamil Nadu) who had instilled the basics of concrete technology in me through their engineering courses early in my career.

I am more than just fortunate to have Mr. Sapan Prasad Gaur to assist me in my experimental ventures, without whom this journey would not have been as easy it seemed to be. I am also obliged to acknowledge the contribution of Mr. Phukraj Leelawat, Mr. Ram Babu Meena, Mr. Bijender and Mr. Govind Singh to stepping in whenever the need be.

I would acknowledge the support of Mr. Sadiq Ansari, Mr. Sita Ram Jat, Mr. R. S. Mandolia, Mr. Rajesh Saxena, Mr. Nitesh Kumar Sunaria, Mr. Anil Kumar Sharma and Mr. Om Prakash Gared for their technical assistance. I am also thankful to the staff of Material Research

Centre for their backing in conducting the microstructural studies required for completion of this thesis.

I am also obligated towards my material suppliers, Mr. Saifi, Mr. Abhishek Jain (Savita Scientific and Plastic Products, Jaipur), Ankur Speciality Gases and Technologies (Jaipur), Shree Stones Crusher (Jaipur), Gomathi Marbles (Jaipur), Maheshwari Kiln Company (Jaipur) and Rohit Traders (Jaipur); and experimental setup manufacturers, Yamberzal International (Jaipur), HEICO (New Delhi), Industrial Corporation (Jaipur), Stylco India (New Delhi), Jet Technocrats (Jaipur), Shahzad Engineering Works (Jaipur), Precision Industries (New Delhi) and Rakshita Electrical and Hydrolic (Jaipur) for providing me with their best efforts to complete my experimental programme.

It is an honour to acknowledge the blessings of my mother Mrs. Kousar Afshan and father Mr. K. M. Iqbal Ahmed for their continuous support and motivation for the completion of my thesis. I am also humbled by the love shown by my brother Mr. K. I. Junaid Ahmed and sister – in – law Ar. Asma Syed towards me. I am also lucky to have countless prayers of my aunts Mrs. Firdouse Anjum, Mrs. Tahira Jabeen and Mrs. Rasheeda Matheen and uncle Dr. Ahmed Mudassar Ali for the successful completion of my research work.

The contribution made by my dearest friend Dr. Sanjeev Kumar K. S. to my life is also profound, who inspired me to take up this doctoral degree. So just thanking him will be an understatement. I also recognize how lucky I was to have an humble but short company of Mr. Prabu Dhandapani during my stay at Jaipur. Mrs. Anuja Baheerathan, Dr. Nishant Roy, Dr. T. Jothi Saravanan, Mr. K. R. Tabraze Ahmed, Dr. Kunal Bisht, Mrs. Nithya V. J., Mrs. Shikha Sharma and Mr. Mohammad Arif have been the best of friends whose influence in my life is more than just sublime during the difficult times. I am delighted to acknowledge Mr. Ajay Dhenwal, Mr. Ajay Kumar Vash, Mr. Dunger Ram, Mr. Prashant Chandra and Mr. Yogeshwar Dilta for being my family away from home.

I am thankful to my fellow research scholars, Dr. Sudarshan D. Kore, Mr. Lalit Kumar Gupta, Dr. Salman Siddique, Dr. Pankaj Kumar, Dr. Arnav Anuj Kasar, Mr. Shashi Narayan and Mr. Harshwardhan Singh Chauhan, along with Mr. Ankit Goyal and Ms. Mitlesh Kumari; post graduate students Mr. Rajendra Kumar Khyaliya, Mr. Vikash Kumar, Mrs. Anjali Chawla and Mr. Vikas Babu; and undergraduate students Mr. Kamlesh Kumar, Mr. Sunil Kumar Meena, Mr. Bharat Singh, Mr. Kamlesh Kumar Jat, Mr. Shushil Mundel, Mr. Chandra Prakash, Mr. Jay Prakash Tak, Mr. Rahul Singh and Mr. Naveen Kumar Nirala and my dear friend Late Mr. Shivnath Mehra.

**K. I. SYED AHMED KABEER**

## ABSTRACT

The scarcity of river sand has triggered the utilization of industrial waste for the production of concrete and mortars. One such waste is marble slurry which is being produced in huge quantities during marble processing. This waste was evaluated as a substitute to sand for the production of mortars. Four different mix proportions (1:3, 1:4, 1:5 and 1:6) of mortars were prepared by substituting river sand by dried marble slurry (marble powder) in steps of 20% from 0% to 100%. These mortars were evaluated in terms of workability, drying shrinkage, compressive strength, bond and adhesive strengths, density, water absorption and dynamic Young's modulus. Results showed that mortar mixes with 20% substitution of river sand by marble powder increased the compressive strength by 25% to 90% for mix proportions 1:3 and 1:6 respectively. Outcomes from the other above tests also showed that mortar mixes with 20% substitution of river sand by marble powder can be used for masonry and rendering purposes. However, with the aim of increasing the utilization further, a coarser river sand was used to combine with marble powder. By doing so, an additional 10% of marble powder could be incorporated for the production of mortars. Further analysis of these mortars showed that they have a distinctively dense microstructure which is a consequence of reduced water requirement and formation of superior quality of hydration products. These were confirmed by scanning electron microscope, X – ray diffraction, thermogravimetric analysis and Fourier transform infrared spectroscopy techniques. For studying the durability properties, marble powder incorporation was limited to a range of 20% - 30% based on the sand grading on two mix proportions of 1:3 and 1:6. Cycles of salt crystallization proved to be detrimental to the lean mixes with marble powder. Whereas mixes with 20% marble powder had comparable performance when compared to conventional mortars after exposure to cycles of rapid freezing and thawing. Nevertheless alternate wetting and drying cycles did not produce any substantial damage to the new mortar composites. The capacity of marble powder to neutralize acids imparted mortars better resistance to such environments. At the end of the test period conventional mortars had 40% residual strength, when compared to 65% to 72% residual strength of marble based mixes of proportion 1:3. These mortars were also stable when exposed to chloride reagent. The conventional mix of proportion of 1:6 had no residual strength, whereas the marble based mixes had strength higher than the initial value when subjected to sulphate attack. They are also less susceptible to undergo alkali carbonate reaction. However the decarbonation effect makes the mortars with marble powder stable up to 600°C only. Such mortars also resist carbonation efficiently but with increased carbonation shrinkage. On evaluating the environmental and economic performance mortars, with marble powder perform at par with conventional mortars. Hence, by replacing sand to the tune of 20% by marble powder irrespective of the durability requirements, would enable the construction industry to reduce their dependency on this natural resource.





## TABLE OF CONTENTS

Sl. No.	CHAPTER	Pg. No.
	<b>DECLARATION</b>	<b>i</b>
	<b>CERTIFICATE</b>	<b>iii</b>
	<b>ACKNOWLEDGMENT</b>	<b>v</b>
	<b>ABSTRACT</b>	<b>vii</b>
	<b>LIST OF TABLES</b>	<b>xiii</b>
	<b>LIST OF FIGURES</b>	<b>xv</b>
	<b>ABBREVIATIONS AND SYMBOLS</b>	<b>xxi</b>
<b>1</b>	<b>INTRODUCTION</b>	<b>1</b>
1.1	General	1
1.2	Challenges linked with waste management	1
1.3	Construction Industry	2
1.4	Waste materials used in the production of cement composites	3
1.5	Marble dimension industry	4
1.6	Excerpts from literature pertaining to usage of marble waste	5
1.7	Specific objectives	8
1.8	Organisation of the thesis	8
<b>2</b>	<b>LITERATURE REVIEW</b>	<b>9</b>
2.1	General	9
2.1.1	Utilization of marble slurry for soil stabilization and road construction	9
2.1.2	Utilization of marble slurry for the production of clay bricks	11
2.1.3	Marble waste as coarse aggregate for production of concrete	12
2.1.4	Marble slurry as supplementary cementitious material	15

<b>Sl. No.</b>	<b>CHAPTER</b>	<b>Pg. No.</b>
2.1.5	Marble slurry as supplementary cementitious material in production of concrete	17
2.1.6	Composites of marble slurry and other supplementary cementitious material in production of binders	18
2.1.7	Marble waste as fine aggregate for production of concrete	20
2.1.8	Marble waste as fine aggregate / filler in self-compacting concrete	22
2.1.9	Marble waste as fine aggregate in mortars	23
2.1.10	Other niche domains	25
2.1.11	Summary	26
<b>3</b>	<b>MATERIALS AND METHODS</b>	<b>27</b>
3.1	General	27
3.2	Materials	27
3.2.1	Cement	27
3.2.2	Fine aggregate	27
3.2.3	Marble powder	28
3.3	Mix proportions	30
3.4	Research methodology	31
3.5	Experimental methodology	32
3.5.1	Casting and curing of specimens	32
3.5.2	Workability	35
3.5.3	Fresh bulk density	35
3.5.4	Compressive strength	35
3.5.5	Tensile strength	36
3.5.6	Flexural strength	37
3.5.7	Tensile bond strength	37
3.5.8	Adhesive strength	38
3.5.9	Drying shrinkage	39
3.5.10	Water absorption by immersion, bulk and apparent densities and voids	40
3.5.11	Water absorption by capillarity	40
3.5.12	Dynamic modulus of elasticity	41

<b>Sl. No.</b>	<b>CHAPTER</b>	<b>Pg. No.</b>
3.5.13	Salt crystallization	42
3.5.14	Wet – dry cycles	43
3.5.15	Sulphate attack	43
3.5.16	Acid attack	44
3.5.17	Carbonation	44
3.5.18	Rapid freezing and thawing	45
3.5.19	Chloride ion penetration	46
3.5.20	Alkali carbonate reaction	47
3.5.21	Effect of fire	47
3.5.22	Environmental evaluation	48
3.5.23	Economic evaluation	49
3.5.24	Consolidated evaluation	50
<b>4</b>	<b>RESULTS AND DISCUSSIONS</b>	<b>51</b>
4.1	General	51
4.2	Evaluation of Physical and Mechanical Properties	51
4.2.1	Workability	51
4.2.2	Fresh bulk density	52
4.2.3	Drying shrinkage	53
4.2.4	Compressive strength	55
4.2.5	Tensile bond strength between brick and mortars	57
4.2.6	Adhesive strength of renderings on substrates	58
4.2.7	Density, water absorption and porosity	59
4.2.8	Dynamic modulus of elasticity	61
4.2.9	Microstructure	62
4.3	Usage of Coarse River Sand to Improve Extent of Marble Powder Utilization	64
4.4	Evaluation of Tensile and Capillary Water Absorption Characteristics	69
4.4.1	Flexural and tensile strength	69
4.4.2	Capillary water absorption	71
4.4.3	Scanning electron microscopy	72

<b>Sl. No.</b>	<b>CHAPTER</b>	<b>Pg. No.</b>
4.4.4	X – ray diffraction analysis and Fourier transform infrared spectroscopy	74
4.5	Performance Evaluation of Mortar Mixes when Exposed to Aggressive Environments	76
4.5.1	Salt crystallization	76
4.5.2	Wet – dry cycles	81
4.5.3	Rapid freezing and thawing	85
4.5.4	Exposure to fire	89
4.5.5	Acid attack	94
4.5.6	Sulphate attack	102
4.5.7	Chloride penetration	107
4.5.8	Carbonation	110
4.5.9	Alkali carbonate reaction	113
4.6	Consolidated evaluation	114
<b>5</b>	<b>CONCLUSIONS</b>	<b>117</b>
	<b>REFERENCES</b>	<b>123</b>
	<b>LIST OF PUBLICATIONS</b>	<b>133</b>
	<b>BIODATA OF THE AUTHOR</b>	<b>135</b>

## List of Tables

<b>Table No.</b>	<b>Title</b>	<b>Pg. No.</b>
1.1	Percentage waste generated depending upon the mining technology used during processing	5
3.1	Physical properties of materials used to prepare mortars	28
3.2	Oxide composition of materials used to prepare mortars	28
3.3	Quantities of materials required to produce 1 m <sup>3</sup> of mortar with FS	31
3.4	Quantities of materials required to produce 1 m <sup>3</sup> of mortar with CS	31
3.5	A summary of different curing regimes followed	34
3.6	Life cycle inventory data of mortar constituents	48
3.7	Cost of mortar constituents	49
4.1	Variation of adhesive strength of mixes on substrate	59
4.2	Weight loss (%) of specimens when subjected to heat	64
4.3	Summary of mechanical properties of mortar mixes	69



## List of Figures

Figure No.	Title	Pg. No.
1.1	Marble cutting waste dumped in a landfill near a quarrying site in the Indian state of Rajasthan	4
1.2	Marble processing waste dumped in a parched river bed near an industrial zone of Jaipur district in the Indian state of Rajasthan	5
2.1	A mix design monogram designed by Alyamac and Ince (2009)	22
3.1	Scanning electron micrograph of PPC	27
3.2	A comparative statement of particle size distribution of two different samples of river sand with the required specifications	29
3.3	Dried marble powder	29
3.4	X-ray diffraction pattern of dried marble powder	30
3.5	SEM micrographs of dried marble powder	30
3.6	A flow chart showing the research methodology	32
3.7	One batch of cast mortar mix	33
3.8	Curing regimes: a) water curing; b) curing at ambient RH and temperature and c) moist curing	34
3.9	Measurement of flow value of mortar mixes	35
3.10	Measurement of weight of fresh mortar mix in a standard container	35
3.11	Compression testing machine	36
3.12	Experimental setup to test tensile strength of mortars	36
3.13	Experimental setup to test flexural strength of mortars	37
3.14	Experimental setup to test tensile bond strength of mortars	38
3.15	Preparation of sample to test adhesive strength	39
3.16	Experimental setup to measure the length of mortar prisms	39
3.17	Experimental setup to for conducting the capillarity test of mortar specimens	41
3.18	Samples subjected to a 5% solution of sodium sulphate	44
3.19	Carbonation chamber	45
3.20	Environmental chamber to simulate rapid freezing and thawing	46
3.21	Colour change when 0.1M solution of AgNO <sub>3</sub> is sprayed on samples soaked in NaCl	46
3.22	Gas fired furnace	47
3.23	Standard fire curve	47
4.1	Water requirement of mortars to attain the desired flow value of 105% to 115%	52
4.2	Variation of fresh bulk density of mortar mixes	53
4.3	Drying shrinkage of series A (1:3)	53
4.4	Drying shrinkage of series B (1:4)	54
4.5	Drying shrinkage of series C (1:5)	54

<b>Figure No.</b>	<b>Title</b>	<b>Pg. No.</b>
4.6	Drying shrinkage of series D (1:6)	54
4.7	Twenty eighth day compressive strength of mortar mixes	55
4.8	Variation of tensile bond strength for all mixes	57
4.9	Variation of hardened bulk density of mortar mixes	59
4.10	Variation of apparent density of mortar mixes	60
4.11	Variation of water absorption capacity of mortar mixes	61
4.12	Variation of permeable pores space of mortar mixes	61
4.13	Variation of dynamic modulus of elasticity of mortar mixes	62
4.14	FTIR spectra of mortar mixes ASF0, ASF20, ASF40 and ASF60	63
4.15	Thermogravimetric analysis (TGA) of mortar mixes ASF0, ASF20, ASF40 and ASF60	63
4.16	Variation of compressive strength of mixes using CS as fine aggregate	64
4.17	Variation of tensile bond strength of mixes using CS as fine aggregate	65
4.18	Variation of water absorption capacity of mixes using CS as fine aggregate	66
4.19	Variation of drying shrinkage of mixes using CS as fine aggregate	66
4.20	Variation of compressive strength of mixes using CS as fine aggregate	67
4.21	Variation of water absorption capacity of mixes using CS as fine aggregate	67
4.22	Variation of tensile bond strength of mixes using CS as fine aggregate	68
4.23	Variation of drying shrinkage of mixes using CS as fine aggregate	68
4.24	Variation of flexural strength of mortar mixes with increase in percentage of MS	70
4.25	Variation of tensile strength of mortar mixes with increase in percentage of MS	71
4.26	Variation of capillary water absorption of mortar mixes with increase in percentage of MS for series A	71
4.27	Variation of capillary water absorption of mortar mixes with increase in percentage of MS for series D	72
4.28	Elemental mapping of mortar mix ASF0	73
4.29	Elemental mapping of mortar mix ASC30	74
4.30	X-Ray diffractograms of mixes ASF0, ASF20, ASC20 and ASC30	75
4.31	FTIR spectrum of two mixes ASC20 and ASC30	76
4.32	Change in weight of samples when subjected to cycles of salt crystallization	77
4.33	Appearance of samples of series a) A and b) D when subjected to cycles of salt crystallization	77
4.34	Variation of capillary water absorption after the salt crystallization cycles	78
4.35	Compressive strength of mortar mixes when subjected to cycles of salt crystallization	79



<b>Figure No.</b>	<b>Title</b>	<b>Pg. No.</b>
4.36	Scanning electron micrographs of a) ASF0, b) ASF20, c) ASC20 and d) ASC30 after salt crystallization cycles, e) glauberite and f) thenardite crystals	80
4.37	FTIR spectra of mortar mixes after salt crystallization cycles	81
4.38	Change in weight of samples when subjected to wet – dry cycles	82
4.39	Appearance of samples of series a) A and b) D when subjected to wet – dry cycles	82
4.40	Compressive strength of mortar mixes when subjected to wet – dry cycles	83
4.41	Variation of capillary water absorption after wet – dry cycles	84
4.42	Scanning electron micrographs of mixes of series A after wet – dry cycles	84
4.43	FTIR spectra of mortar mixes of series A after wet – dry cycles	85
4.44	Variation of compressive strength of mortar mixes of series A after rapid freezing and thawing	86
4.45	Change in length undergone by mixes after rapid freezing and thawing	86
4.46	Extent of weight loss suffered by mortar mixes of series A after rapid freezing and thawing	87
4.47	Change in appearance of mortar mixes of series a) A and b) D after rapid freezing and thawing	87
4.48	Extent of weight loss suffered by mortar mixes of series D after rapid freezing and thawing	88
4.49	Change in compressive strength of mortar mixes of series D after rapid freezing and thawing	88
4.50	FTIR spectra of mortar mixes of series A after rapid freezing and thawing	89
4.51	Change in compressive strength of mortar mixes of series A after exposure to fire	90
4.52	Mass loss pattern when CS and FS are heated up to 900°C	91
4.53	X-ray diffraction pattern of ASF0 and ASF20 after exposure to fire at 800°C	92
4.54	Extent of weight loss suffered by mortar mixes of series A after exposure to fire	93
4.55	Change in compressive strength of mortar mixes of series D after exposure to fire	93
4.56	Extent of weight loss suffered by mortar mixes of series D after exposure to fire	94
4.57	Compressive strength of mortar mixes of series A when subjected to an acidic medium	95
4.58	X-Ray diffractograms of mix ASF0 after 0,1 and 14 days of exposure to acid attack	95
4.59	Weight loss of mortar mixes of series A when subjected to an acidic medium	96

<b>Figure No.</b>	<b>Title</b>	<b>Pg. No.</b>
4.60	X-Ray diffractograms of mix ASF20 after 0 and 1 day of exposure to acid attack medium	97
4.61	FTIR spectra of mixes ASF0 and ASF20 after subjecting to an acidic medium for 1 day	97
4.62	X-ray diffraction pattern of ASF0 and ASF20 after different periods of exposure to acidic medium	98
4.63	Scanning electron micrographs of ASF0 and ASF20 after exposure to different periods of acidic environment	99
4.64	Compressive strength of mortar mixes of series D when subjected to an acidic medium	100
4.65	Weight loss of mortar mixes of series D when subjected to an acidic medium	101
4.66	Appearance of mortar mixes of series a) A and b) D when subjected to an acidic medium for 84 days	101
4.67	Compressive strength of mortar mixes of series A when subjected to sulphate attack	102
4.68	X-ray diffraction pattern of ASF0 and ASF20 after exposure to sulphate attack for 164 days	103
4.69	Change in length of specimens of series A due to sulphate attack	104
4.70	Weight loss of mortar mixes of series A when subjected to sulphate attack	104
4.71	FTIR spectra of ASF0 and ASF20 after exposure to sulphate attack for 164 days	105
4.72	Appearance of mortar mixes of series a) A and b) D when subjected to a sulphate solution for 168 days	106
4.73	Change in length of specimens of series D due to sulphate attack	106
4.74	Compressive strength of mortar mixes of series D when subjected to sulphate attack	106
4.75	Weight loss of mortar mixes of series D when subjected to sulphate attack	107
4.76	Position of colour change front of mixes after exposure to sodium chloride	108
4.77	X-ray diffraction pattern of ASF0 and ASF20 after 84 days of exposure to sodium chloride	109
4.78	FTIR spectra of mixes ASF0 and ASF20 after 84 days of exposure to sodium chloride	110
4.79	Position of colour change front of mixes after exposure to carbon dioxide	111
4.80	X-ray diffraction pattern of ASF0 and ASF20 after 84 days of carbonation	112
4.81	FTIR spectra of ASF0 and ASF20 after 84 days of carbonation	112
4.82	Change in length undergone by mixes after carbonation	113
4.83	Change in length of specimens due to alkali aggregate reaction	114

<b>Figure No.</b>	<b>Title</b>	<b>Pg. No.</b>
4.84	Performance evaluation of mortar mixes	115
4.85	Consolidated performance evaluation of mortar mixes	116



## Abbreviations and Symbols

A	Cement mortar mix with a proportion 1:3
Afm	Hexacalcium aluminate monosulphate hydrate / monosulphate
Aft	Hexacalcium aluminate trisulphate hydrate / ettringite
AgNO <sub>3</sub>	Silver nitrate
AP	Acidification potential
ASTM	American Society for Testing and Materials
B	Cement mortar mix with a proportion 1:4
BS	British Standard
C	Cement mortar mix with a proportion 1:5
CaCl <sub>2</sub>	Calcium chloride
CaCO <sub>3</sub>	Calcium carbonate / calcite
CAH	Calcium aluminate hydrate / katoite
Ca(OH) <sub>2</sub>	Calcium hydroxide / Portlandite
CaMg(CO <sub>3</sub> ) <sub>2</sub>	Calcium magnesium carbonate / Dolomite
CASH	Calcium aluminate silicate hydrate / gismondine
CaSO <sub>4</sub> .0.5H <sub>2</sub> O	Calcium sulphate hemihydrate / bassanite
CaSO <sub>4</sub> .2H <sub>2</sub> O	Calcium sulphate dihydrate / gypsum
CO <sub>2</sub>	Carbon dioxide
CS	Coarse sand
CSH	Calcium silicate hydrate / tobermorite
CSM	Cement – sand – marble powder
D	Cement mortar mix with a proportion 1:6
ECM	Consolidated performance index
EDAX	Energy dispersive X – ray spectroscopy
FESEM / SEM	Field emission scanning electron microscope
FS	Fine sand
FP	Fossil fuel depletion
FTIR	Fourier transform infrared
GWP	Global warming potential
IS	Indian Standard
ISF	Imperial Smelting Furnace
LCI	Life cycle inventory
LOI	Loss on ignition
Mg(OH) <sub>2</sub>	Magnesium hydroxide / brucite
MS	Marble powder
MSME	Ministry of Micro, Small and Medium Enterprises
NaCl	Sodium chloride
NaSO <sub>4</sub>	Anhydrous sodium sulphate / thenardite

$\text{NaSO}_4 \cdot 10\text{H}_2\text{O}$	Hydrous sodium sulphate / mirabilite / Glauber's salt
$\text{Na}_2\text{Ca}(\text{SO}_4)_2$	Sodium calcium sulphate / glauberite
NMR	Nuclear magnetic resonance
NT	Nordtest
OBC	Optimum binder content
OPC	Ordinary Portland cement
PET	Polyethylene terephthalate
PPC	Portland pozzolana cement
SCC	Self-consolidating concrete
SCM	Supplementary cementitious material
TGA	Thermogravimetric analysis
UPV	Ultrasonic pulse velocity
XRD	X – ray diffraction

## CHAPTER 1

### INTRODUCTION

#### 1.1 General:

All organisms on planet Earth, both living and inorganic, cooperate with each other to preserve the conditions that would support life by forming a self – adaptable and synergic complex system. This concept is called as the Gaia hypothesis formulated in 1974 by James Lovelock and Lynn Margulis. However, this hypothesis was never really accepted by humanity, which led to the exploitation of other natural resources. Industrialization was given preference so that nations could achieve economic growth targets at higher pace. Upsurge in growth of industries not only increased consumption of natural resources but also increased the amount of wastes and by products generated. Improper disposal of these wastes on landfills has damaged our planets' ability to regulate its surface temperature, composition of the atmosphere and salinity of the oceans.

#### 1.2 Challenges linked with waste management:

The world population has risen from 1.5 billion to 6 billion through the course of the 20<sup>th</sup> century (Hameed et al., 2012). Today this figure stands at 7.2 billion with half of this population being accommodated in cities (Dong et al., 2017). The physical social well-being of this population is closely linked to its access to infrastructure (Steckel et al., 2017). Resources wise, construction of infrastructure consumes 30 billion tonnes of raw materials extracted worldwide each year (Behera et al., 2014).

With rise in population accompanied by infrastructure and industrial growth, the annual quantity of waste generated has also increased substantially. In India alone 69 million tonnes of waste is generated annually out of which only 17% is treated. The remaining portion is dumped on open lands which contribute to the generation of greenhouse gases. The leachate produced from such dumpsites is also harmful (Mohan et al., 2018). Hence in order to improve the quality of waste management, global governments of late have specified rules for waste handling. The measures taken up for handling different types of wastes by different industries are briefed below.

It is believed that agricultural wastes if recycled, 25% of the nutrient needs of crops can be met. Animal dung, crop residues and spoilt fruits, grains and vegetables can be used

as amendment of soils and composts. In particular, rice husk ash has found tremendous utilization potential for the manufacture of bricks, cement, steel etc (Fiksel and Lal, 2018). Moreover, when combined with metakaolin, rice husk ash has the ability to improve the compressive strength of self-consolidating concrete (SCC) mixes by 27%.

Steel slags have been used to replace the conventional coarse aggregates completely when available in proper particle size distribution (Jiang et al., 2018). Though waste originating from electrical and electronic equipment contain several hazardous elements, the developing countries recycle 80% of the generated waste (Ohajinwa et al., 2018). With regard to automobile industries, stringent European regulations make it mandatory that at least 85% of components used in the manufacturing of automobiles must be recyclable (Ortego et al., 2018).

The extent of generation of the construction and demolition wastes is around 3 billion tonnes globally which has brought it under the scanner of the environmentalists. Processing of aggregates from such sources is considered to be an energy intensive process where the removal of adhered mortar and aggregate porosity dampen the extent of recycling in new construction activities. However when material like glass is used to replace 10% of cement, can simultaneously allow replacement of 50% of coarse aggregate by recycled aggregates (Akhtar and Sarmah, 2018). It is worth mentioning that, unlike other sectors, construction industry has the potential to consume waste from other industries as well. The following section outlines the measures taken up by this industry to reduce dependency on natural resources by using wastes from a variety of sources.

### **1.3 Construction Industry:**

As mentioned earlier, the construction industry consumes around 30 billion tonnes of raw materials every year and thereby contributing to 25% of the global carbon emissions. Discretely, when the greenhouse gas emissions due to production of construction materials like bricks, tiles, steel, aluminium and wood are compared on pure volume basis, emissions associated with concrete manufacturing are the least (Gartner and Hirao, 2015). This is because, water and aggregates have very low associated CO<sub>2</sub> emissions, whereas for the manufacture of 1 tonne cement, it is only 0.83 tonnes. This is very minimal when compared to other materials like steel and aluminium's contribution of 3 and 15 tonnes of CO<sub>2</sub> for one tonne of their production respectively. Further, cement is only used to the extent of 10% in concrete manufacturing while aggregates, water and steel constitute the remaining



volume (Gartner and MacPhee, 2011). However high extent of utilisation of this cement aggregate composite which is second only to the usage of water has made it to be a producer of 7% of global CO<sub>2</sub> emissions.

Therefore, in the quest to achieve sustainability by reducing dependency on natural resources and to prevent global environmental catastrophe by waste disposal, construction sector has evaluated the waste to resource route. Industrial slags, construction and demolition wastes, dimensional stone by products have piqued the interests of researchers, scientists and environmentalists to scrutinize their potential to replace conventional construction materials.

#### **1.4 Waste materials used in the production of cement composites:**

There are many waste materials that have been tested as potential replacement of conventional cement binder and natural aggregates. Few of them have already been approved by the regulatory authority. IS 1489 (1991) allows 25% replacement of OPC by fly ash. Ground granulated blast furnace slag can be used to replace 65% of OPC (IS 455, 1989). IS 383 (2016) in its latest iteration specifies to what extent the use of iron slag, steel slag, recycled aggregate, recycled concrete aggregate and bottom ash can be used as replacement of fine and coarse aggregate in plain and reinforced concretes.

Apart from these, there are various other waste materials and by products that are being/have been tested as potential concrete making materials. Farinha et al. (2012) have reported that 20% replacement of natural aggregates by sanitary-ware waste can be made for the production of concrete. Siddique et al. (2018) used tableware ceramic waste to completely replace fine aggregate for the production of concrete. Toxic waste in the form of imperial smelting furnace (ISF) slag and crumb rubber can also be used to replace fine aggregate (Bisht and Ramana, 2017; Tripathi et al., 2013). This also helps in effectively binding heavy metals in the form of lead and slag within the cement matrix hence preventing environmental degradation.

Stone quarrying waste like limestone, granite, marble and sandstone have also been evaluated for utilization in concrete. Rana et al. (2016) were able to replace the entire fine aggregate component in the concrete manufacture by limestone waste comprising slurry and crushed stone particles. On the other hand Singh et al. (2015) was able to replace 25% of river sand by granite cutting waste which produced durable concrete mixes. In case of utilization of sandstone wastes, usage of super-plasticizer becomes mandatory to reduce

the required water content and hence arrive at the necessary strength as shown by Kumar et al. (2017). Marble waste can also be used to replace conventional coarse aggregates, where the extent of substitution depends on the strength of concrete (Chawla et al., 2018; Kore and Vyas, 2016).

### **1.5 Marble dimension industry:**

Marble is the most preferred dimension stone in India which is available in nature as a metamorphic rock, formed from calcite or dolostone minerals when subjected to pressure and heat. As of 2010, marble resources in the country stand at 1655 Mega tonnes, 64% of which comes from the state of Rajasthan. Mining and processing of dimension stones like marble is different from other rocks because, blocks of stones have to be removed from the rock formation without any cracks or damages (Indian Bureau of Mines, 2015). Though the mining activities have developed over the years, the amount of waste still generated is about 60% the extracted block.

The waste generated at this stage is in forms of small blocks, powder and slurry which are dumped in landfills nearby. Fig. 1.1 shows the amount of marble waste disposed in a landfill near a quarry site near the city of Kishangarh in Ajmer district of the Indian state of Rajasthan.



**Fig. 1.1: Marble cutting waste dumped in a landfill near a quarrying site in the Indian state of Rajasthan**

After extraction these blocks are sent for processing. Based on the mechanism used for sawing, grinding and polishing, the marble slurry generated here is about 10% of the stone block. This depends on the technology used as shown in Table 1.1. The generated slurry is indiscriminately dumped in vacant lands, river banks or forest areas as shown in Fig. 1.2. These slurry particles being fine enough are capable of filling pores of the soil,

preventing water percolation and reducing its fertility. On drying, these particles are lifted by air which result in respiratory problems in humans (MSME Development Institute, 2009). Uncontrolled disposal of marble industrial effluents had led to increase in pollutants in groundwater, endangered aquatic biodiversity along with causing kidney, skin and eye diseases in humans (Khan et al., 2012).

**Table 1.1: Percentage waste generated depending upon the mining technology used during processing** (Source: MSME Development Institute, 2009)

Stage	Mechanised mines with gang saw cutting machines	Mechanised mines with using blasting	Semi – mechanised mines using blasting	Weighted average
Cutting	10%	15%	18%	15%
Grinding and polishing	5%	5%	5%	5%



**Fig. 1.2: Marble processing waste dumped in a parched river bed near an industrial zone of Jaipur district in the Indian state of Rajasthan**

### **1.6 Excerpts from literature pertaining to usage of marble waste:**

There are plenty of attempts reported where different types of marble waste have been evaluated as a construction material. These wastes have been tested as potential replacement for coarse and fine aggregates and cement for the production of concrete, in the manufacture of bricks, construction of pavements, soil neutralization etc. Marble waste in the form of slurry has been used to produce clay bricks where an optimum utilization ratio of 10% - 20% is recommended (Montero et al., 2009a). On incorporation of this waste, the bricks attain the required mechanical properties at lower firing temperatures itself,

hence enabling cost saving. Due to their increased porosity they tend to have better thermal properties also (Sutcu et al., 2015).

Marble has good soil neutralizing capacity and therefore limestone has been reported to be replaced by marble waste to alleviate the properties of contaminated soils (Ercikdi et al., 2015). These waste increase the soil's pH and hence promote microbial activity for plant growth (Melgar-Ramírez et al., 2012). On combination with clayey soils, marble waste has the capacity to improve its geotechnical properties (Gurbuz, 2015). They have also been used as a filler for the construction of asphaltic pavements, rubber and plastics.

Marble waste resulting from quarrying activities is sufficiently coarser in nature to be used as a replacement of conventional coarse aggregates for the manufacture of concrete. Studies have shown that marble waste based coarse aggregates are the best alternative to limestone aggregates (Binici et al., 2008). However when conventional aggregates of other geological origins have to be replaced, an additional parameter of dry bulk density has to be evaluated (André et al., 2014). Using this parameter an optimum partial substitution of conventional aggregates can be derived to design concrete mixes of necessary performance (Kore and Vyas, 2016).

Marble fines impart necessary cohesivity and prevent segregation of self-consolidating concrete (SCC) mixes. When added as fillers, they can prevent high usage of cements for the production of composites with such specific performance characteristics (Alyamaç and Ince, 2009).

Marble powder, due to its similarity to limestone has emerged as one of the possible substitutes for cement in concrete and mortars. Results have shown that replacement of 10% of cement by marble powder has improved the performance of concrete mixes (Şahan Arel, 2016). This improvement has been credited to number factors like, presence of reactive silica, chemical reaction between calcium hydroxide and tri-calcium aluminate and pore filling nature of marble slurry. However since marble powder does not participate in the hydration process, substitution greater than 10% has been shown to be of adverse effect to the strength of concrete mixes (Aliabdo et al., 2014; Vardhan et al., 2015).

On other hand, it was reported that the positive effect of marble powder was more pronounced when it was used in place of sand than as a cement replacement (Aliabdo et al., 2014). Workability of concrete mixtures decreased with increase in percentage

incorporation of marble even though the grading curve was kept as a constant. This led to higher w/c ratio and reduced compressive strength when compared to mixes made with river sand, basalt sand and granite sand (Silva et al., 2013). Reduction in workability was reported by (Hebhoub et al., 2011) also, however on evaluation of mechanical properties marble incorporated mixes performed better than control mixes which were made using limestone as fine aggregate. With regard to durability of the concrete mixes, Gameiro et al. (2014) stated that water absorption by capillary action and immersion was the least for 20% substitution. Resistance to chloride penetration improved with addition of marble. The aggregates geometry improved the shrinkage behaviour also.

In the particular case of production of masonry and rendering mortars, marble waste of different sizes has been evaluated to determine their optimum utilization potential. Corinaldesi et al. (2010) used calcite marble sludge of fineness 1500 m<sup>2</sup>/kg and was able to produce mortars of acceptable quality at a replacement level of 10%. Rai et al. (2011) tested the extent of usage of marble granules having fineness modulus of 2.72 as fine aggregate replacement, and approved 15% substitution. Keleştemur et al. (2014) replaced sand finer than 0.25 mm with dried marble slurry of both calcite and dolomitic origin and tested them for resistance against fire and rapid freezing and thawing. Based on the results of compressive and flexural strengths after exposure to fire, the authors reported 50% substitution of sand by dried marble slurry can be done. However in the case of freezing and thawing, usage of dried marble slurry proved detrimental. Another detailed examination on marble mining waste (fineness modulus of 1.45) conducted by Khyaliya et al. (2017) stated, though 50% substitution is possible based on mechanical performance, the extent of utilisation has to be limited to 25% owing to durability considerations. The niche domain of cement based adhesive mortars was also evaluated by (Buyuksagis et al., 2017) to assess the possible utilisation of marble waste as a replacement of dolomite powder. Even complete substitution was endorsed but with the caution of increased water requirement to produce such mortars.

Hence it can be pointed out that, there are only countable studies which evaluate waste marble powder (waste resulting from cutting and polishing activities) as a fine aggregate in the production of mortars for masonry and rendering purposes when compared to other domains. Studies pertaining to the evaluation of dolomitic marble powder are limited to only assessment of high strength mortars to elevated temperature and rapid freezing and thawing. Deciphering the existence of this gap in literature, this study makes

an attempt to contribute to the knowledge base of mortars made with dolomitic marble powder as a replacement of fine aggregate for both short and long term behaviour in order to bring out guidelines for consuming this huge amount of waste for some useful applications.

### **1.7 Specific objectives:**

1. To characterize the waste marble powder obtained from dolomitic marble processing units in terms of detailed physical/chemical properties pertaining to the intended application.
2. To evaluate of physical and mechanical properties of cement sand mortars containing waste marble powder.
3. To assess the durability characteristics of mortars made with marble powder when subjected to aggressive environments.
4. Based on the results of the test runs, to derive optimal usage of marble powder for different possible applications in the construction sector.

### **1.8 Organisation of the thesis:**

The research program presented in this thesis is divided into five chapters. As presented earlier, *Chapter 1* explains recycling and reuse of waste as an important aspect to achieve sustainability. The problems associated with marble waste disposal are also briefly described. The following chapter; *Chapter 2* provides an extensive review of literature which deals with the attempts made to evaluate construction materials produced using marble waste. Production of concrete, mortars, self-compacting concrete, asphalt pavements and clay bricks with marble waste has been reviewed. Ability of marble waste to stabilize and neutralize acids is also presented. The first section of the *Chapter 3* presents the results from the characterization tests carried out on marble waste as well as other materials like cement and fine aggregate used for the production of mortars. The next section discusses the research methodology followed to scrutinize the mortars made with marble waste. The final and third section of this chapter deals with the experimental methodology used for the each of the conducted tests. In *Chapter 4* results of different laboratory tests conducted have been discussed in detail. Micro-structural studies have been presented in support of the discussions. The thesis concludes with the *summary of test results* appended with *recommendations for future scope* in the areas regarding the use of waste marble.

## CHAPTER 2

### LITERATURE REVIEW

#### 2.1 General:

Attempts have been made to study the utilization of marble waste of different sizes in the production of construction materials. Marble waste in the form of coarse and fine aggregate have been used frequently in the past for the production of concrete. It has also been evaluated as a supplementary cementitious material for the production of the concrete and mortars. Many researchers have also used it to stabilize soils and for road construction. The following paragraphs present a review of performance all construction materials made with marble waste.

##### *2.1.1. Utilization of marble slurry for soil stabilization and road construction:*

###### *Modification of geotechnical properties*

From the traced literature, waste marble slurry found its first application in stabilizing lateritic soils in 1999. Okagbue and Onyeobi (1999) evaluated the usage of marble dust and found that, incorporation of marble dust reduced plasticity of the soils and hence improved workability. According to Ural et al. (2014) this modification was due to the coarser nature of marble slurry when compared to the clayey soil. They also pointed out that the unconfined compressive strength was maximum for 10% addition. Akinwumi and Booth (2015) stated that the ability of marble slurry to react with silica rich soil to form hydrates of calcium silicates and calcium aluminates was credited to be the reason for increase in the reported unconfined compressive strengths. Gurbuz (2015) also stated that the ductility behaviour of soils improved due to the usage of marble. Additionally, when the modified soils samples were subjected to 12 freeze thaw cycles, the residual strength was higher than samples with only clay.

###### *Construction of asphaltic pavements*

Chandra et al. (2002) citing the limitation in effective utilization of marble dust in the building construction industry, the authors evaluated its utilization in the preparation of asphaltic pavements as filler. Comparisons were made with limestone and rock dust which are conventionally used fillers in road constructions. The results showed that OBC increased with increase in filler content which decreased air voids in the mix. Maximum

performance in terms of unconfined compressive strength, Young's Modulus, fatigue capacity and tensile strength were maximum at 7% marble dust incorporation.

Akbulut and Gürer (2007) evaluated marble waste of size 20 mm to 0.075 mm with the aim of utilizing the same for the production asphaltic pavements. On comparison with limestone aggregates, it was found that mixes made with marble waste had high stability and flow values. Hence such mixes were deemed suitable for the construction of asphalt pavements with light to medium traffic. Kardeşahin and Terzi (2007) also recommended the usage of waste marble dust as a filler in place of limestone for the construction of roads with low volume. This limitation was set based on the higher plastic deformation characteristics of asphalt pavements with marble waste.

#### *Soil neutralization*

Pérez-Sirvent et al. (2007) analysed the potential of marble dust to immobilize heavy metals in contaminated soils. The authors concluded that marble waste was capable of stabilizing the sediments by immediately increasing the pH values from 3 to 8. Heavy metals like zinc which was around 10 mg/l in the lixiviates of the untreated samples was not detected in the treated samples.

Zanuzzi et al. (2009) evaluated the usage of waste marble along with organic waste like pig manure and sewage sludge as soil amendment. In addition to increase in pH value of the soil, marble waste also helped in the formation of organic matter. With the increase in soil organic matter, soil's capacity to hold nutrients increased which satisfy the requirement for microbial and plant growth. Zornoza et al. (2012) extended the research conducted by Zanuzzi et al. (2009) to five years, at the end of which they could see that pig manure and sewage sludge along with marble waste were able to maintain the quality of soil. Melgar-Ramírez et al. (2012) used horticulture waste composite along with marble waste and detected enzyme growth, which was an indication of microbial activity in the soils.

Fernández-caliani and Barba-brioso (2010) showed that of all the heavy metals, arsenic's concentration in the extracted liquids dropped by 94%, where significant reduction was noticed within one month. Presence of sulphate ions in the soil led to the formation of gypsum which was confirmed by scanning electron microscopy. Formation of gypsum aided the fall in electrical conductivity also. All these conditions led to plant growth after application of the soil amendment. Tozsın et al. (2014) added that coarser



marble waste with highest calcite content (99%  $\text{CaCO}_3$ ) was more effective in reducing the acidity of soil.

Calcite marble slurry waste was used as an additive to produce cemented paste backfill of tailings consisting sulphides by Ercikdi et al. (2015). Addition of this waste helped in improving the compressive strength of the backfill by 1.27 to 1.77 times higher than backfills without marble waste. These wastes also delayed the damage caused by the acidic sulphate environment on the cement hydration products. Tozsin et al. (2015) reconfirmed the fact that marble waste can be effectively utilized as a material which neutralizes acids and regulates mineral composition of soils.

### ***2.1.2. Utilization of marble slurry for the production of clay bricks:***

Marble waste has been evaluated as additive for the production of bricks since 2005. A Brazilian research group had used marble waste along with granite residue to produce clay in first of their three studies (W Acchar et al., 2006; Wilson Acchar et al., 2006; Segada et al., 2005). The temperature ranges in all these three studies were same but the heating rates were kept at 8.33°C/min, 10°C/min and 5°C/min respectively. By using these three heating rates different optimum substitutions were derived. After the bricks were sintered, linear shrinkage, apparent density, water absorption and flexural strength were determined. These mechanical properties were within acceptable limits which were achieved at lower firing temperatures itself. At a heating rate of 10°C/min, 50% incorporation was recommended, whereas for 8.33°C/min and 5°C/min rates, the maximum substitution was limited to 30%.

Sarkar et al. used saturated steam pressure to make clay-quartz-marble composite bricks. They pointed out that since these bricks had high porosity and low density they can be considered suitable for controlling humidity and temperature in buildings (Sarkar et al., 2006).

Saboya et al. (2007) were the first to use marble waste as a lone additive for the manufacture of bricks. The sintering temperature used in their study were between 750°C to 950°C with a heating rate of 5°C/min. Porosity and water absorption were the least at all firing temperatures when the substitution was around 15%. At the same level flexural and tensile strengths were also maximum, with no significant change in linear shrinkage. Hence the authors had recommended a maximum substitution of 15%.

In 2009, Montero et al. (2009a) reiterated the same facts as that presented by Saboya et al. (2007). Additionally in a follow up study, Montero et al. (2009b) used sewage sludge along with marble waste. By incorporating 1% - 2% of sludge along with 15% to 20% of marble waste, heavy metals were successfully immobilized in clay bricks without any substantial damage to their mechanical and physical properties.

Unlike the studies presented earlier, Bilgin et al. (2012) heated the raw materials to up to a temperature of 1100°C at a heating rate of 5°C/min. After evaluating a few physical and mechanical properties, the authors recommended a utilization of 10% of marble waste. Eliche-Quesada et al. (2012) evaluated the same properties of bricks sintered to the same temperatures as Bilgin et al. (2012) but with a heating rate of 3°C/min (Eliche-Quesada et al., 2012). By changing this heating rate they could allow a maximum substitution of 25% of marble waste.

Kirgiz in 2015 attempted to produce a clay and marble slurry cement which can be equivalent to conventional cement clinker (Kirgiz, 2015). Based on the LOI values of cement produced by using 77% to 81% of marble waste with brick powder the author was successful in producing a celite based cement clinker.

In addition to all the above properties determined, Sutcu et al. (2015), evaluated the thermal conductivity of bricks made with marble slurry. The results show that, since marble incorporation increases porosity of the bricks, a substitution of 30% of marble waste reduces the thermal conductivity by 60%, thereby improving thermal insulation.

Munir et al. (2018) studied properties like ultrasonic pulse velocity, efflorescence, resistance to freeze and thaw and sulphate agents of clay bricks with marble powder. All these properties were seen to deteriorate even for the minimal substitution of 5%.

### ***2.1.3 Marble waste as coarse aggregate for production of concrete:***

Marble waste was judged as a potential replacement for conventional coarse aggregates first by Binici et al. (2008). They had compared the behaviour of concrete mixes completely made with marble waste as coarse aggregate with mixes containing limestone aggregate. On evaluating the properties, it was found that density of concrete mixes did not vary much on utilization of marble waste. However the compressive strength of the these mixes increased by 76% after 28 days of curing. Flexural and tensile strengths along with Young's modulus of elasticity were also higher in the range of 57% to 64% when compared

to mixes made with limestone aggregates. These marble incorporated mixes had better durability properties also. Resistance to chloride ions was increased by 71% and the residual compressive strength after exposure to sulphate solution for 12 months was up by 2.4 times when compared to limestone based concrete.

The study conducted by Hebhouh et al. (2011), used limestone aggregate for the production of control concrete. These limestone aggregates were replaced by marble waste in the steps of 25% from 0% to 100%. The results show that mixes made with marble waste had slightly lesser fresh bulk density values when compared to control concrete. The workability also reduced significantly on increment of marble waste incorporation. However, compressive strength improved on inclusion of marble, where maximum performance was achieved at 75% substitution level. This was higher by 25% when compared to the control mix. Split tensile strength was also higher at the same substitution level.

Gencil et al. (2012) had used crushed stone as a baseline for comparison of marble waste as coarse aggregate, where substitution was done in steps of 10% from 0% to 40%. The results showed that with increase in replacement level of marble waste, the unit weight of concrete mixes reduced along with compressive strength. At 40% substitution, the compressive strength was only 78% of the control concrete. There were similar variations in split tensile strength, Young's modulus, UPV and Schmidt hardness values also. Only positive attribute of marble based concretes is that they have been reported to have lesser water absorption capacity, hence their resistance to freeze and thaw was also higher. At the end of the freezing and thawing testing regime the fall in compressive strength was around 4% to 7% for mixes with 40% marble waste, whereas for the control mixes it was around 13% to 15%.

Martins et al. (2014) and André et al. (2014) used limestone, basalt and granite as their baselines for evaluating performance of marble waste as coarse aggregate. Marble waste was used to replace these conventional aggregates by 20%, 50% and 100% levels. Mixes made with marble aggregate were equivalent or marginally better in resisting compressive and tensile strengths when compared to limestone counterparts. Resistance to water penetration was higher by 40% at complete substitution. However there was significant reduction in Young's modulus values which was lesser by 28% at complete

substitution when compared to the control mix. There was no significant variation in resisting chloride ions and carbonation when marble was used as coarse aggregate.

However when comparison was made with granite based concrete mixes, marble based concrete mixes have higher or equal performance characteristics at 50% substitution levels. A similar conclusion can be drawn when comparison is made with basalt aggregates also, with exceptions of Young's modulus and water absorption. As in the case of limestone aggregates, replacement of basalt aggregates by marble waste also resulted in drop of Young's modulus by the same extent. These mixes absorb higher water (60% increase at 50% substitution) also.

Based on the results presented above, André et al. (2014) conclusive remarks have been that, most if not all, durability parameters improve with the increase in bulk density of the concrete mix, which they achieved through partial substitution (25 – 50%) of conventional aggregates by marble waste.

Hence, to further enhance the utilization of marble waste, the packing of the concrete mix was improved by Kore and Vyas (2016) using an alternative mix design method based on packing density. This design method allowed mixes to incorporate 75% of coarse aggregates as marble waste. Since this design technique results in increase in aggregate content, marble based mixes required higher super - plasticizer content to attain required workability. Mechanical properties like compressive and flexural strengths of marble incorporated mixes were equivalent to control concrete. With increased packing, the water absorption of marble based mix was lesser by 15%. This resulted in higher resistance to chemical attack from carbonation and chloride ions which were lesser by 11% and 29% respectively. Residual compressive strength after exposure to sulphate reagents was equivalent to control concrete at the end of the test period.

However residual compressive strength of these marble based aggregate mixes when exposed to a sulphuric acid medium was lesser by 8% due to their acid soluble nature. When they were subjected to standard fire at 600 °C, the only significant change noticed was reduction in flexural strength which was lesser by 68% when compared to control concrete (Kore Sudarshan and Vyas, 2017). Finally, with this sufficient knowledge base on performance of marble waste as coarse aggregate, Tekin et al. (2017) had gone one step ahead and used marble waste as a conventional coarse aggregate itself to conduct their study on concrete with fly ash.

From the results presented in the above articles, it can be resolved that marble waste is a better coarse aggregate material than limestone. However when comparison is made with granite based concrete mixes, marble based concrete mixes have higher or equal Youngs' modulus only, while the other remaining performance parameters showed a decline. Mixes having crushed stone or basalt aggregates, perform better than marble waste coarse aggregates in both mechanical and chemical durability parameters. Hence based on the availability of type of conventional coarse aggregate, complete replacement can be made; or a partial substitution can be made where a particular combination of marble and conventional aggregates achieve a maximum dry bulk density value.

#### ***2.1.4. Marble slurry as supplementary cementitious material:***

Agarwal and Gulati (2006) were able to produce mortars with up to 20% marble waste (by replacing cement) from dolomitic origin which had same strength as that of control mortars after 28 days of curing for a mix proportion of 1:3. After 180 days of curing, the increase in strength was at a lower rate, which resulted in a disadvantage in performance of 12% to 25% for 10% and 20% substitutions respectively. By using a proportion of 1:6, the gain in strength was more predominant with 10% and 20% substitutions having 42% and 8% more strength than control mixes. These advantages however were wiped out on usage of a super-plasticizer in both the proportions, with mixes having marble waste reporting negative performance.

Corinaldesi et al. (2010) characterized the rheological properties of composite binders by replacing cement by marble slurry in the levels 10% and 20% with and without super-plasticizing admixture and with two w/c ratios of 0.4 and 0.5. It was reported that presence of marble powder improved yield stress of the cement pastes i.e. improved cohesiveness necessary for self-compacting concrete. Marble powder also improved segregation resistance. Thixotropy values of cement pastes with marble powder were low, indicating better flow through narrow sections when set in motion. On replacing cement by 10% for the production of mortars, compressive strength of the mixes was less by 10% when compared to conventional mortars. Rai et al. (2011) also echoed the same results as depicted by Corinaldesi et al. (2010) where the compressive strength of cement mortars reduced even for the 10% substitution level.

Aliabdo et al. (2014) used calcite marble of fineness 3996 cm<sup>2</sup>/g to replace OPC in variations of 5%, 7.5%, 10% and 15%. On evaluating the fresh and hardened properties it

was summarized that there was no change noticed in the water requirement of pastes to achieve the necessary consistency. Both initial and final setting times were also identical for all variations. The expansion of the composite cement pastes was also within limits. Maximum compressive strength was obtained for pastes with 10% replacement where an increment of 12% in performance was recorded.

Mashaly et al. (2015) had also recorded fresh and hardened properties of cement composites prepared by substituting cement by marble waste in the steps of 10% from 0% to 40%. On evaluating their consistency, these samples required more water than the pure cement pastes. This might be because, marble powder used in this study had fineness twice as much as cement it was replacing ( $6700 \text{ cm}^2/\text{g}$ ). Both the setting times recorded were very much lower than others for a substitution of 10%. With higher water contents in them, mortars prepared with these pastes recorded reduced resistance to compression even for the smallest substitution value.

The sample used by Vardhan et al. (2015) to replace cement was of dolomitic origin. This marble waste reduced the water quantities required even from minimal substitution level of 10% to a maximum substitution level of 50%. Flow time of cement pastes was also notably lower with significant reduction in time noted for 10% substitution level itself. This waste also prolonged both initial and final setting times of OPC. However the time gap between initial and final setting times reduced for a substitution range of 10% – 20%. On further increase in incorporation this time gap broadened. Similar results were also presented by Singh et al. (2017).

Vardhan et al. (2015) had reported that 10% replacement of OPC would produce cement paste with the same strength as that of control samples, whereas Singh et al. (2017) had sanctioned usage of 25%. This advantage could be because of two specific reasons. Firstly, Singh et al. (2017) had used marble waste was finer than cement they were replacing, which improves the chances of filler effect. Secondly the paste with 25% MS had 8% lesser water also in order to achieve necessary consistency.

Kirgiz (2016b) used calcite marble slurry to replace OPC and tested the composite cement mortars for their compressive strengths. Substitutions were done in variations of 6%, 20%, 21% and 35% to prepare mortars of proportion of 1:3 with a constant water cement ratio of 0.5. Maximum compressive and flexural strengths were obtained for 6% replacement only.

Li et al. (2018) used marble waste particles finer than 150 microns to replace cement in the production of mortars. They had evaluated four different w/c ratios of 0.4, 0.45, 0.5 and 0.55 and replaced cement in ranges of 5%, 10%, 15% and 20%. Durability properties like drying shrinkage, carbonation and water absorption of these mortars were studied. By using marble waste as a binder and reducing the water content by usage of a superplasticizer, carbonation depth of these mortars was significantly reduced by around 30% – 40%. Water absorption and drying shrinkage were also reduced by more than 40%.

Fall in compressive strength seems to be more predominant in case of air cured samples as exhibited by Toubal Seghir et al. (2018). The apparent density of pastes made with replacing cement with marble slurry in variations of 5%, 10%, 15% was noticed to reduce with significant increase in porosity values also.

#### ***2.1.5. Marble slurry as supplementary cementitious material in production of concrete:***

There have been six studies which could be traced, that discuss the effect of marble slurry as a supplementary cementitious material (SCM) in the production of concrete.

Based on the outcome of the traced literature, these could be categorised in two categories. First, the studies presented by Rana et al. (2015) and Rodrigues et al. (2015) show that on usage of MS in place of cement, the direct consequence is reduction in compressive strength, even for the meniscal substitution of 5%. Thereby all other connected mechanical properties also show a negative trend. However, at this substitution, the target strength in compression was achieved by the concrete mixes in both the studies.

Nevertheless, Rana et al. (2015), have reported that, addition of marble slurry leads to reduction in porosity and hence improved resistance to chloride and water penetration was noted. These parameters have shown improvement as compared to control mixes at a substitution range of 5% - 10%. Corrosion resistance of the mix with 5% marble waste was maximum among all the reported mixes.

Contrastingly, Rodrigues et al. (2015) showed increased susceptibility to damage by carbonation, chloride penetration, water, abrasive wear and drying shrinkage. This difference in results presented by the two studies might be due to the difference in surface area of marble slurry used. The sample used by Rana et al. (2015) had a surface area of 7350 mm<sup>2</sup>/kg whereas Rodrigues et al. (2015) had used a sample of surface area 2150 mm<sup>2</sup>/kg. Hence in order to improve the quality of these mixes with marble slurry, the

authors introduced the usage of two different kinds of superplasticizer by which they could improve these durability properties by 9% to 33%. The only drawback of these mixes was their increased drying shrinkage values which was higher by 20% to 93% based on the superplasticizer used.

Secondly the studies presented by Aliabdo et al. (2014) and Mashaly et al. (2015) show that, there is reduction in porosity, and this advantage has transpired in to better compressive strength also at 20% and 10% substitutions respectively. Ergün (2011) produced concrete mixes having the best resistance to compression at 7.5% substitution of OPC.

Aliabdo et al. (2014) have shown mixes with 7.5% to 10% marble waste have better steel concrete bond. On the other hand Mashaly et al. (2015) have reported mixes with 20% marble waste have higher resistance to freeze and thaw, improved bulk density, better resistance to water penetration and reduced abrasive wear. These properties improved by 11% to 26% as compared to control mixes.

#### ***2.1.6. Composites of marble slurry and other supplementary cementitious material in production of binders:***

Understanding the fact that marble slurry cannot be substituted in place of conventional cement, researches later turned their focus on combining it with other supplementary cementitious materials and then replace cement. Materials that have been evaluated with this intention include fly ash, slag and silica fume along with other mineral admixtures like diatomite, pumice, nano-graphite and granite dust.

Agarwal and Gulati (2006) were successful in producing mortars of proportions 1:3 and 1:6 by replacing 20% of cement by equal proportions of dolomite marble waste with either fly ash, silica fume or slag. Leaner the mix, greater was the advantage of gain in compressive strength (a minimal increment of 17% and 20% for 1:3 and 1:6 mix proportions respectively), which was negated partially or fully with use of a superplasticizer. The maximum increment in compressive strength was noticed when marble dust was combined with silica fume, fly ash and slag were 170%, 114% and 20% respectively for the mix proportion 1:6.

Ergün (2011) used diatomite (a type of sedimentary rock) to offset the fall in compressive strength when marble waste was used in place of OPC. He too could reduce



cement consumption by 20% on using equal proportions of diatomite and marble waste. Such mixes had equivalent performance in terms of compressive and flexural strength after 28 days of water curing.

However Bacarji et al. (2013) results were not much encouraging when they used a composite waste material of granite and marble to replace OPC. Their results showed a maximum substitution of 5% only is possible to prevent any significant fall in compressive strength. At this substitution level, modulus of elasticity reduced and water absorption was higher than the control concrete mixes.

Sancak and Özkan (2015) used a combination of equal proportions of pumice and fly ash along with marble, which also produced concrete mixes of inferior quality. Composite cement pastes made with the above combination required more water to achieve consistency and set faster. When used to prepare concrete, they produced mixes whose compressive and flexural strengths were lesser by 32% – 58% and 36% - 61% respectively. Their resistance to external sulphate attack was also low.

Nano-graphite was used in the visionary research conducted by Kirgiz (2016) where he could recover the loss in performance of compressive strength by replacing 35% of OPC by marble waste. More realistically Ashish (2018) used marble slurry of dolomitic origin to replace both OPC cement and sand. With a marginal fall in workability, by replacing 30% of OPC and sand combined, the concrete mix had 4.65% more compressive strength. Tensile strength was even higher with no change in UPV values.

Taking account of the research conducted by Agarwal and Gulati (2006), Khodabakhshian et al. (2018) used silica fume to increase the utilization of marble slurry. Their initial study could allow them replace 5% of OPC with marble waste, which could be increased to 20% by replacing an additional 10% OPC by silica fume. These mixes had reduced workability but had higher stiffness and compressive and tensile strengths by a very minimal margin. They slightly absorbed more water but still had better electrical resistivity which was higher by 2.28 times than the control concrete. These mixes also performed equivalent to the conventional mixes when subjected to sulphate attack. Significant improvement against acid attack was noticed where the residual compressive strength at the end of the 63 days test period was 1.63 times more than control mix (Khodabakhshian et al., 2018b).

### ***2.1.7. Marble waste as fine aggregate for production of concrete:***

Marble waste has been tested as a possible replacement of fine aggregate for the production of concrete mixes having w/c ratio in the range 0.4 – 0.6. Most of the studies have used calcite based marble waste for their studies. As in the case of replacing coarse aggregate by marble waste, Hanifi Binici here too was the pioneer in carrying out the research in this domain. Binici et al. (2007) used marble waste finer than 1 mm to replace sand of the same size, in proportions of 5%, 10% and 15%. They stated that with inclusion of marble waste, compressive strength of the concrete mixes improved by 24% at 15% substitution level. After exposure to a 7% sulphate solution the compressive strength of the same mix reduced by only 15% when compared to control concrete which lost 58% of original compressive strength. This mix had the best resistance to abrasive wear and water penetration also. These improvements were credited to marble wastes' pore filling ability but at the expense of reduced workability. Hence a superplasticizer had to be used to compensate this loss.

Ural et al. (2014) repeated the above exercise, but with the use of pozzolana based cement as the binder and without any superplasticizer. They could achieve equivalent performance to that of control concrete at 10% substitution despite a marginal increase in water content to achieve necessary workability. (Kırgız, 2016b) also reiterated the same claims when he replaced sand by marble waste finer than 0.075 mm. He could achieve maximum compressive strength (higher by 8% when compared to control concrete) at 20% replacement level. Additionally he evaluated flexural strength, Schmidt surface hardness and resonant frequency which were very much in line with the variation in compressive strength. These improvements however were largely insignificant.

Demirel (2010) used dolomitic marble slurry of size smaller than 0.25 mm to replace sand of the same size. Concrete properties like compressive strength, modulus of elasticity, unit weight and ultrasonic pulse velocity (UPV) were enhanced because of reduced porosity. Most significant variation was noticed for the change in modulus of elasticity which was about 24%, whereas for the remaining parameters the increase was limited to only 10%.

Unconventionally, Hebhouh et al. (2011) used marble waste (fineness modulus 3.12) to replace comparatively finer sand (fineness modulus 1.92). He could achieve an improved performance in terms of compressive (an improvement of 24%) and tensile

strength at 50% substitution. At 100% replacement, these parameters were lesser than control concrete.

Alyamac and Aydin (2015) and Aliabdo et al. (2014) used marble waste of fineness 4372 cm<sup>2</sup>/g and 4000 cm<sup>2</sup>/g to replace river sand. Alyamac and Aydin (2015) used a super-plasticizer to compensate for the loss in workability, by which they could replace 90% of the fine aggregate. The mechanical performance and resistance to abrasion for mixes with 40% – 50% marble waste was equivalent to control concrete. Sorptivity was also acceptable within the same range. While Alyamac and Aydin (2015) study proved maximum compressive strength can be obtained at 20%, Aliabdo et al. (2014) stated that maximum gain is obtained at 10% replacement of river sand. This improvement ranged between 7% to 15%. Both these studies show that the ratio of tensile to compressive strengths increases, which indicate a stronger interfacial transition zone when marble waste is used. Apart from compressive and splitting tensile strengths, Aliabdo et al. (2014) also evaluated steel concrete bond strength, UPV and porosity. While the bond strength was maximum at 10% substitution, UPV values showed no change and porosity was least at 15% substitution.

Gameiro et al. (2014) and Silva et al. (2013) also evaluated the utilization of marble mining waste as fine aggregate for the production of concrete. They used river sand, basalt sand and granite sand as the base lines for comparison of marble waste. Unlike other studies, the grading curve of individual and composite fine aggregates was kept the same across all mixes in order to remove the variations in performance arising due to change in particle size distribution. The results show that irrespective of the nature of the conventional fine aggregate, compressive strength of all concrete mixes reduced. A significant reduction of 20% was noticed when comparison was made to concrete with river sand. When compared to mixes made with the aggregates of basalt and granite, the reduction was 4% to 8%. However the reduction in tensile strength and modulus of elasticity was not as significant as that of compressive strength. This again was an indication of a stronger ITZ in marble incorporated mixes when compared to the mixes made with aggregates of non – carbonate sources. Durability properties like water absorption, carbonation and chloride ion penetration depended on the porosity of the mix, in which the aggregates did not play any significant role in changing the cement's chemistry. Drying shrinkage was the least in mixes with marble waste which the authors credited to its better geometric features.

### 2.1.8. Marble waste as fine aggregate / filler in self-compacting concrete:

Alyamaç and Ince (2009) aimed at constructing a monogram for the design of self-compacting concrete (SCC) with marble waste as a filler. To achieve this, the authors had used marble from three different sources, and added them at different levels to concrete mixes from 0 to 400 kg/m<sup>3</sup>. Cement content and w/c were also varied between 300 to 500 kg/m<sup>3</sup> and 0.36 to 0.7 respectively. These variables resulted in design of 47 different mix proportions. Based on the results of fresh and hardened properties which were analysed statistically led to the design of the monogram as shown in Fig. 2.1. This single graph makes it possible to estimate the quantities of cement, water and powder content to achieve desired compressive and split tensile strengths with two different flow values.

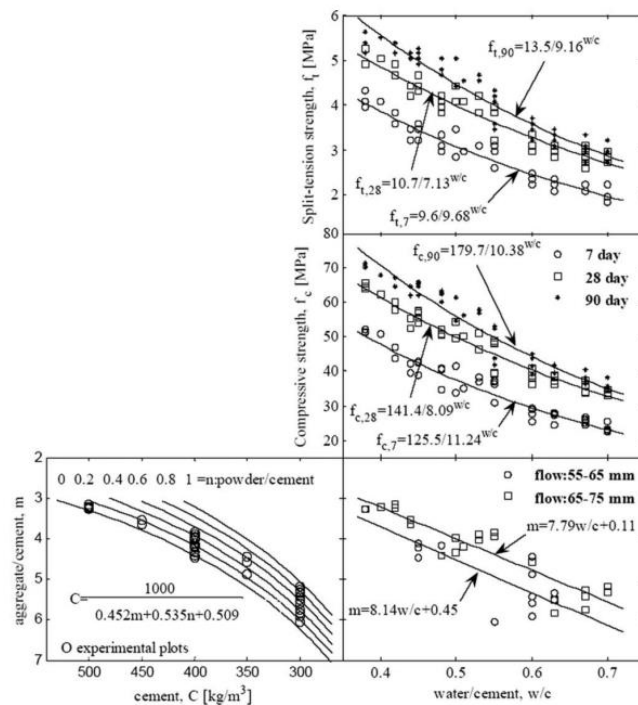


Fig. 2.1 A mix design monogram designed by Alyamac and Ince (2009)

Hameed et al. (2012) aimed at completely replacing river sand with crushed rock dust and incorporating marble waste as a filler for the production of SCC. The authors were successful in replacing the entire river sand with crushed rock dust and incorporation of marble waste helped in reducing pores. Hence, such concrete mixes had better compressive and split tensile strengths. This increment varied between 2 to 17% for both the above mechanical parameters. Water permeability which increased by 21% on replacing river sand by rock dust was reduced by the same extent when marble waste was used as a filler.

Such mixes also had higher penetration resistance to chloride ions and better electrical resistivity.

Sadek et al. (2015) tried to combine granite and marble waste and use them as fillers for the production of SCC. On analysing the results the authors justified that marble waste imparted better mechanical and durability properties when combined with granite waste. Best performance was obtained when these wastes were used as 50% by weight of cement. Compressive strength of such mixes were higher by 28% when compared to mixes made with 10% silica fume (added by weight as a percentage of cement content). Water absorption was also reduced by 17% when these two mixes were compared. This enhanced behaviour of these mixes was due to suspected pozzolanic property of granite waste, whereas marble waste acted only as a filler. These mixes also had a marginal advantage over resisting attack from sulphate reagents. Utilization of such waste also proved to be an eco-friendly alternative to attain the necessary fresh properties of SCC without increasing the cement content or without utilization of fines like silica fume.

Tennich et al. (2015) compared the mechanical performance of SCC made with marble waste as a filler with those mixes made with conventional limestone fillers in first of their two studies. The authors pointed out mixes made with marble waste had comparable fluidic and hardened properties to that of control mixes. However, sulphate resistance of mixes with marble waste was significantly better than those mixes without any filler. The mixes made with marble waste could better retain the required elastic modulus for a longer period of exposure to sulphate solutions (14 to 20 months) when compared to control mixes (5 to 8 months). Weight loss experienced by such mixes was also lesser. However, SCC mixes with limestone showed lower deterioration characteristics than those made with marble waste. Tennich et al., (2017) reasoned this variation in performance to be because of higher alumina content in marble waste when compared to limestone filler, i.e. higher the alumina content greater is the susceptibility to damage by the sulphate reagents.

#### ***2.1.9. Marble waste as fine aggregate in mortars:***

Buyuksagis et al. (2017) had used marble waste particles finer than 1 mm as replacement for dolomite aggregate in the production of adhesive mortars. They had substituted this conventional aggregate from 0 to 100% in steps of 20%. They measured workability in terms of flow table test in which they had recorded a minimal decline from 60% substitution onwards. The authors had also recorded a fall in setting times of mortars

with increase in substitution of marble waste. With regard to compressive strength they could not find any specific pattern in variation, whereas the tensile strength was equivalent for all mixes. Adhesive strengths however have been reported to improve with used of marble slurry which was maximum at 80% substitution level. These mixes had also marginal increase in water absorption capacity.

With regard to production of masonry mortars, the most recent published literature available is of Khyaliya et al. (2017). The authors used marble waste of particles ranging from 4.75 mm to 75  $\mu$  to substitute fine aggregate from 0% to 100%. The flow value of these mortars was fixed at 105% to 115%. The results showed that, water requirement was the least for 50% substituted mix. Consequently compressive strength was maximum at 50% substitution while the completely substituted mix had 125% more strength than the control mix.

Romania's Molnar and Manea (2016) explored the suitability of calcite based marble slime in plaster (1:5) as a replacement for fine aggregate. Each size fraction was substituted in proportions of 25%, 50%, 75% and 100%. The authors reported that with regard to consistency, inclusion of marble reduced workability which was reasoned out to be because of the binding nature of marble powder. Seventh day compressive strength for the mix with 25% marble sludge was more than control mortar's strength by 8%. But evaluation of the 28<sup>th</sup> and 60<sup>th</sup> day strength, specimens recorded a decline of 5% and 40% respectively for the same mix. However even 100% substitution satisfied the criteria of attaining a minimum strength of 6 MPa after 28 days of curing. Lastly, on evaluation of strength of adhesion to the support layer, mix with 25% marble waste had 160% more strength than control mortar. Substitution of 75% and upwards showed a decline in performance for the same property.

Earlier in 2014, Keleştemur et al. (2014b) examined the utilization of marble sludge produced by the Turkey's marble cutting and sawing industry, as a replacement of fine sand (<0.25 mm) in the substitution of 20%, 40% and 50% (by volume). A w/c ratio of 0.5 was kept constant for the mix ratio 1:3 by volume. Compressive and flexure strengths were evaluated after 30 cycles of freeze and thaw. The author's conclusion was that since marble was finer than the sand it replaced, it served the purpose of a filler resulting in better compressive and flexural strengths. But however the same filler effect reduced the mortars resistance to freeze and thaw cycles. This is because, pores help reduce the tensile stresses

created in the cement paste by the expanded frozen water. Reduction of these pores led to a significant fall in flexural strength than compressive strength when specimens were treated to freeze and thaw cycles.

In a preceding research conducted by the same research group (Keleştemur et al., 2014a), the effect of elevated temperature on compressive strength and porosity values were studied. It was found that, the filler effect of marble helped reduce porosity, thereby achieving higher compressive strength. Alteration of aggregate cement paste was also linked to lesser reduction of porosity and compressive strength at elevated temperature.

Rai et al. (2011) investigated the effect of marble granules as a replacement of fine aggregate in mortar. Replacement was done by weight in variations of 5%, 10%, 15% and 20% for a mix ratio of 1:3 with a constant w/c of 0.44. On testing, mortars attained a peak compressive strength for 10% substitution after which resistance to compression dropped.

Corinaldesi et al. (2010) characterized marble powder generated from marble shaping and cutting industry with a view of using the same in mortars and concrete. To evaluate compressive strength, mortars of ratio 1:3 (cement:sand) were prepared in which marble slurry was used in place of sand (10% substitution). The flow value was kept constant for both the mixes. Slurry was used in wet state and subsequent corrections were made to the required w/c ratio based on the moisture content of the marble slurry. On recording the compressive strength, there was a fall by 10% in performance. Hence they concluded that marble slurry played the role of filler and showed no sign of taking part in the hydration process.

#### ***2.1.10 Other niche domains:***

Calcium carbonate is used as a filler to reinforce rubber formulations. An experimental evaluation conducted by Marras and Careddu (2017) has proved that dried marble sludge of calcite origin can produce tyre mixtures with same or even better physical, rheological and mechanical properties when used in place of reagent grade calcium carbonate. Marble slurry can also help in alleviating the properties of discarded polyethylene terephthalate (PET) products. On incorporation of about 25%, marble slurry of calcite origin can improve tensile and bending stresses bearing capacity with improved hardness value also. Marble inclusion also renders this composite relatively more non-flammable. While the thermal behaviour of original polymer remains intact, the modified heat conductivity coefficient classifies the new composite polymer as a construction

material. However the inclusion of marble makes PET more brittle which breaks at lower energy values. With these characteristic features, it thought that such products can be used as an anti-corrosion coating for reinforcement as well as an electrical insulator Çınar and Kar, (2018). Marble waste can also be used as fillers for the production of polymer concrete (Tawfik and Eskander, 2006).

#### **2.1.11 Summary:**

From the above literature survey it can be summarized that marble waste of sufficient fineness can reduce segregation of self-compacting concrete mixes and help improve flowability with lesser water content itself at a cement replacement level of 10%. This would in turn help in improving the compressive resistance of cement composites. This advantage can also be obtained when marble waste are able to fill pores left between other constituents of concrete and mortars for conventional concrete mixes. At a cement replacement level of 10% the durability properties are improved with no change in mechanical properties. To enhance mechanical performance of such composites marble waste can be combined with silica fume and fly ash at the same replacement level.

The geotechnical properties of soils can be alleviated with an addition of 10% of marble slurry waste. This can also replace conventional fillers for the construction of pavements. Calcite based marble waste have appreciable acid neutralizing capacity hence can be used to lower the pH of acidic soils. On replacement of up to 30% cement in cemented backfills, the resistance of these composites towards attack from sulphate reagents increases. Marble waste along with granite or sewage sludge can be used to produce clay bricks too. The extent of utilization (15% - 50%) depends on the sintering temperature and combination of waste materials.

It can also be safely pointed out that marble powder has been tested as fine aggregate relatively to a lesser extent for utilization in mortars than any other domain. Properties like tensile bond strength of mortars with substrates, drying shrinkage, resistance to salt crystallization, and wet – dry cycles have not yet been reported so far. Marble being acid soluble in nature, performance evaluation of mortars with marble powder when exposed to acidic mediums becomes crucial. Mechanisms pertaining to sulphate attack on mortars containing marble waste also needs to be studied. Additionally, utilization of such waste can also reduce the dependency on natural river sand leading to reduction in cost and burden on landfills around marble processing industries.



## CHAPTER 3

### MATERIALS AND METHODS

#### 3.1 General:

This chapter presents the characterization of materials used to prepare mortars after which the methodology used to arrive at the optimum level of utilization of marble powder is discussed. Experimental methodology of the laboratory tests conducted on the various mortar samples is also elaborated here.

#### 3.2 Materials:

The materials used to prepare mortars were Portland pozzolana cement, natural sand and marble powder (dried marble slurry). These materials were characterized using relevant standards and specifications as discussed below.

##### 3.2.1 Cement:

Portland pozzolana cement (PPC) complying with IS 1489 (1991) was used. The physical properties of this cement are listed in Table 3.1. A scanning electron micrograph as seen in Fig. 3.1 shows presence of spherical fly ash particles and irregular cement clinker. Quantitatively, the oxide composition is listed in Table 3.2.

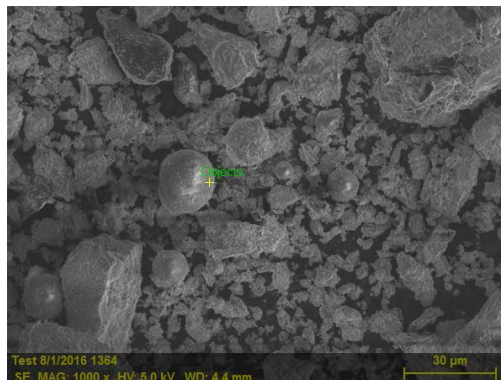


Fig. 3.1: Scanning electron micrograph of PPC

##### 3.2.2 Fine aggregate:

River sand of two different particle size distributions were used. As mentioned above they are designated as fine sand (FS) and coarse sand (CS). Their grading is as shown in Fig. 3.2. Their physical properties like bulk density, water absorption, specific gravity and fineness modulus are shown in Table 3.1.

Table 3.1: Physical properties of materials used to prepare mortars

Property	Material			
	Cement (PPC)	Fine sand (FS)	Coarse sand (CS)	Marble powder (MS)
Initial setting time (min)	127	-	-	-
Final setting time (min)	232	-	-	-
28 <sup>th</sup> day compressive strength (MPa)	37	-	-	-
Consistency (%)	33	-	-	-
Specific gravity	2.9	2.67	2.65	2.7
Bulk density (kg/m <sup>3</sup> )	1100	1560	1685	1380
Water absorption (%)	-	6.2	1.8	-
Fineness modulus	-	2.13	2.44	-
Shrinkage limit (%)	-	-	-	18
Specific surface area (m <sup>2</sup> /g)	0.361	-	-	0.35

Table 3.2: Oxide composition of materials used to prepare mortars

Radical	Material			
	Cement	Fine sand (FS)	Coarse sand (CS)	Marble powder (MS)
Calcium oxide (CaO)	44.75	2.57	2.2	32.05
Silica (SiO <sub>2</sub> )	32.01	79.57	79.04	1.57
Alumina (Al <sub>2</sub> O <sub>3</sub> )	8.47	8.28	9	0.18
Ferric oxide (Fe <sub>2</sub> O <sub>3</sub> )	3.83	1.74	1.68	1.18
Magnesium oxide (MgO)	1.11	0.5	0.56	19.95
Sodium oxide (Na <sub>2</sub> O)	0.23	1.53	1.78	0.03
Potassium oxide (K <sub>2</sub> O)	0.42	2.53	2.52	0.03
Manganese oxide (MnO)	-	0.05	0.05	0.05
Titanium dioxide (TiO <sub>2</sub> )	-	0.19	0.18	0.02
Phosphorous pentoxide (P <sub>2</sub> O <sub>5</sub> )	-	0.05	0.05	0.2

### 3.2.3 Marble powder

Wet marble slurry was acquired from a firm which processes marble slabs in an industrial area of Jaipur. The slurry was sun dried, hammered to reduce the dried blocks to a powder passing through 1.18 mm sieve (Fig. 3.3). In addition to specific gravity and bulk density, specific surface area and shrinkage limit (IS 2720 (Part 5), 1985) for MS were

identified and listed in the Table 3.1. On particle size analysis, 50% of MS particles were found to be smaller than  $49.68 \mu\text{m}$  with a surface area of  $0.35 \text{ m}^2/\text{g}$ . This shows that MS is as fine as conventional cement. Table 3.2 lists out the chemical composition of MS used, which shows that marble has significant amount of magnesium and calcium ions. On conducting X-ray diffraction analysis (Fig. 3.4) marble powder was found to consist of calcium and magnesium carbonate, predominantly in the form of dolomite crystals indicated by the peak at a diffraction angle of  $31.027^\circ$ . SEM micrographs were also taken (Fig. 3.5) which showed MS have rough texture with irregular shape.

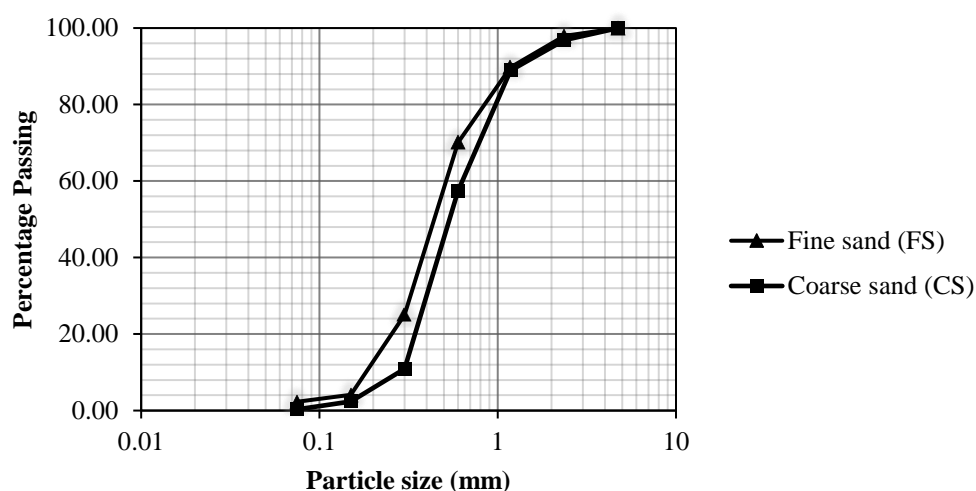
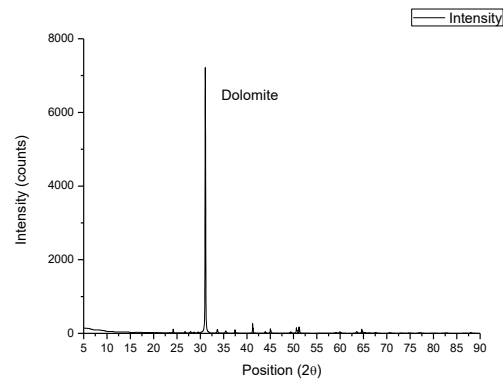


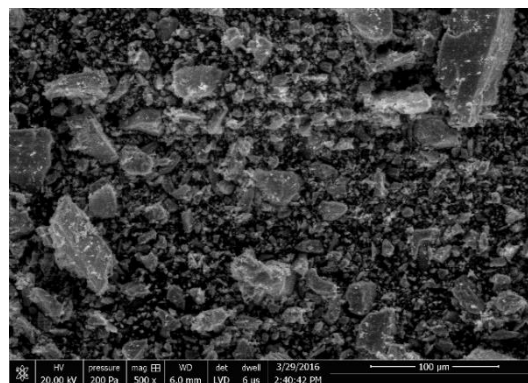
Fig. 3.2: A comparative statement of particle size distribution of two different samples of river sand with the required specifications



Fig. 3.3: Marble powder



**Fig. 3.4: X-ray diffraction pattern of dried marble powder**



**Fig. 3.5: SEM micrograph of marble powder**

### 3.3 Mix proportions

Four volumetric proportions of cement and sand in the ratios 1:3, 1:4, 1:5 and 1:6 were chosen. These four series were named A, B, C and D respectively. For the first stage of the study MS was used to replace FS volumetrically, in steps of 20% from 0% to 100%. Hence mixes were named by the series, the type of sand used and percentage of MS content. For e.g. Mix ASF0 would indicate, a mix proportion of 1:3 with FS and 0% MS content, whereas mix DSC40 would imply a mix proportion of 1:6 with CS and 40% MS content. Water content was adjusted such that the mortars had sufficient workability (as detailed in section 3.1.1). The quantities of materials required to prepare one cubic meter of mortar is detailed in Table 3.3 and Table 3.4 for mixes with FS and CS respectively.

Table 3.3: Quantities of materials required to produce 1 m<sup>3</sup> of mortar with FS

Designation	Substitution of FS (%)	Cement (kg)	FS (kg)	MS (kg)	Water (L)
ASF0	0	356	1517	0	320
ASF20	20	356	1213	268	303
ASF40	40	356	910	536	360
ASF60	60	356	607	804	434
ASF80	80	356	303	1072	509
ASF100	100	356	0	1340	573
BSF0	0	274	1556	0	334
BSF20	20	274	1245	275	304
BSF40	40	274	934	550	351
BSF60	60	274	623	825	416
BSF80	80	274	311	1100	490
BSF100	100	274	0	1375	562
CSF0	0	220	1562	0	352
CSF20	20	220	1250	276	297
CSF40	40	220	937	552	328
CSF60	60	220	625	828	403
CSF80	80	220	312	1104	477
CSF100	100	220	0	1380	552
DSF0	0	190	1619	0	342
DSF20	20	190	1295	286	287
DSF40	40	190	971	572	314
DSF60	60	190	648	858	399
DSF80	80	190	324	1144	475
DSF100	100	190	0	1430	551

Table 3.4: Quantities of materials required to produce 1 m<sup>3</sup> of mortar with CS

Designation	Substitution of CS (%)	Cement (kg)	CS (kg)	MS (kg)	Water (L)
ASC0	0	356	1636	0	320
ASC10	10	356	1472	133	295
ASC20	20	356	1308	268	303
ASC30	30	356	1145	402	331
ASC40	40	356	981	536	338
ASC60	60	356	654	804	427
ASC80	80	356	327	1072	498
DSC0	0	190	1746	0	352
DSC10	10	190	1571	143	298
DSC20	20	190	1397	286	286
DSC30	30	190	1222	429	289
DSC40	40	190	1048	572	314

### 3.4 Research Methodology:

Marble powder (MS) was used to prepare Portland pozzolana cement (PPC) mortars by replacing river sand (FS) in percentages of 20%, 40%, 60%, 80% and 100% by volume. The river sand (FS) used as fine aggregate conformed to IS 2116 (1980) for use in mortars for masonry purposes. Four volumetric proportions (1:3, 1:4, 1:5 and 1:6) of PPC and FS

were chosen for the study to evaluate properties like workability, fresh bulk density, compressive strength, tensile bond strength, adhesive strength, dynamic modulus of elasticity, water absorption and drying shrinkage. Based on the results obtained from the above set of experiments, it was estimated that a coarser grading of sand might help in improving the extent of utilization of MS. Hence a coarser sand (CS) was chosen which satisfied the grading requirements of IS 2116 (1980). The same set of experiment was repeated on two proportions (1:3 and 1:6). With these results in hand, four mixes were chosen for two mix proportions (1:3 and 1:6). These mixes were then evaluated for their performance when subjected to durability tests. Hence this methodology can be summarized with the help of a flow chart in Fig. 3.6.

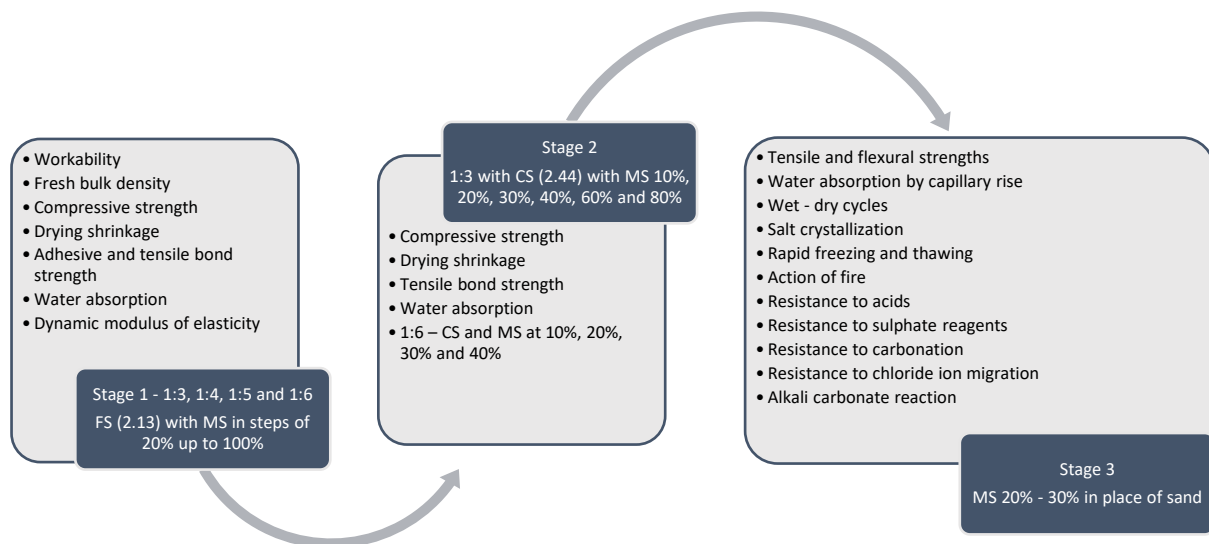


Fig. 3.6: A flow chart showing the research methodology

### 3.5 Experimental Methodology:

The following section elaborates how the mortar mixes were prepared and tested for their various physical, mechanical and durability properties.

#### 3.5.1 Casting and curing of specimens:

Mortar mixes were prepared by mixing the required ingredients in proportions given in Table 3.3 and Table 3.4. Mixing of dry constituents was done first in tilting drum mixer, after which the predetermined quantity of water was added. Then for 3 – 5 minutes the mixing was continued until the mix appeared to be homogenous. Tests to be done on fresh mortar samples were carried out as specified in following sections. For testing on hardened samples, the prepared mortar mixes were filled in pre-oiled moulds of appropriate

sizes as shown in Fig. 3.7. Two different curing regimes were followed for specimens to be evaluated for physical and mechanical properties. For measuring length change by shrinkage, sulphate attack, alkali carbonate reaction, rapid freezing and thawing and carbonation a third type of curing method was used. The detailed procedures for curing are explained below.



**Fig. 3.7: One batch of cast mortar mix**

#### *Curing regime 1*

This curing regime was practised as per the stipulations of IS 2250 (1981). The hardened samples were removed from the moulds after 24 hours. Then they were water cured until the day of testing, which in all tests was 28 days of duration.

#### *Curing regime 2*

Samples prepared for evaluating tensile bond strength and adhesive strength were subjected to this curing regime as per ASTM C 952 (2002) and BS EN 1015 (2000) respectively. After the mortar in the prepared samples had sufficiently hardened they were sealed in a polythene bag and left as such for 7 days. Then they were transferred to a room where the temperature and relative humidity was maintained at  $20^{\circ}\pm 2^{\circ}\text{C}$  and  $50\% \pm 5\%$  respectively till the time of testing.

#### *Curing regime 3*

The samples cured with this method were prepared only for conducting length change experiments. This curing regime consisted of moist curing the samples in their moulds for two days with the help of wet jute gunny bags. Drying shrinkage (ASTM C 1148, 2002) was evaluated on samples which were moist cured for one additional day after de-moulding. Measurements for evaluating alkali carbonate reaction (ASTM C 1105, 2008)

were done on samples which were moist cured after demoulding for the entire test period. Samples prepared for measuring length due to rapid freezing and thawing, carbonation and sulphate attack were cured in a saturated solution of lime water for 26 days after demoulding (ASTM C1012/C1012M-15, 2015). Following table (Table 3.5) summarizes the curing regimes used for measuring different physical and mechanical properties. The different curing regimes carried out for the different sample types are as shown in Fig 3.8.

**Table. 3.5: A summary of different curing regimes followed**

Curing regime 1	Curing regime 2	Curing regime 3	Tests
<i>Water curing for 28 days</i> 1. Compressive strength 2. Flexural strength 3. Tensile strength 4. Dynamic modulus of elasticity 5. Water absorption 6. Capillarity 7. Salt crystallization 8. Wet – dry cycles 9. Acid attack 10. Chloride penetration 11. Effect of fire	<i>Sealed in polythene bags for 7 days then stored in a room with RH 50% ± 5% and temperature 20°±2°C for 21 days</i> 1. Tensile bond strength 2. Adhesive strength	<i>Moist curing for 3 days and then stored in a room with RH 50% ± 5% and temperature 20°±2°C</i>	Drying shrinkage
		<i>Moist cured for the entire test period</i>	Alkali carbonate reaction
		<i>Cured in saturated lime water for 28 days</i>	Sulphate attack, carbonation and rapid freezing and thawing
Testing age: 28 days	Tests Compressive strength, Flexural strength, Tensile strength, Dynamic modulus of elasticity, Water absorption, Capillarity		
Testing age: 1, 7, 14, 21, 28, 56, 84, 112, 140 days	Drying shrinkage and alkali aggregate reaction		
Testing age: 1, 7, 14, 21, 28, 56, 84 days	Acid attack, carbonation, and chloride penetration		
Testing age: 28, 84 and 168 days	Sulphate attack		
Cycles:	Salt crystallization (15 cycles); Wet – dry cycles (20 cycles)		



**Fig. 3.8: Curing regimes: a) water curing; b) curing at ambient RH and temperature and c) moist curing**



### 3.5.2 Workability:

The consistency of the mortar mixes was considered at a flow value of 110% to 115% as recommended by IS 2116 (1980). The flow mould was centrally placed over the flow table. Mortar mix was filled inside this mould in three layers of 25 mm thickness and each layer was tamped 20 times. The mould was lifted away from the mortar after which the flow table was dropped 25 times in 15 seconds from a height of 12.5 mm. The resulting diameter was measured in four directions. This increase in diameter was represented as percentage of the original inner base diameter. The measurement of flow value of one such mortar mix is shown in Fig. 3.9.

### 3.5.3 Fresh bulk density:

Bulk density in the fresh mortar state was evaluated as per ASTM C 185 (2002). After mixing the constituents in the required proportions, a standard metal container of volume 400 mL was filled with the prepared mortar in three layers. Each layer was tamped 20 times. After tamping the final layer, the side of the container was slightly struck with the tamping stick four times. Then the excess mortar was struck off using a straight edge. The container and its constituents were weighed as shown in Fig. 3.10. By knowing the weight of the container, the fresh bulk density was calculated using the following expression:

$$\text{Fresh bulk density (g/cc)} = \frac{\text{Mass of container with mortar sample} - \text{Mass of empty container (g)}}{\text{Volume of container (mL)}} \quad (1)$$



Fig. 3.9: Measurement of flow value of mortar mixes



Fig. 3.10: Measurement of weight of fresh mortar mix in a standard container

### 3.5.4 Compressive strength:

Compressive strength of mortar mixes was evaluated based on the stipulations set by IS 2116 (1980). Three cubes of 50 mm size were tested immediately after removing from the curing tank. Cubes were placed centrally on the loading platform and loaded at a

rate of 2 to 6 N/(mm<sup>2</sup>.min) until failure occurred. The peak load was noted and compressive strength was calculated using the following expression:

$$\text{Compressive strength (N/mm}^2\text{)} = \frac{\text{Peak load at failure (N)}}{\text{Cross sectional area (mm}^2\text{)}} \quad (2)$$



Fig. 3.11: Compression testing machine

### 3.5.5 Tensile strength:

Tensile strength of the mortar samples was evaluated as per ASTM C 307 (2003). Three briquet samples were prepared and water cured for 28 days. After which they were oven dried for 24 hours at a temperature of 60°±5°C. The specimens were positioned centrally between the clips of the machine as shown in Fig. 3.12.



Fig. 3.12: Experimental setup to test tensile strength of mortars

The loading rate was kept constant at 5 to 6.4 mm/min. Load was applied until failure and peak tensile strength was calculated using the following expression:

$$\text{Tensile strength (N/mm}^2\text{)} = \frac{\text{Peak load at failure (N)}}{\text{Width at the waist of briquet} \times \text{depth of briquet (mm}^2\text{)}} \quad (3)$$

### 3.5.6 Flexural strength:

Three prisms of size 40 x 40 x 160 mm of each mix were water cured for 28 days to evaluate their flexural strength as per ASTM C 348 (2002). The samples were oven dried at  $60^{\circ}\pm 5^{\circ}\text{C}$  for 24 hours before testing. For testing, the specimens were centrally placed over the base plate as shown in Fig. 3.13. The load was applied at a rate of 2 to 3 kN/min till failure occurred. The flexural strength of the mixes was calculated using the following expression:

$$\text{Flexural strength (N/mm}^2\text{)} = 0.0028 \times \text{peak load (N)} \quad (4)$$



Fig. 3.13: Experimental setup to test flexural strength of mortars

### 3.5.7 Tensile bond strength:

Tensile bond strength of bricks and mortar samples for all mixes was evaluated using brick couplets. This test was conducted as per ASTM C 952 (2002). Clay bricks were pre-wet for a period of 24 hours before the test. A square mould of side 92 mm and depth 13 mm was centrally placed over a brick and mortar sample was filled into it. Then the mould was removed from the mortar bed. Another brick was placed over the mortar bed in perpendicular direction of the lower brick. Then the frame of the drop hammer was placed on top brick and the drop hammer was dropped from an approximate height of 40 mm. If

there was any extrusion of mortar it was wiped away. Then the samples were cured by the curing regime 2. After 28 days from the preparation of the samples, they were placed between the two tripods. The setup was placed in a compression testing machine as shown in Fig. 3.14 and load was applied such that the samples fail within 2 minutes of applying initial load. Tensile bond strength was calculated using the following expression:

$$\text{Tensile bond strength (N/mm}^2\text{)} = \frac{\text{Peak load at failure (N)}}{\text{Cross sectional area in load (mm}^2\text{)}} \quad (5)$$



Fig. 3.14: Experimental setup to test tensile bond strength of mortars

### 3.5.8 Adhesive strength:

Three pre-wet clay bricks were used for this test. The sample mortars prepared with required proportions of the constituents, were coated on the side of the brick without the frog in upright position as shown in Fig. 3.15. The thickness of the coated layer was maintained at  $10 \pm 1$  mm. The samples were cured according to the curing regime 2. Curing was followed by creating a circular groove of diameter 50 mm into the brick layer for depth of around 2 mm through the plaster layer. Then a metal pull head was glued on this circular groove with a suitable adhesive. This adhesive was allowed to set for 48 hours. Then with the help of a pull-off machine, a tensile load on the glued metal pull head was applied at a rate such that the mortar brick interface or mortar or brick within the groove enclosed area failed within 2 minutes of initial load. The peak load and the type of failure were noted. Adhesive strength between the brick and plaster was calculated using the following expression:

$$\text{Adhesive strength (N/mm}^2\text{)} = \frac{\text{Peak load at failure (N)}}{\text{Cross sectiona of the loaded area (mm}^2\text{)}} \quad (6)$$

The type of failure was also noted with the following notations: E – Adhesive fracture:- failure of mortar brick interface; F – Cohesive fracture:- failure of mortar; and G – Cohesive fracture:- failure of brick.



**Fig. 3.15: Preparation of sample to test adhesive strength**

### **3.5.9 Drying shrinkage:**

Drying shrinkage of five prisms of size 25 x 25 x 285 mm were measured using the stipulations set by ASTM C 1148 (2002) using the setup shown in Fig. 3.16.



**Fig. 3.16: Experimental setup to measure the length of mortar prisms**

Samples were cured using the curing regime 3. Initial reading was noted on the third day. Further readings were taken 7, 14, 21, 28 days and then every 30 days until the end of 5<sup>th</sup> month. Drying shrinkage was calculated using the following expression:

*Shrinkage (%) =*

$$\frac{\text{Initial measurement after removal from moist cure (cm)} - \text{measurement during or after drying (cm)}}{\text{effective gage length}} \quad (7)$$

### **3.5.10 Water absorption by immersion, bulk and apparent densities and voids:**

ASTM C 642 (2006) was used as a guideline to evaluate water absorption by immersion, bulk and apparent densities and void content of the mortar mixes. After 28 days of water curing, three samples of 70 mm cubes were oven dried for a two consecutive periods of at least 48 and 24 hours in oven of temperature  $110 \pm 5^\circ \text{C}$  and their weights were noted each time. If the variation in weight was less than 0.5%, they were immersed in water at approximately  $21^\circ \text{C}$ , else they would be returned to the oven for another period of 24 hours and this shall be repeated until the variation in weight between two successive readings is less than 0.5%. After placing the specimens in water for two consecutive periods of 24 hours, the weights were noted by wiping off the loose water by damp cloth. If the weights varied by less than 0.5%, then the samples in the same state were suspended using a wire basket into a container filled with water. The apparent weight was noted. The following parameters were calculated using the expressions given below:

$$\text{Water absorption by immersion (\%)} = \frac{(B-A) \times 100}{A} \quad (8)$$

$$\text{Bulk density } (g_1) = \frac{A \times \rho}{B - D} \quad (9)$$

$$\text{Apparent density } (g_2) = \frac{A \times \rho}{A - D} \quad (10)$$

$$\text{Volume of permeable pore space (\%)} = \frac{(g_2 - g_1) \times 100}{g_2} \quad (11)$$

Where:

- A = weight of oven dried sample in air (g)
- B = weight of surface dry sample in air after immersion (g)
- D = apparent weight of sample in water after immersion (g)
- $\rho$  = density of water, (1 g/cc)

### **3.5.11 Water absorption by capillarity:**

Rate of water absorption by capillarity was determined using three specimens of 50 mm cubes of each of the eight mixes as per ASTM C 1403 (2006). After 28 days of curing, the samples were oven dried for 24 hours at  $110 \pm 5^\circ \text{C}$  and the oven dried weight was noted.

Then the dimensions of the specimens were measured to calculate the area of the exposed. After which a mark was made on the specimens to indicate a distance of 3 mm from the exposed side. The samples were then placed on a steel mesh in a container such that the exposed surface was greater than 90% of the exposed side. Water was added to the container in a way that water rises only to the level of 3 mm mark on the side perpendicular to the exposed surface as shown in Fig. 3.17. After adding water, weight of the specimens was noted by wiping the wet surface dry by a damp cloth at intervals of 0.25, 1, 4 and 24 hours. After each reading the specimens were returned back to the container immediately. For each reading taken, water absorption was calculated using the following expression:

$$A_T = \frac{(W_T - W_0) \times 10000}{L_1 - L_2} \quad (12)$$

Where:

- $A_T$  = Water absorption in 100 g / cm<sup>2</sup>,  
 $W_T$  = the weight of the specimen at time T (g),  
 $W_0$  = the initial oven dried weight of the specimen (g),  
 $L_1$  and  $L_2$  = average length and width of the specimen (mm).



Fig. 3.17: Experimental setup to for conducting the capillarity test of mortar specimens

### 3.5.12 Dynamic modulus of elasticity:

The pulse velocity method was used to calculate the dynamic modulus of elasticity as given by Pozo-Antonio (2015). For this experiment, three prisms of 40 x 40 x 160 mm were used. Two transducers having a frequency of 54 kHz were placed on the two phases of 40 x 40 mm size. The time taken for the ultrasonic pulses to travel from one end to the other was recorded and dynamic modulus of elasticity (MPa) was calculated using the following expression.

$$E_{dyn} = 0.001 * v^2 * \rho \quad (13)$$

Where,

v = velocity of ultrasonic waves (m/s);

$\rho$  = bulk density of mortars (g/cm<sup>3</sup>)

### 3.5.13 Salt crystallization:

The effect of salt crystallization cycles was evaluated using the stipulations set by BS EN 12370 (1999). To evaluate the change in compressive strength, weight and water absorption capacity, three cubes each of 50 mm and 70 mm dimensions were used. After 28 days of water curing, the specimens were oven dried at 110±5° C for 24 hours. After which the 70 mm cubes were weighed and their initial weight was noted. Then all the specimens were transferred to containers with 14% solution of sodium sulphate decahydrate. They were allowed to be there for 2 hours. Then all the specimens were transferred to an oven with temperature of 110±5° C. After 15 hours, these samples were removed and were allowed to reach room temperature. From immersion of samples into the solution and removing them from the oven constituted one cycle. This cycle was repeated for 14 more times. After the completion of the 15<sup>th</sup> cycle, 50 mm cubes were subjected to capillary water absorption test as detailed in section 3.1.11. Then the same samples were used to evaluate the compressive resistance as mentioned in section 3.1.4. The 70 mm cubes were used to measure the change in weight. After evaluating the compressive resistance, the change in compressive resistance was calculated using the expression:

$$C_{\%} = \frac{(C_{28} - C_D) \times 100}{C_{28}} \quad (13)$$

Where:

C<sub>%</sub> = Change in compressive strength (%)

C<sub>28</sub> = Compressive strength after 28 days of curing (MPa)

C<sub>D</sub> = Compressive strength after the durability test (MPa)

The change in capillary water absorption was calculated using the following expression:

$$P_{\%} = \frac{(P_{28} - P_D) \times 100}{P_{28}} \quad (14)$$

Where:



$P_{\%}$  = Change in capillary water absorption (%)

$P_{28}$  = water absorption capacity after 28 days of curing (100 g / cm<sup>2</sup>)

$P_D$  = water absorption capacity after the durability test (100 g / cm<sup>2</sup>)

The change in weight was calculated using the following expression:

$$W_{\%} = \frac{(W_{28} - W_D) \times 100}{W_{28}} \quad (15)$$

Where:

$W_{\%}$  = Change in weight (%)

$W_{28}$  = Weight after 28 days of curing (g)

$W_D$  = Weight after the durability test (g)

#### **3.5.14 Wet – dry cycles:**

This test was performed on the same lines as that of salt crystallization test with the difference in the conditioning regime. The immersion phase lasted for 6 hours where the samples were dipped in clean water at 20° C. Then all of the samples were transferred to an oven at 70° C and left there for 18 hours. After the completion of drying period they were immediately transferred to the containers with water at 20° C. This alternate wetting and drying was done in 20 cycles, after which the same properties were evaluated as those evaluated for the salt crystallization. These stipulations for conducting the test of wet – dry cycles test can be found in BS EN 14066 (2013).

#### **3.5.15 Sulphate attack:**

Resistance of the mortar mixes to an attack from sulphate ions was judged as per the stipulations of ASTM C 267 (2001). Three each of 50 mm and 70 mm cubes were water cured for 28 days, after which they were exposed to a 5% sodium sulphate solution as shown in Fig. 3.18. The extent of damage was evaluated in terms of compressive strength and weight. Before exposing the samples to sulphate solutions, the oven dry weight of the 70 mm cubes was noted. Then after exposure, compressive strength was tested as detailed in the section 3.1.4 along with weight, at durations 1, 7, 14, 28, 56 and 164 days of exposure to the solution. The change in these parameters was estimated using the expressions 13 and 15 given in section 3.1.12. In addition to the above mentioned parameters, the amount of extent of change in length mortar samples was also noted. For this purpose five prisms of size 25 x 25 x 285 mm were used. After the curing regime (as given in section 3.4.1) the specimen's initial length was measured. Then these samples were also exposed to the same

solution for the same amount of duration. At each measuring interval the change in length was calculated using the expression 7.



Fig. 3.18: Samples subjected to a 5% solution of sodium sulphate

### 3.5.16 Acid attack:

This test was conducted on the similar lines of sulphate attack test. Stipulations of ASTM C 267 (2001) hold good for this test too. Acidic medium used here consisted of 5% 1M sulphuric acid solution. Three numbers of 50 mm and 70 mm cubes which were water cured for 28 days were used. With these samples, the resistance of the mortars to the acidic medium was evaluated in terms of change in compressive strength and weight at durations 1, 7, 14, 28, 56 and 84 days of exposure.

### 3.5.17 Carbonation:

The penetration of carbon dioxide into the mortar mixes was evaluated as per recommendations set by RILEM CPC 18 (1988). Mortar samples of size 40 x 40 x 160 mm prisms were water cured for 28 days. Then they were oven dried at temperature range of  $60^{\circ}\pm 5^{\circ}\text{C}$  for a period of 24 hours. After which they allowed to reach room temperature. Then they were painted by two coats of an epoxy paint on five faces of the prism leaving one of the two 40 x 40 sides uncoated. After the paint had sufficiently hardened they were transferred to the carbonation chamber (as shown in Fig. 3.19) where the relative humidity was maintained at 50% and carbon dioxide concentration at 5%. The testing periods were fixed at 1, 7, 14, 28, 56 and 84 days at which three samples of each mortar mix were removed from the chamber and split open in the longitudinal direction. Phenolphthalein solution of 1% strength in 70% ethanol was sprayed on to the split samples. The portion of samples where colour remained unchanged, signified that carbonation of the hydration

products had occurred to an extent that the pH of the cement matrix has degraded to a value less than 9. The portion of sample where the colour of the specimen became pink on spraying the solution indicated that cement matrix's pH was above 9. Based on the position of the colour change front from the uncoated face, the extent of penetration of carbon dioxide was noted.

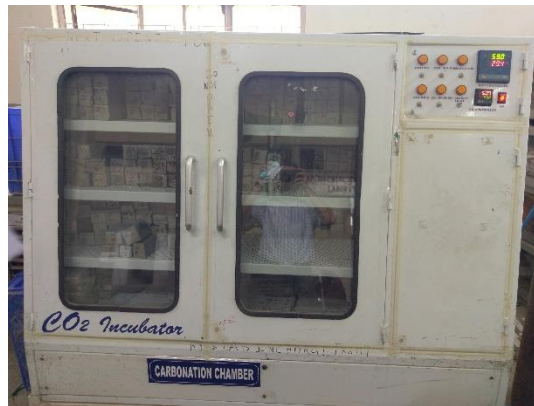


Fig. 3.19: Carbonation chamber

### 3.5.18 Rapid freezing and thawing:

Resistance of mortar mixes to cycles of freezing and thawing was evaluated as per ASTM C 666 (2003). The freezing cycle consisted of reducing the temperature to  $-18^{\circ}\text{C}$  within a span of 3 hours and 30 minutes, after which the thawing cycle was initiated where the temperature was raised to  $4^{\circ}\text{C}$  in the span of 2 hours and 30 minutes. This constituted the one freezing and thawing cycle. Performance of the mixes after they have been subjected to 20, 50, 100 cycles of rapid freezing and thawing was quantified in terms of change in compressive strength and weight loss. For this, three numbers of 50 mm and 70 mm cubes each were used respectively. Additionally change in length was also noted using five 25 x 25 x 285 mm prisms. The curing regime for these three types of samples is given section 3.4.1. After the curing regime, initial lengths and weights were noted for the respective samples. Then they were transferred to a chamber where the effect of freezing and thawing was simulated (Fig. 3.20). After the completion of one exposure period, compressive strength, was evaluated as given in section 3.1.4 along with change in weight. Change in compressive strength and weight were calculated using the expressions 13 and 15 respectively. Change in length of the prism samples was calculated using the equation 7.



Fig. 3.20: Environmental chamber to simulate rapid freezing and thawing

### 3.5.19 Chloride ions penetration

The curing regime and the sample preparation for this test is the same as that for evaluating the extent of carbonation. After the samples had been coated with an epoxy paint, three samples for each mix were immersed in a solution of 1% NaCl. The extent of penetration of chloride ions into the mortar matrix was evaluated at 1, 7, 14, 28, 56 and 84 days. During each of the testing period, as per the Nordtest method, NT BUILD 492 (1999), samples were split open along the longitudinal direction and 0.1M AgNO<sub>3</sub> solution was sprayed. The depth from the uncoated face of 40 x 40 mm side where the colour of AgCl's white precipitate changes to brown colour of AgNO<sub>3</sub> (shown in Fig. 3.21) was noted to be extent of free chloride ions.



Fig. 3.21 Colour change when 0.1M solution of AgNO<sub>3</sub> is sprayed on samples soaked in NaCl

### 3.5.20 Alkali carbonate reaction:

Possibility of alkalis present in cement to react with the carbonate ions present in dolomite MS was evaluated as per stipulations set by ASTM C 1105 (2008). Five specimens of 25 x 25 x 285 mm prisms were cast and moist cured in the moulds for two days. Initial length was noted at the beginning of the third day and moist curing continued until the end of the test. Subsequent length measurements were noted for 7, 28, 56 and 84 days of testing. Length change was calculated using the expression given in equation 7.

### 3.5.21 Effect of fire:

To understand the extent of damage fire could make to mortars with marble powder, samples were exposed to fire in a gas fired furnace (shown in Fig. 3.22) at 200°C, 400°C, 600°C and 800°C. The rate of increase in temperature of the fire followed the standard fire curve (ISO 834) as shown in Fig. 3.23.



Fig. 3.22: Gas fired furnace

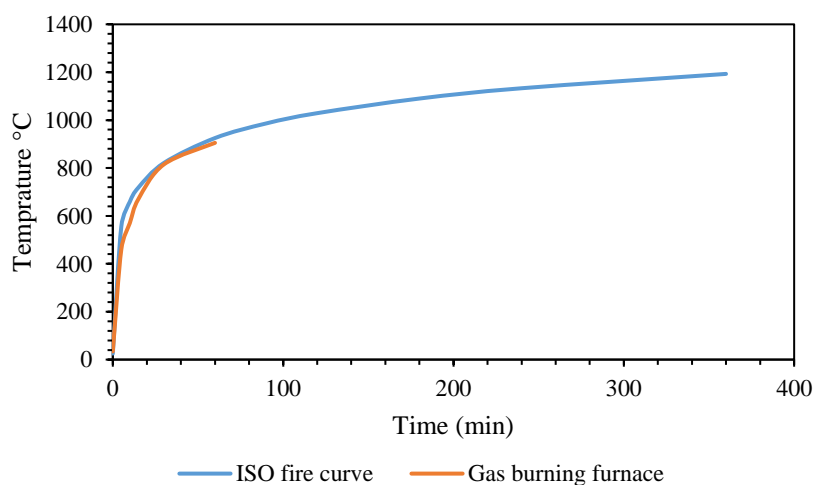


Fig. 3.23: Standard fire curve

Three samples of sizes 50 mm and 70 mm used for this test were water cured for 28 days. Initial weight of 70 mm cubes was noted and then both the types of samples were exposed to the fire until the required temperature was attained. After the exposure, compressive strength was evaluated as detailed in section 3.1.4. Using the expressions 13 and 15, change in compressive strength and weight were calculated respectively.

### 3.5.22 Environmental evaluation:

The methodology adopted by Khodabakhshian et al. (2018a) to calculate the environmental performance of concrete mixes has been used here. Environmental evaluation has been divided in to three heads viz., global warming potential, fossil fuel depletion index and acidification potential.

Global warming potential (GWP) uses the life cycle inventory (LCI) data to calculate the quantity of emissions made to land, water and air for the provision of a service or a product. This also takes in to account of inputs made by any means of materials and energy. These emissions are calculated in terms of CO<sub>2</sub> (grams) released per unit product. The life cycle inventory data for individual materials used in the production of mortar which represents their contribution to global warming is given in Table 3.6.

**Table 3.6: Life cycle inventory data of mortar constituents**

Constituent	Cement	Sand	Water
GWP (CO <sub>2</sub> – eq)	0.855	0.0032	0.0025
AP (SO <sub>2</sub> – eq)	0.0053	0.00002	0.0045
FP (MJ/kg)	1.49	0.0063	0.01

Hence GWP (in grams of CO<sub>2</sub>) for production of one cu.m of mortar can be given as

$$GWP = 0.885 * C + 0.0032 * S + 0.0025 * W \quad (16)$$

Fossil fuel depletion (FP) associated with the production of the above material constituents can be given by the following equation

$$FP = 1.49 * C + 0.0063 * S + 0.01 * W \quad (17)$$

The ability to release H<sup>+</sup> ions in to the environment relative to SO<sub>2</sub> (sulphur dioxide) is termed as acidification potential (AP). LCI data to estimate the AP and FP for the production of mortar constituents is given in Table 3.6 Acidification potential linked with the production of mortars can be given by the following equation

$$AP = 0.0053 * C + 0.00002 * S + 0.0045 * W \quad (18)$$

Where C, S and W are the quantities (in kg) of cement, sand and water required for the production of one cu.m of mortar. Since marble powder is a waste material associated with the manufacturing of marble slabs, the environmental impact associated for the production of this is assumed as zero.

A cumulative score was then calculated for each mortar mix after normalizing each of the above three parameters. The mathematical expression used is as follows

$$EnvScore = \frac{GWP}{Max(GWP \text{ of a given series})} + \frac{AP}{Max(AP \text{ of a given series})} + \frac{FP}{Max(FP \text{ of a given series})} \quad (19)$$

### 3.5.23 Economic evaluation:

The cost involved in conditioning marble powder so that it can be used in the production of mortars is as follows

An unskilled labour charge = Rs 400 / day

Daily output (manually hammering and sieving through 1.18 mm sieve) = 320 kg

This would translate to a cost of Rs 1.25 for conditioning one kg of dried marble powder. Cost of other materials is given in Table 3.7

**Table 3.7: Cost of mortar constituents**

Constituent	Cost	Normalized value
<b>Cement</b>	Rs 300 / 50 kg bag	1
<b>Sand</b>	Rs 1920 / m <sup>3</sup>	0.2
<b>Marble powder</b>	Rs 400 / 320 kg	0.21

Hence the cost involved for the production of mortars can be given by the following expression

$$Cost = 1 * C + 0.2 * S + 0.0034 * W + 0.21 * MP \quad (20)$$

Where C, S, W and MP are the quantities in kg of cement, sand, water and marble powder required for the production of one cu.m of mortar. The normalized value of water has been obtained from literature. After obtaining the cost for the production of each mix in both the series, all the values are then normalized.

### 3.5.24 Consolidated evaluation:

Mortar specimens were also ranked based on their mechanical and durability performances. Two different normalized factors were determined. One factor ( $N_1$ ) for properties like compressive strength, bond and adhesive strengths and flexural and tensile strengths where maximum performance is desirable. Second ( $N_2$ ) for properties like drying shrinkage, penetration of chloride ions, carbonation, length change due to carbonation, sulphate attack and freezing and thawing. For this second parameter, least change in their physical property is desirable. Mechanical and durability performance can hence be calculated by the following expression:

$$MD_{per} = \frac{N_1}{N_2} \quad (21)$$

$$ECM = \frac{MD_{per}}{EnvScore+Cost} \quad (22)$$

After analysing the mechanical performance and gaging the environmental and economic performance a consolidated index (ECM) was used (Eq. 22) to judge the overall benefits/drawbacks derived by using marble waste as fine aggregate in the production of mortars.



## CHAPTER 4

### RESULTS AND DISCUSSIONS

#### 4.1 General:

Properties of cement mortar mixes containing marble powder in different ratios were evaluated and compared with control mortars. Later a coarser grading of sand was adopted in mortars to seek the possibility of enhancing incorporation of marble powder in the mixes. Vital mechanical and durability properties were evaluated and optimum replacement level of fine aggregate by marble powder was determined in two widely used mix proportions in construction sector.

#### 4.2 Evaluation of Physical and Mechanical Properties:

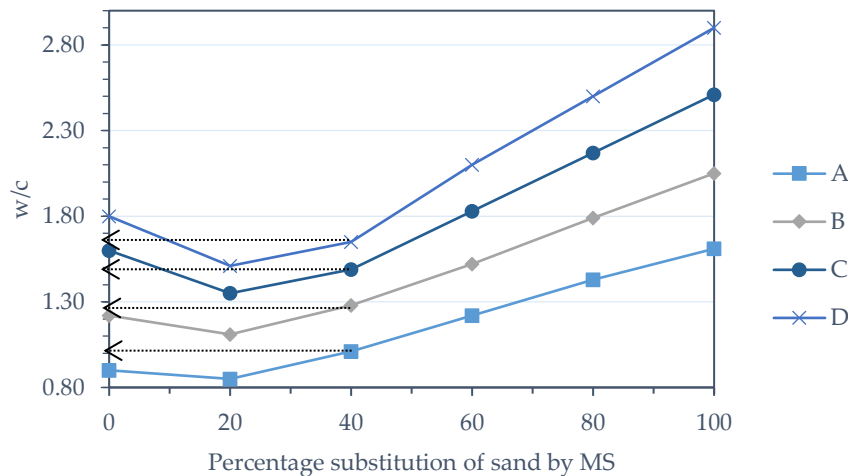
Marble powder (MS) was used to replace fine sand (FS) for the preparation of cement sand mortars. Four volumetric mix proportions, 1:3, 1:4, 1:5 and 1:6 were studied in stage 1, where FS was replaced by MS in the range of 20% to 100% by volume. Properties such as workability, fresh bulk density, drying shrinkage, compressive strength, tensile bond strength, adhesive strength, hardened bulk and apparent densities, water absorption capacity, permeable voids and dynamic modulus of elasticity were evaluated. The results of the above tests are discussed below.

##### 4.2.1 Workability:

The water requirement of mortars to attain the desired flow is shown in Fig 4.1. For the series A, w/c ratio for control mix was 0.9, but when FS was completely replaced by MS (mix ASF100), the w/c ratio increased to 1.61 which is 79% more than that of control mix ASF0. However mix ASF20 required 5.6% less amount of water in comparison to control mortar to attain the same flow value. The same pattern of results were obtained for the other three mix proportions also. When compared to control mortars ASF0 and BSF0, more water was required when substitution was greater than 20% (refer Fig. 4.1) for series A and B. Whereas for series C and D, a substitution greater than 40% resulted in greater water demand when compared to the corresponding control mixes.

The characteristic variation in water demand to attain the required workability of MS incorporated mortar mixes can be because of the distinguishing thixotropic nature of MS as pointed out by Corinaldesi et al. (2010). This would be the reason why mortar mixes

with 20% to 40% substitution of FS appear to be stiff but flow easily when a force is applied. This fall in water requirement is actually a consequence of fall in rheological parameters of the mortar mixes, where this dolomitic MS plays a role of a weak super-plasticizer. Szybilski and Nocun-Wczelik (2015) also noticed similar behaviour of paste samples when they replaced cement with dolomitic powder.



Key to legend: A, B, C and D represent mixes of proportions 1:3, 1:4, 1:5 and 1:6 respectively

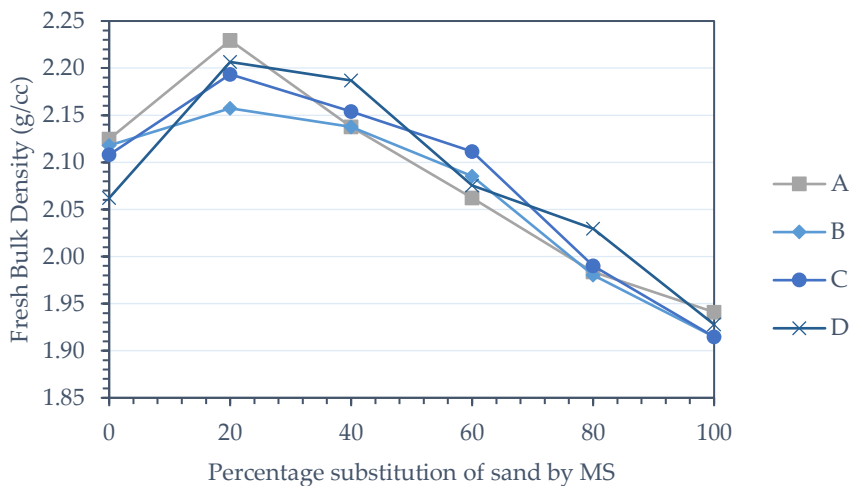
**Fig. 4.1: Water requirement of mortars to attain the desired flow value of 105% to 115%**

Beyond 20% - 40% substitution of FS, the thixotropic property seems to be overcome by the fineness of MS. Initially the voids left between the large sand particles provide large internal friction resulting in high plastic viscosity. When MS is added, these occupy the voids helping reduce internal friction and consequently plastic viscosity. When the MS content is increased further, their surface area starts playing a dominating role which in return increases plastic viscosity. Haach et al. (2011) also deemed the same reason was responsible for the increase in water content when coarse sand was replaced by fine sand in the production of mortars. Hence mixes with fines content greater than 20% for series A and B and 40% for series C and D require more water to achieve consistency equal to that of mortars with only river sand.

#### **4.2.2 Fresh bulk density:**

The variation of fresh bulk density of mortars with increase in substitution of FS by MS is as shown in Fig. 4.2. For all the four series, maximum density was obtained at 20% replacement of FS. This peak was recorded because of the fact that, MS has the ability to fill the voids formed between FS and cement. Also water content for this mix was the least when compared to other substitutions. At 40% incorporation of MS, the density was equal

or greater than the corresponding control mixes. On further increase there was steady decline, and the least fresh density was seen at complete substitution of FS. This decrease is a consequence of variation in water content, which increases with increase in FS content. Molnar and Manea (2016) have also reported that the least density was obtained when sand was completely substituted by marble slime.



Key to legend: A, B, C and D represent mixes of proportions 1:3, 1:4, 1:5 and 1:6 respectively

**Fig. 4.2: Variation of fresh bulk density of mortar mixes**

### 4.2.3 Drying shrinkage

Variation of drying shrinkage of mortars with increase in MS utilisation has been plotted in Fig. 4.3 to Fig. 4.6 for series A to D, respectively.

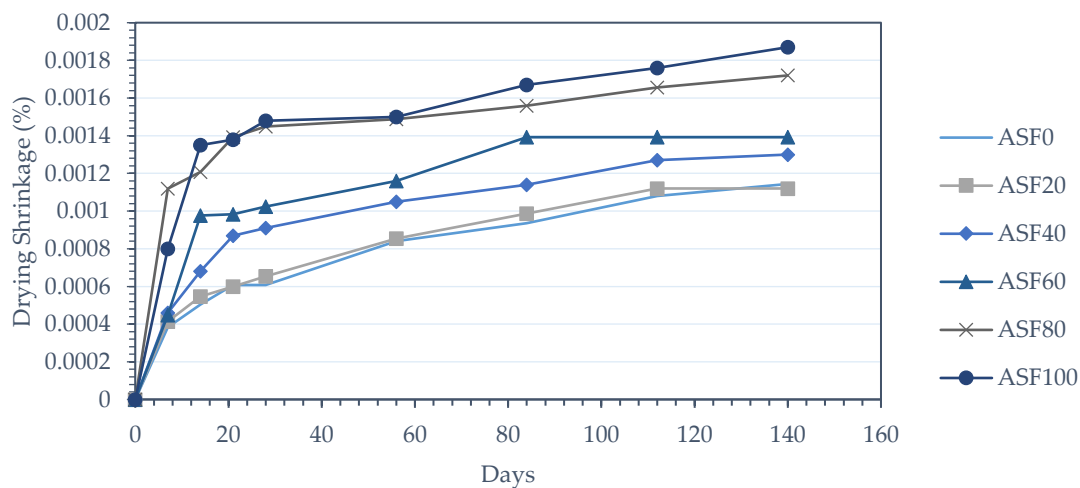


**Fig. 4.3: Drying shrinkage of series A (1:3)**

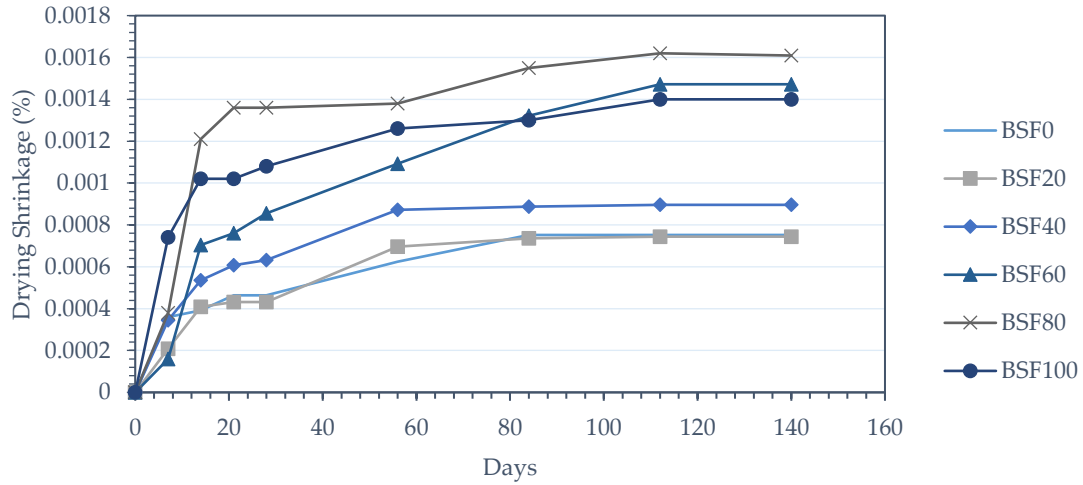


Fig. 4.4: Drying shrinkage of series B (1:4)

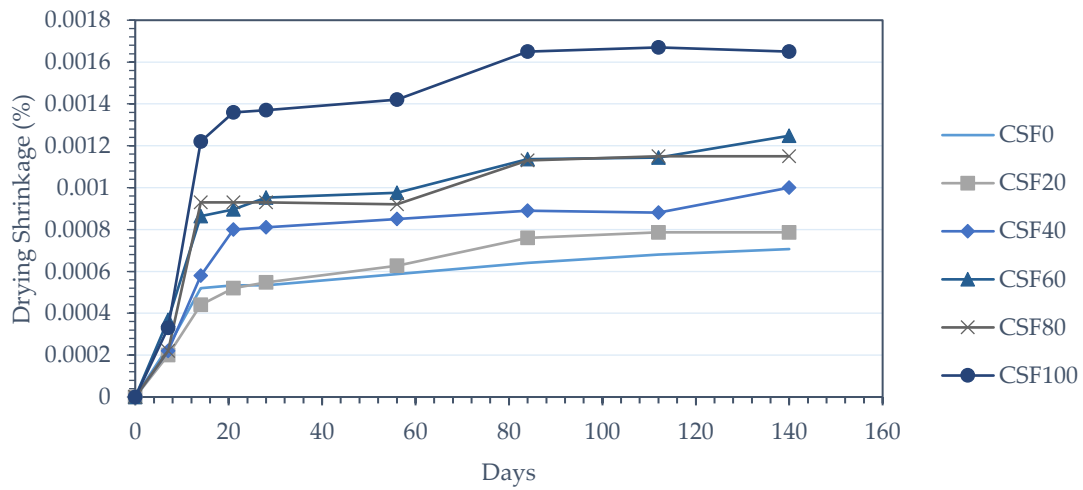


Fig. 4.5: Drying shrinkage of series C (1:5)

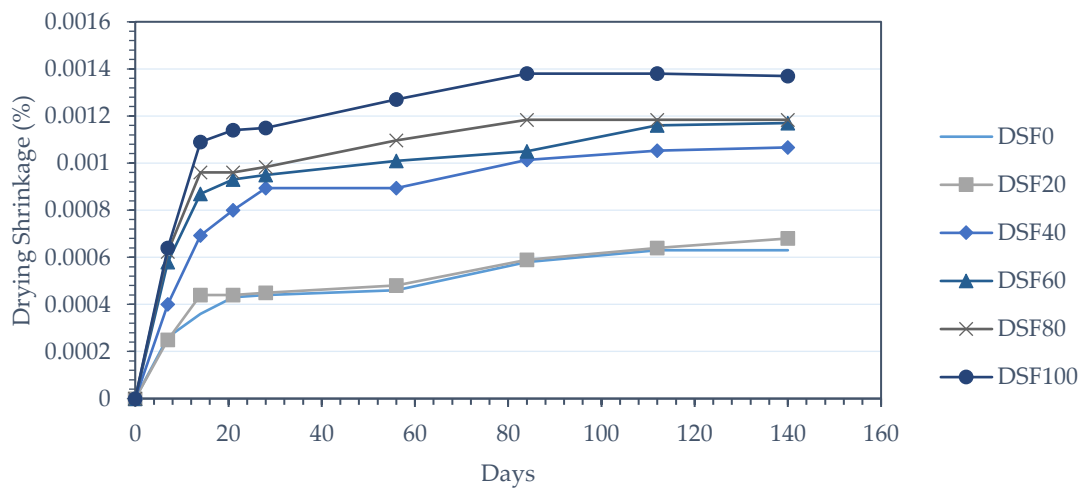


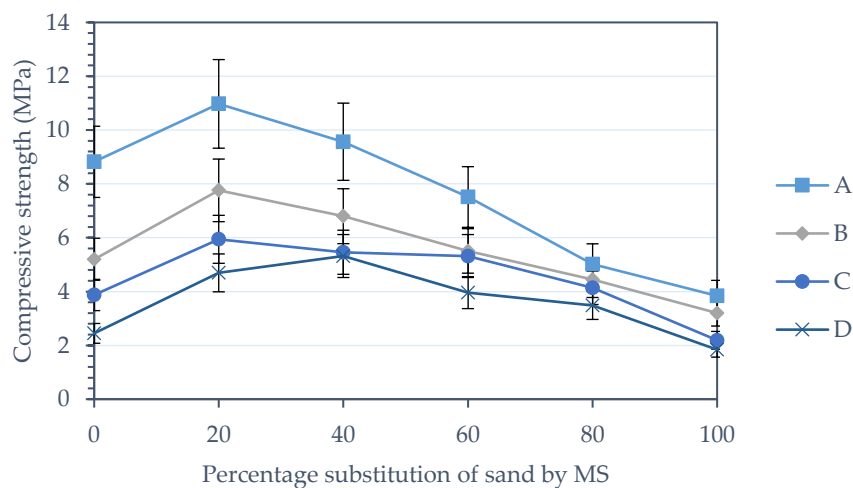
Fig. 4.6: Drying shrinkage of series D (1:6)

For all the mixes, drying shrinkage increased when MS content increased from 0 to 100% substitution. Since, drying shrinkage is a consequence of loss of water from the mortar mixes, marble incorporated mixes have greater water content when compared to their corresponding control counterparts. This might be the reason why their drying shrinkage is greater than the corresponding control mixes. Similar increase in drying shrinkage of mortars was noticed by Bilir et al. (2015) when they used fly ash, which was comparatively fine than the sand it replaced.

However, mixes with 20% substitution of river sand of all mixes have water content lesser than that of corresponding control mixes. This should have made these perform better than the corresponding control mixes. But according to Imamoto and Arai (2007) drying shrinkage is also dependent on aggregates surface area. Therefore, when MS is used to substitute river sand, the positive effect due to reduced water content has been negated by MS's fineness.

#### 4.2.4 Compressive strength

The compressive strength values of mortar mixes after twenty eight days of water curing is plotted graphically in Fig. 4.7. Maximum resistance to compression was exhibited by mixes having 20% substitution of river sand by MS. The increase in compressive strength at this substitution for mixes ASF20, BSF20, CSF20 and DSF20 is 24%, 49%, 53% and 91% when compared to their control mortars ASF0, BSF0, CSF0 and DSF0.



Key to legend: A, B, C and D represent mixes of proportions 1:3, 1:4, 1:5 and 1:6 respectively

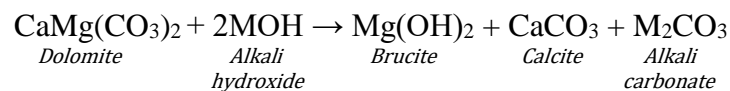
**Fig. 4.7: Twenty eighth day compressive strength of mortar mixes**

The variation in strength across a same series for various sand replacement ratios

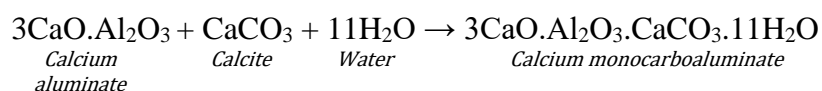
may be because of combination of several factors. Primarily as seen from Fig. 4.1 mixes ASF20, BSF20, CSF20 and DSF20 have lesser water cement ratios than their corresponding control mortars. It is very well understood that for a given cement content, lesser the water cement ratio greater is the strength. Thus this gain in strength is noticed. The subsequent fall in strength of mixes with MS content greater than 20% can hence be justified for the same reason of higher water content in these mixes. However a good number of marble incorporated mixes having same or greater water cement ratio have greater compressive strength when compared to the mortars with only sand.

Apart from reduction in water cement ratio, dolomitic marble is capable of accelerating the hydration reaction of alite as shown by the calorimetric studies conducted by Szybalski and Nocun-Wczelik (2015). This would mean that there is an excess of  $\text{Ca(OH)}_2$  in the cement matrix when compared to mixes without dolomite marble. When there is sufficient quantity of  $\text{Ca(OH)}_2$  present in the matrix, Antiohos and Tsimas (2004) pointed out that solubility of silica of fly ash increases. Hence this might be reason for the enhancement the secondary pozzolanic reaction.

Dolomitic aggregates are unstable in alkaline environments. It has been proved that these aggregates enhance the microstructure of cement matrix by the process of dedolomitization. The chemical reaction taking place between dolomite aggregate and alkalis of cement as given by Beyene et al. (2013) is



Where ‘M’ are alkali elements (lithium, sodium and potassium). Brucite thus formed has a capability to form a Mg-Si-Al complex which is thought to be concentrated near the aggregate – cement boundary resulting in better interlocking and higher compressive strength of the mortar matrix. Such a complex was first traced by Štukovnik et al. (2014) where they studied the mechanism of alkali carbonate reactivity of dolomite based aggregate. On the other hand calcite is capable of reacting with calcium aluminate hydrates to form calcium carboaluminates whose reaction is given by Carlson and Berman (1960)



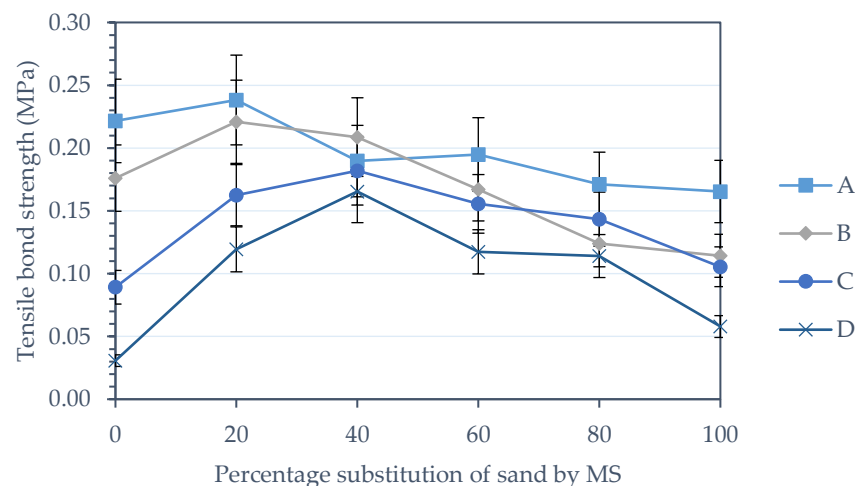
There are other phases that have been reported as well, calcium tricarboaluminate and calcium hemicarboaluminates being common as detected by Trezza and Lavat (2001). These carboaluminates enhance the compressive strength of cement matrix by

retarding/preventing the formation of katoite ( $C_3AH_6$ ) from the other metastable calcium aluminate hydrates.

The strength gain by these reactions is so significant that it overcomes the negative effect of greater water cement ratio in mortar mixes up to 60% substitution of MS as fine aggregate. But when MS is used to substitute more than 60% of sand, the pores formed due to excess of water is sufficient enough to reduce the compressive strength.

#### 4.2.5 Tensile bond strength between brick and mortars

The change in tensile bond strength is similar to the variation seen in compressive strength with increasing proportion of MS in mortars. This variation is plotted in the form of a graph in Fig. 4.8.



Key to legend: A, B, C and D represent mixes of proportions 1:3, 1:4, 1:5 and 1:6 respectively

**Fig. 4.8: Variation of tensile bond strength for all mixes**

For mixes of proportion of 1:3 and 1:4, maximum strength was obtained for mixes ASF20 and BSF20. For lean proportions of 1:5 and 1:6 best performance was obtained at 40% substitution of sand by MS. When MS content was increased beyond 20% for A and B series and 40% for C and D, tensile bond strength reduced. This fall was gradual for series A, while for series B, C and D it was significant. For series A, any substitution greater than 20% had strength lesser than the control mortar, whereas for series B, BSF0 and BSF60 had almost similar strength. Justifiably, for series C and D all mixes with MS have strengths greater than their corresponding control mortars respectively.

According to Venkatarama Reddy and Gupta (2008) the rise and fall of this parameter can be correlated to one controlling parameter: fineness of aggregate. It has been reported that by increasing the fineness of aggregate, tensile bond strength reduces. But

however, for incorporation of 20% MS for series A and B and 40% for series C and D are accompanied by fall in water requirement as compared to corresponding control mortars as seen in Fig. 4.1. Therefore strength of the hydration product plays a dominant role up to these incorporation levels. Hence, incorporating MS which is finer than FS beyond 20% for series A and B and 40% for series C and D can be the reason behind reduction in performance.

#### **4.2.6 Adhesive strength of renderings on substrates**

The variation of adhesive strength of mortars when applied as a rendering on substrates is similar to compressive strength and tensile bond strength. The strength values are tabulated in Table 4.1. Here the type of failure of brick – mortar bond is also noted. As we move from rich to lean mixes, mode of failure changes from failure of mortar to failure at interface. This might be because of insufficient hydration products developed at the interface due to a lower cement content. For a given series, with varying substitution of MS, strength seems to peak out at 20% substitution. Further increase in MS content in mortar mixes reduces the adhesive strength. For series A, B, C and D, comparable strengths are obtained between ASF0, BSF0, CSF0 and DSF0 and ASF40, BSF60, CSF80 and DSF80.

Farinha et al. (2012) had evaluated the effect of ceramic wastes on adhesive strength. They had concluded that ceramic wastes improved the penetration of the hydration products into the substrate and hence at a substitution level of 20% of river sand, improved adhesive performance was achieved (Farinha et al., 2012). Hence here too the performance advantage can be credited to the ability of the hydration products to penetrate in to the bricks. With MS's capacity to accelerate hydration process, the strength gain of the hydration products as well as the mechanical bond between the mortar and brick has improved. Molnar and Manea (2016) have also recorded a 160% increase in adhesive strength to the support layer when calcite marble was substituted in place of 25% of river sand. Adhesive strengths could not be determined for mixes CSF100 and DSF100 mixes because the specimens were damaged during the operation of core cutting or even before the load could be applied.



Table 4.1: Variation of adhesive strength of mixes on substrate

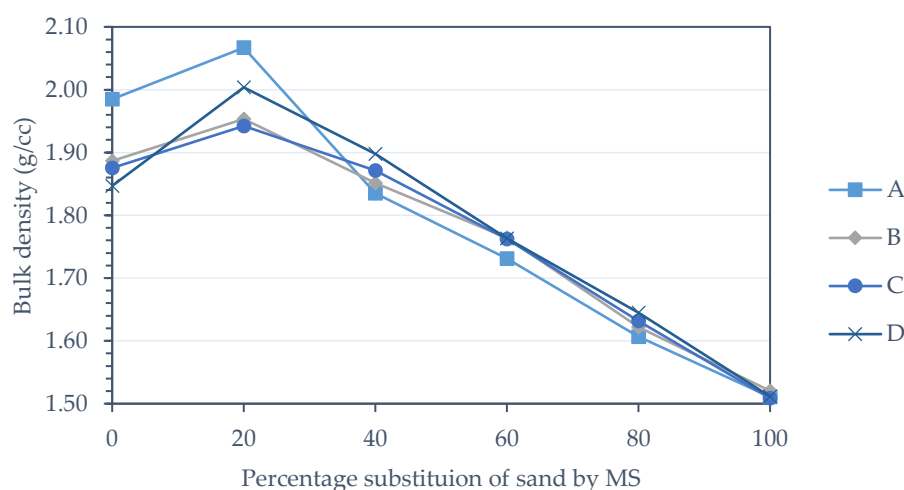
Mix/Substitution	Adhesive strength (MPa)			
	A	B	C	D
0%	0.33	0.16	0.12	0.10
	<i>F</i>	<i>F</i>	<i>E</i>	<i>E</i>
20%	0.46	0.38	0.28	0.20
	<i>F</i>	<i>F</i>	<i>E</i>	<i>E</i>
40%	0.41	0.27	0.20	0.18
	<i>F</i>	<i>E</i>	<i>E</i>	<i>E</i>
60%	0.27	0.26	0.20	0.13
	<i>E</i>	<i>E</i>	<i>E</i>	<i>E</i>
80%	0.26	0.13	0.12	0.09
	<i>F</i>	<i>E</i>	<i>E</i>	<i>E</i>
100%	0.18	0.14	Could not be determined	
	<i>E</i>	<i>E</i>		

E- Adhesive fracture: fracture at the interface of mortar and substrate

F- Cohesive fracture: fracture in the mortar itself

#### 4.2.7 Density, water absorption and porosity

The variations in hardened bulk density and apparent density of mortar mixes due to substitution of sand by MS are graphically represented in Fig. 4.9 and Fig. 4.10 respectively. It can be seen that bulk density (includes volume taken up by permeable voids also) is maximum at 20% substitutions for all mix proportions as predicted by fresh density values shown in Fig. 4.2. This increase in bulk density can be because mortars with this percentage of MS have less water cement ratio. At higher substitutions there is a steady decline of this parameter.

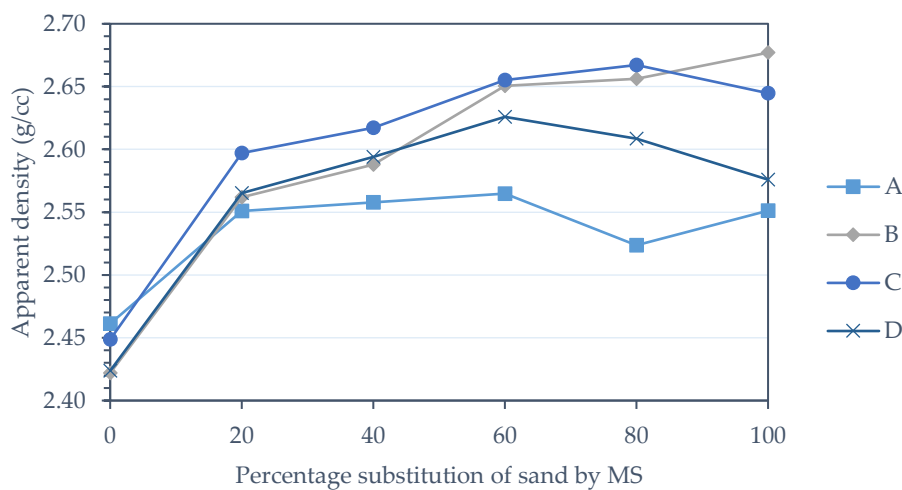


Key to legend: A, B, C and D represent mixes of proportions 1:3, 1:4, 1:5 and 1:6 respectively

Fig. 4.9: Variation of hardened bulk density of mortar mixes

Apparent density (does not include volume taken up by permeable voids) increases

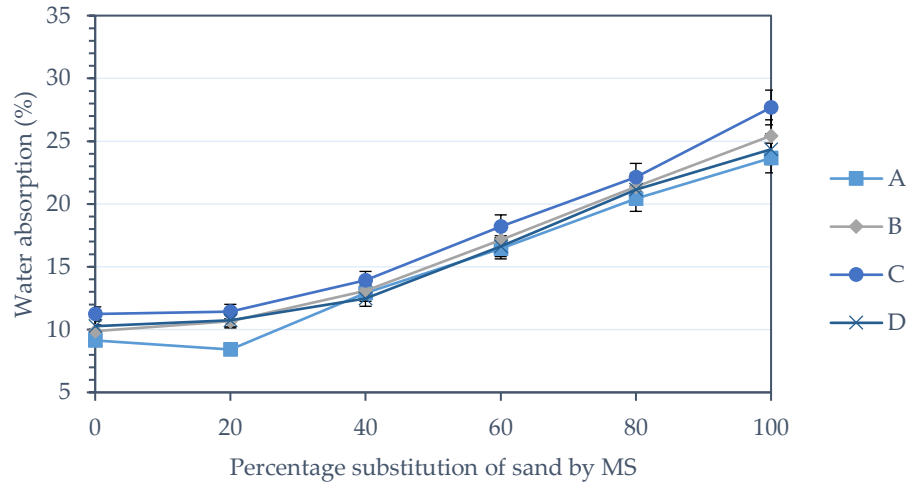
with increase in marble substitution. The extent of rise of apparent density when 20% sand was substituted by MS is between 3% to 6% for all the mixes. Along with reduced water cement ratio at 20% substitution and MS's capacity of accelerating the hydration process, has led to the increase in apparent density. It is understood that failure of a cement composite is initiated by the crack development in the cement matrix. The increase in density of the hydration products has reduced the generation, propagation and connections of cracks when loaded. This could have imparted greater resistance to compression to mixes even at greater water cement ratios as seen in Fig. 4.7. Similar modification to mortars density was noticed when metakaolin was used in mortar preparations which led to the formation of sodium aluminosilicate hydrate as presented by Huseien et al. (2016).



Key to legend: A, B, C and D represent mixes of proportions 1:3, 1:4, 1:5 and 1:6 respectively

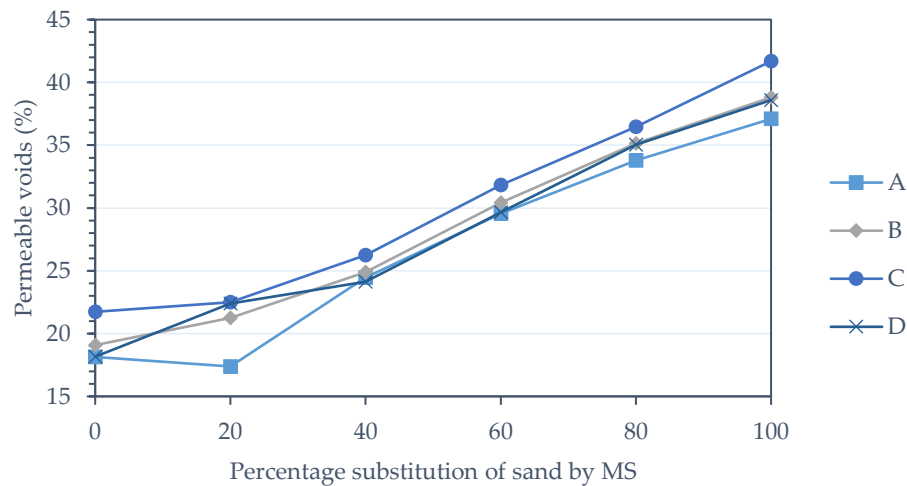
**Fig. 4.10: Variation of apparent density of mortar mixes**

The variation of water absorption and permeable pore space follow the same pattern as seen in the changes of hardened bulk density. These have been graphically represented in Fig. 4.11 and Fig. 4.12. Even at 20% substitution, water absorption is equal or marginally higher than the corresponding control mixes for all series. Primarily this is because of the greater water absorption capacity and fineness of MS than FS. Consequently this has increased the porous volume of mixes.



Key to legend: A, B, C and D represent mixes of proportions 1:3, 1:4, 1:5 and 1:6 respectively

**Fig. 4.11: Variation of water absorption capacity of mortar mixes**



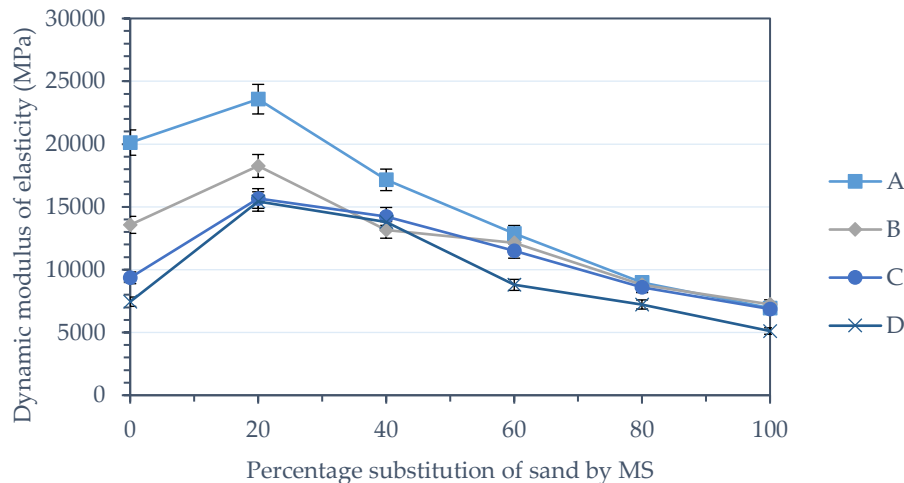
Key to legend: A, B, C and D represent mixes of proportions 1:3, 1:4, 1:5 and 1:6 respectively

**Fig. 4.12: Variation of permeable pores space of mortar mixes**

#### 4.2.8 Dynamic modulus of elasticity

Similar to compressive strength, dynamic modulus of elasticity also attains a peak at 20% substitution of FS by MS as seen in Fig 4.13. At this substitution, increase in elasticity modulus is around 17.1%, 34.6%, 67.6% and 107.1% when compared to ASF0, BSF0, CSF0 and DSF0 mixes respectively. This increase in modulus of elasticity is due to the dolomite MS aggregate which improves load deformation characteristics. Piasta et al. (2017) had also compared the load deformation characteristics of concrete mixes made with aggregates of different geological origins. They concluded that concrete made with dolomite aggregate had the highest modulus of elasticity when compared to mixes made with either granite, basalt or quartzite aggregates. However, for substitution of sand by

dolomite marble waste exceeds 20%, there is a steady fall in this parameter with the minimum value attained for complete substitutions for all series. This fall can be correlated to the increase of porosity of mortars. Because lower the bulk density, lower is the Young's modulus (Wang and Meyer, 2012).



Key to legend: A, B, C and D represent mixes of proportions 1:3, 1:4, 1:5 and 1:6 respectively

**Fig. 4.13: Variation of dynamic modulus of elasticity of mortar mixes**

#### 4.2.9 Microstructure

Since for all the series, the mechanical parameters varied in a similar fashion, microstructure was evaluated only for series A. The four mixes studied with the help of Fourier Transform Infrared (FTIR) spectroscopy are ASF0, ASF20, ASF40 and ASF60 (Fig. 4.14). Of all the observed bands, the discussion worthy change occurs around the wavenumber  $1000\text{ cm}^{-1}$ . Nath et al. (2016) have presented that this peak at the above wavenumber can be assigned to Si-O-Si/Si-O-Al bonds. On addition of marble this wavenumber shifts appreciably, which is  $1010\text{ cm}^{-1}$  for ASF0 reduces to  $1007\text{ cm}^{-1}$  for ASF20 and  $996\text{ cm}^{-1}$  and  $995\text{ cm}^{-1}$  for ASF40 and ASF60 respectively. This reduction in wavenumbers is an indication of increased cross linking of Si-O and Al-O bonds to form C-A-S-H as documented by Chukanov (2014). This better cross linked C-A-S-H network is suggestive of accelerated secondary hydration reaction involving fly ash and portlandite, which has improved mechanical performance of mixes with MS.

Thermogravimetric analysis (TGA) was also conducted on the same four specimens (Fig. 4.15). The weight loss between the temperature range  $100^{\circ}\text{C}$  to  $480^{\circ}\text{C}$  can be considered as the region of decomposition of CSH (along with calcium aluminate hydrates - CAH, monosulphate - Afm and ettringite - Aft). The two regions of  $415^{\circ}\text{C}$  to  $420^{\circ}\text{C}$  and

649°C to 660°C can be considered as the regions of decomposition of CASH. Weight loss occurring between these three temperature ranges is presented in Table 4.3. From this table we can see that the weight loss occurring for mixes with MS are always greater than mix ASF0 across all three temperature ranges. From this we can conclude that extent of hydration is always greater when MS is incorporated in these mixes and hence such mixes have better mechanical properties as shown above.

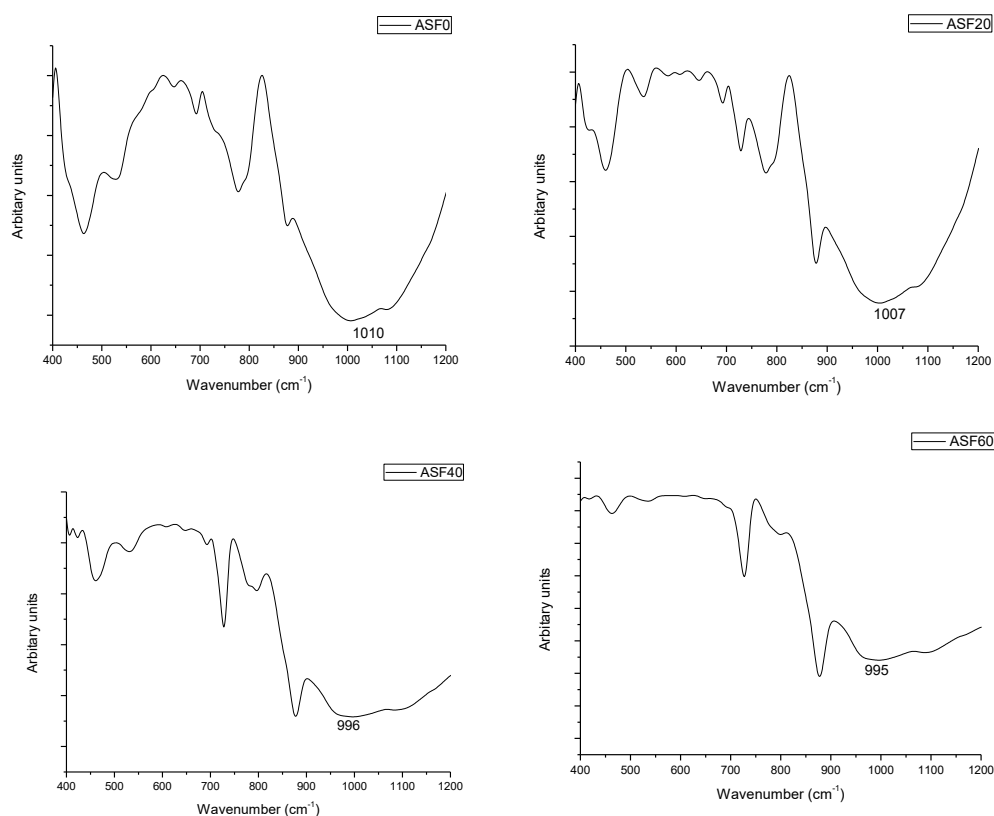


Fig. 4.14: FTIR spectra of mortar mixes ASF0, ASF20, ASF40 and ASF60

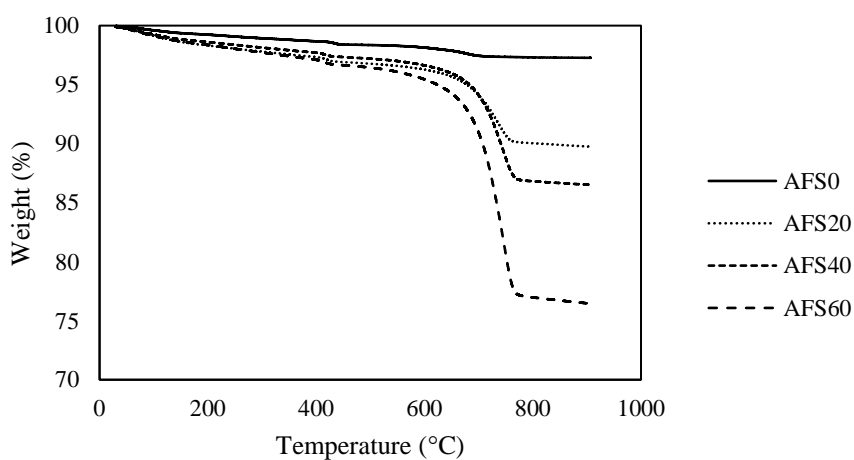


Fig. 4.15: Thermogravimetric analysis (TGA) of mortar mixes ASF0, ASF20, ASF40 and ASF60

Table 4.2: Weight loss (%) of specimens when subjected to heat

Temperature	ASF0 (%)	ASF20 (%)	ASF40 (%)	ASF60 (%)
100°C to 480°C	1.23	2.315	1.989	2.603
415°C to 420°C	0.014	0.077	0.071	0.087
649°C to 660°C	0.078	0.211	0.238	0.423

### 4.3 Usage of Coarse River Sand to Improve Extent of Marble Powder Utilization:

From the above set of experiments it can be concluded that mechanical performance of mixes with 20% MS is comparable to control mortars. The properties that play the most significant role in limiting the utilization potential to this given extent are drying shrinkage and water absorption capacity. The increase in these properties is predominantly due to higher fine content of mortar mixes due to the incorporation of MS. In order to increase the incorporation of MS above 20%, a coarser sand (CS) having fineness modulus of 2.44 was tried. CS was substituted by MS by 10%, 20%, 30%, 40%, 60% and 80% by volume for 1:3 mix proportion. Compressive strength, tensile bond strength, water absorption and drying shrinkage were evaluated for the above mentioned mixes. The results of these parameters are shown graphically in Fig. 4.16 to Fig. 4.19.

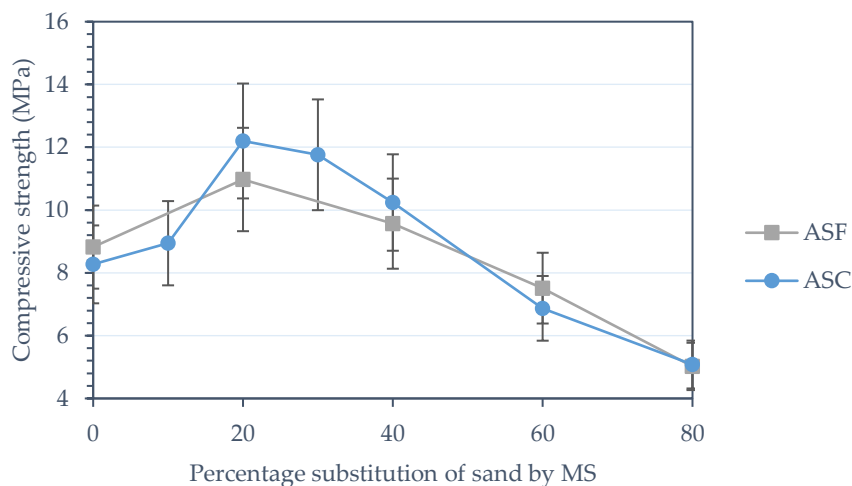
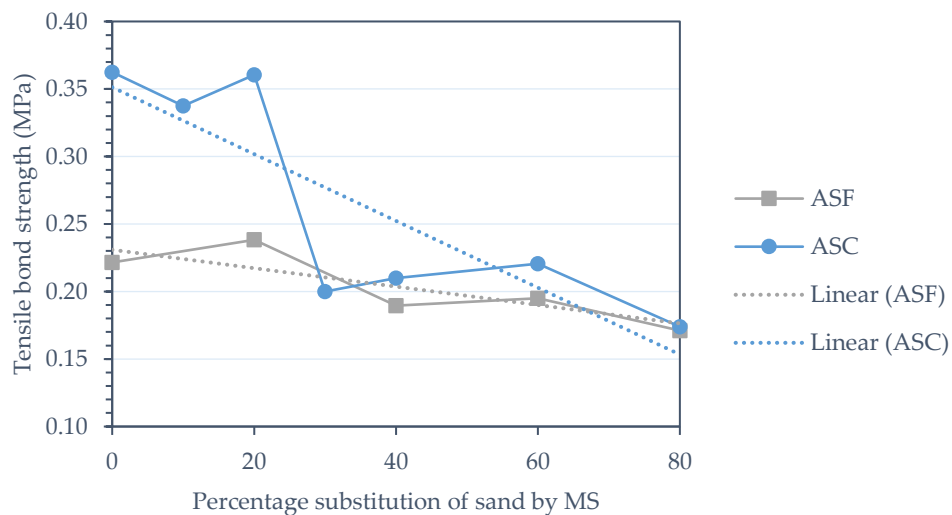


Fig. 4.16: Variation of compressive strength of mixes using CS as fine aggregate

It can be seen that mixes with CS perform marginally better in resisting compressive stresses for 15% - 50% substitution as shown in Fig. 4.16. However, the statistical variation is within 15% for a given percentage substitution of MS for both the series.

Tensile bond strength (Fig. 4.17) has been significantly improved (ASC0 has 64% more strength than ASF0) when CS is used instead of FS for up to 20% incorporation of

MS. ASC20 has 50% more strength than that of ASF20. However, ASC30 has comparable performance with ASF0. As mentioned earlier in section 4.1.5 this improvement in performance for up to 20% substitution of CS by MS is because CS has lesser fine content than FS. With increase in fines, the penetration of the hydration products into the brick substrate is hampered by the penetration of fines itself as presented by Venkatarama Reddy and Gupta (2008). Hence any substitution greater than 20% results in fall in performance of this mechanical property.



**Fig. 4.17: Variation of tensile bond strength of mixes using CS as fine aggregate**

With respect to water absorption capacity, mixes ASC30 and ASC40 absorb 15% and 51% more water than ASF0 (Fig. 4.18), whereas ASF40 absorbs 41% more when compared to the same mix.

The second most significant benefit derived by introducing CS can be seen in the reduction of drying shrinkage for ASC40 when compared to ASF40 as shown in Fig. 4.19. For ASF40 and ASC40, drying shrinkage was 49% and 29% higher than ASF0 at 28 days. At the end of the test period of 140 days, mixes with up to 40% MS undergo lesser drying shrinkage than ASF0. Again, as mentioned earlier, the improvement in this property can be directly linked to reduced fine content in mixes containing CS. Hence by introducing CS, the drying shrinkage has reduced considerably, while compressive strength, water absorption and tensile bond strength remain predominantly unaltered for substitutions greater than 40%. Hence conservatively, the maximum utilization was limited to 40% by volume at this stage for further studies.

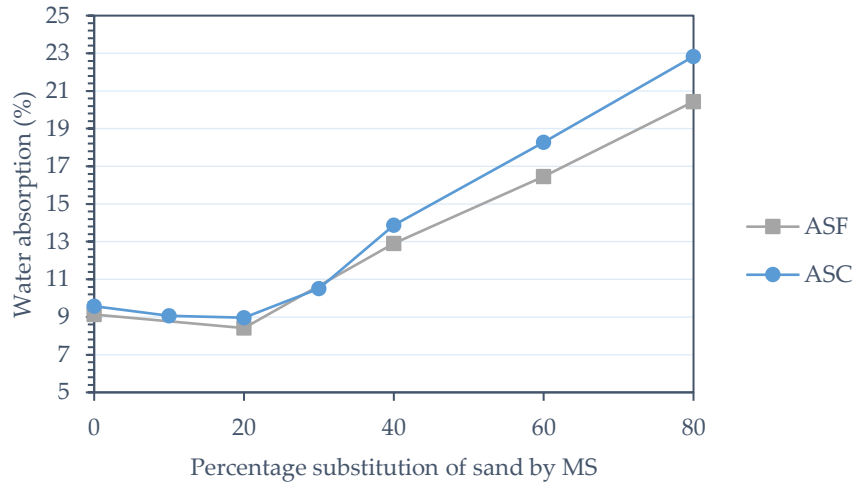


Fig. 4.18: Variation of water absorption capacity of mixes using CS as fine aggregate

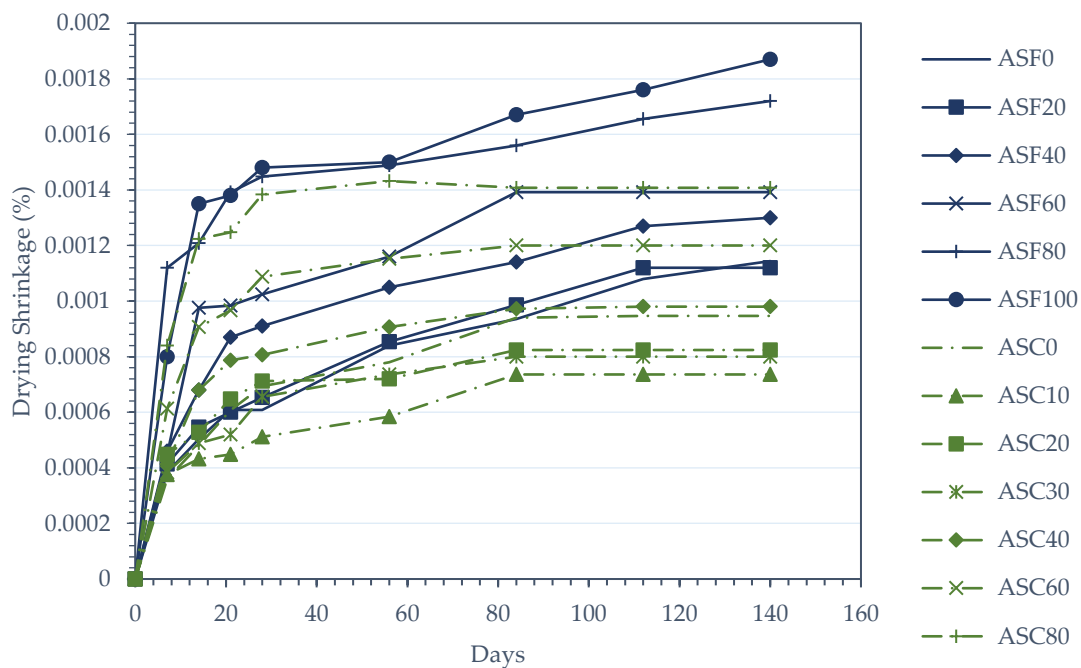
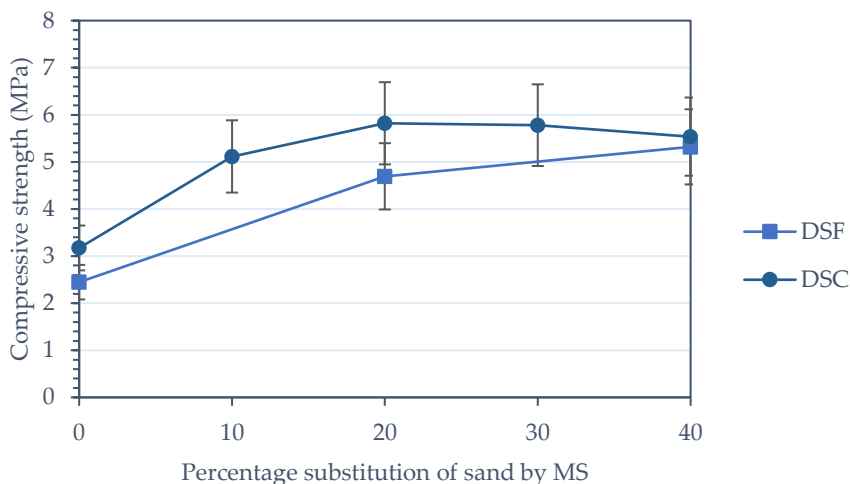


Fig. 4.19: Variation of drying shrinkage of mixes using CS as fine aggregate

Mix proportion of 1:6 was also designed by substituting CS with MS in percentages of 10% to 40% only. On testing, it was noted that compressive strength marginally improved for 1:6 mix proportion also as shown in Fig. 4.20. The variation is higher than 15% between the same substitution levels of 20% MS for the two different sand samples.

The water absorption (Fig. 4.21) tests show that mixes with CS absorb lesser water than mixes with FS. This would imply that a combination of 40% MS with CS has led to reduction of pores due to improved packing, which has also led to the increase in compressive strength to appreciable levels as seen in Fig. 4.20.





**Fig. 4.20: Variation of compressive strength of mixes using CS as fine aggregate**

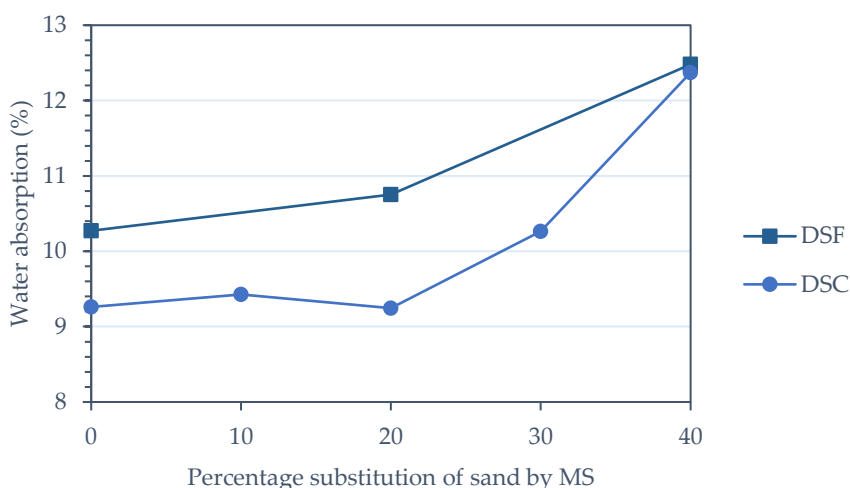


**Fig. 4.21: Variation of water absorption capacity of mixes using CS as fine aggregate**

Bond strength (Fig. 4.22) is maximum for DSC20, and DSC30 performs better than both DSF20 and DSF0. This increase in performance in tensile bond strength can again be credited to reduction in fine content in mortar mixes when CS is used instead of FS as seen in the case of 1:3 mix proportion.

In terms of drying shrinkage (Fig. 4.23), there is no reduction in drying shrinkage on usage of CS instead of FS initially, as noticed in 1:3 proportion. For DSC30, drying shrinkage is 47% more than DSF0 at the end of 28 days. This variation at the end of 140<sup>th</sup> day reduces to 12% only, i.e., drying shrinkage of mixes with CS happens at the early ages of testing itself. This is because FS has higher water absorption capacity than CS, which improves internal curing of these mixes. When water from such mixes undergoes evaporation, the water from the fine aggregate is released in to the cement matrix, hence

compensating the lost water and therefore retarding drying shrinkage to beyond 56 days. Tripathi and Chaudhary (2016) had also reported similar behaviour of concrete mixes when they replaced river sand by porous imperial smelting furnace (ISF) slag.

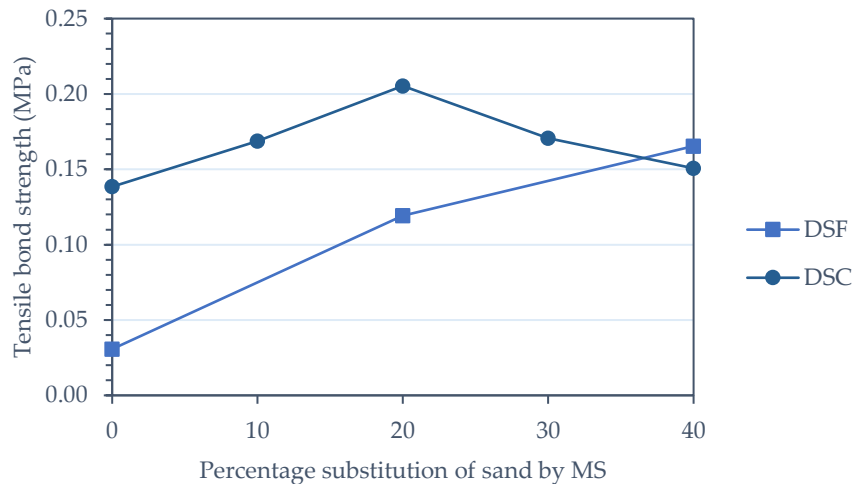


**Fig. 4.22: Variation of tensile bond strength of mixes using CS as fine aggregate**

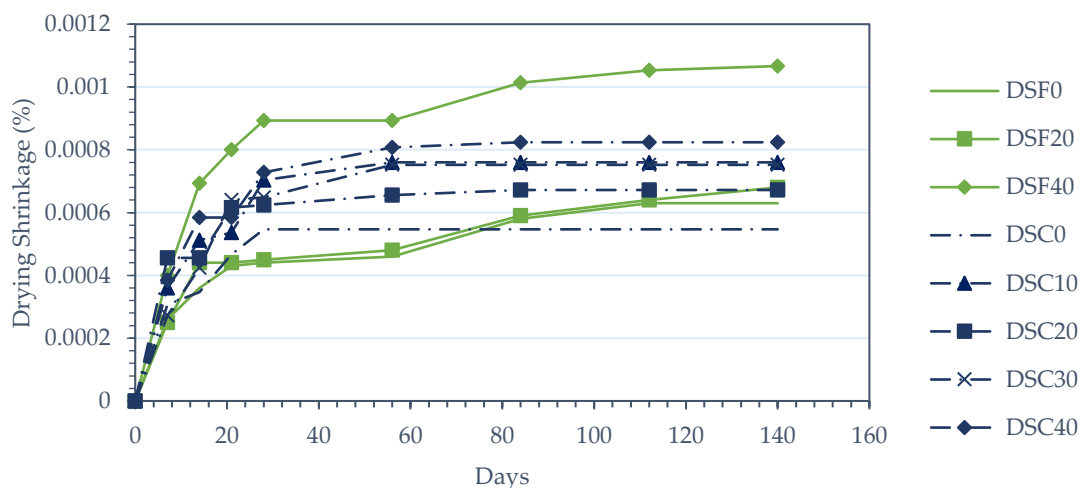


**Fig. 4.23: Variation of drying shrinkage of mixes using CS as fine aggregate**

Hence conservatively considering the above properties for both the mix proportions with CS and FS, the extent of MS utilization was increased to 30% when it is combined with CS and limited to 20% when it is combined with FS. The above mechanical parameters along with permeable voids and dynamic modulus of elasticity have been summarized in Table 4.3 for the following ASF0, ASF20, ASC20 and ASC30 mixes from series A, and DSF0, DSF20, DSC20 and DSC30 mixes from series D. Further durability studies were carried out for the above eight mixes.

Table 4.3: Summary of mechanical properties of mortar mixes

Parameter	Mixes							
	ASF0	ASF20	ASC20	ASC30	DSF0	DSF20	DSC20	DSC30
Water content (w/c)	0.9	0.85	0.85	0.93	1.8	1.51	1.51	1.52
Compressive strength (MPa)	8.82	10.97	12.2	11.76	2.45	4.69	5.82	5.78
Tensile bond strength (MPa)	0.22	0.24	0.36	0.2	0.03	0.12	0.21	0.17
Ultimate drying shrinkage ( $\times 10^{-4}\%$ )	11.4	11.2	8.24	8	6.3	6.8	6.72	7.52
Water absorption (%)	9.14	8.41	8.97	10.52	10.27	10.75	9.25	10.26
Permeable voids (%)	18.14	17.38	18.72	21.34	18.16	22.39	19.01	21.08
Apparent density (g/cc)	2.46	2.55	2.57	2.58	2.42	2.57	2.54	2.6
Dynamic modulus of Elasticity (GPa)	20.11	23.57	24.72	22.27	7.45	15.4	16.97	16.02

#### 4.4 Evaluation of Tensile and Capillary Water Absorption Characteristics:

The above mentioned eight mortar mixes were evaluated for their direct tensile and flexural strengths and their capacity to absorb water by capillary action. Microstructure of the four mixes of series A was also studied using FTIR, X – ray diffraction (XRD) and field emission scanning electron microscope (FESEM). The results of the these tests are presented in the following sections.

##### 4.4.1 Flexural and tensile strength

The variation of flexural strength is shown graphically in the Fig. 4.24. Mixes in series A show a gradual decline in resistance with inclusion of MS with ASC30 mix having the least resistance. The reduction in performance is little greater than 16%. This is despite the fact that mixes with MS have higher compressive strength than the control mortar. This anomaly in this series can be because of alteration in distribution of stresses when flexural strength and compressive strength are compared. A similar relation between compressive and flexural strength was observed by Štukovnik et al. (2014) when they studied the strength development pattern of mortars made with limestone aggregates. Mixes with MS tend to undergo same or slightly higher drying shrinkage even when these mixes have lesser water content. This higher shrinking tendency might have produced micro-cracks in the mortar matrix. These cracks connect more rapidly when in tension than in compression as explained by P. Kumar and Monteiro (2015).

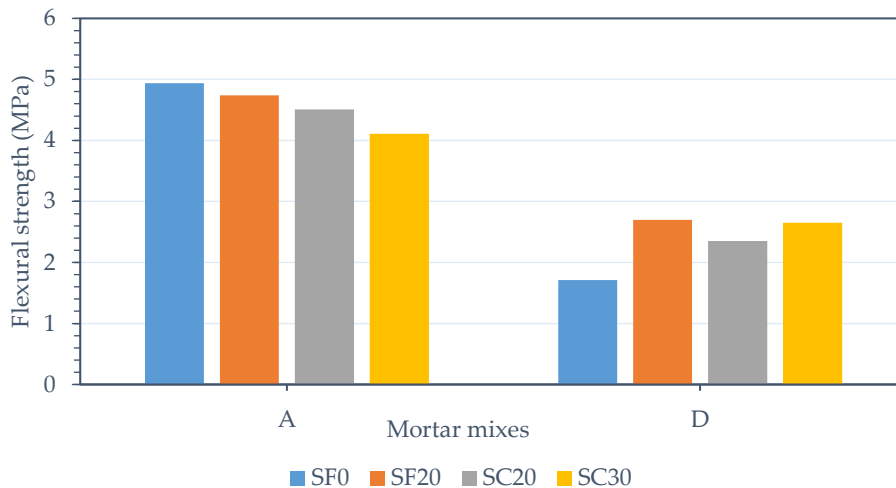


**Fig. 4.24: Variation of flexural strength of mortar mixes with increase in percentage of MS**

Farinha et al. (2012) had used sanitary waste for replacement of fine aggregate for the production of mortars. As the curing period progressed, they had encountered reduction in tensile capacities of such mortar mixes when compared to conventional mortars. They too had reasoned out that, presence of microcracks must have resulted in the decline of this mechanical property. However for series D, mixes with MS have greater resistance to tensile strength when compared to control mortar. The variation ranges between 35% to 58%. This increase in tensile capacity is primarily due to water content which is less by 16% when compared to control mortar with the inclusion of MS. The negative micro-cracking developed due to drying shrinkage might have been undone by the sufficient densification of the cement matrix by the above two reasons.

The variation of tensile strength of all mixes is shown in Fig. 4.25. As seen from this figure, the variation of this mechanical parameter is not significant for the rich mix of proportion of 1:3. Whereas for the series D, there is increase in performance as seen in compressive strength values. The same reason of presence of micro-cracks even before loading as discussed in the variation of flexural strength holds good here too.

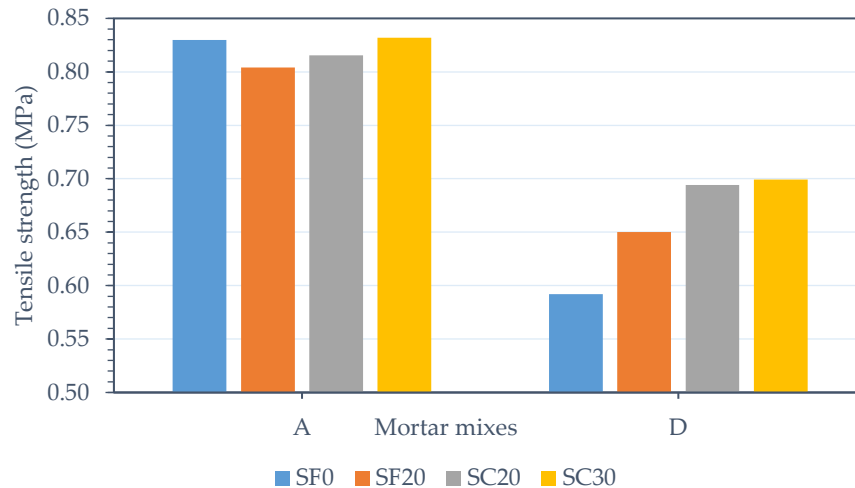


Fig. 4.25: Variation of tensile strength of mortar mixes with increase in percentage of MS

#### 4.4.2 Capillary water absorption

Water absorption by capillary action of mortar mixes is shown in Fig. 4.26 and Fig. 4.27 for series A and D, respectively. For both the series it can be said that, water absorption capacity varies with time. However at the end of 24 hours, the hierarchy obtained in terms of water absorption capacity (by capillary action) matches with that of the variation obtained by immersion tests (Table 4.3).

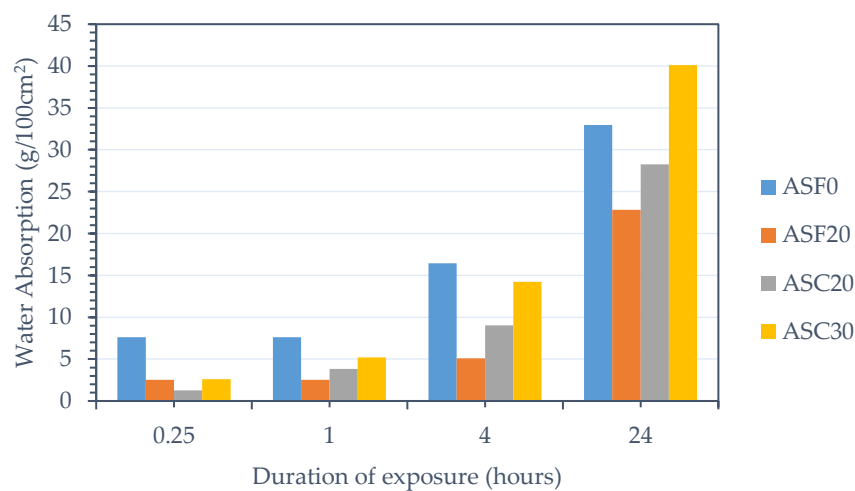
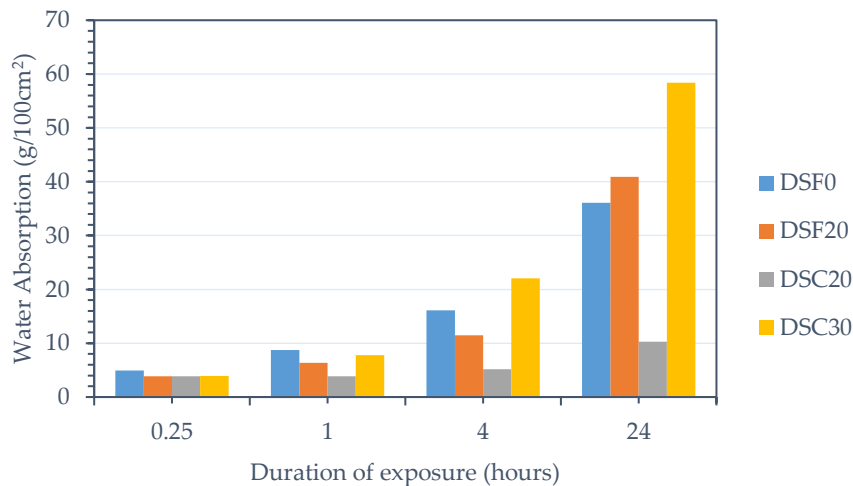


Fig. 4.26: Variation of capillary water absorption of mortar mixes with increase in percentage of MS for series A

The variation of water absorption capacity among mixes might be due to the modification of the composite particle size distribution involving sand and cement, by the inclusion of MS. This helps in filling pores in the case of ASF20, ASC20 and DSC20. But however in the case of ASC30, DSF20 and DSC30, presence of excess fines might have

negatively affected the combined grading and has increased the void content of these mortar mixes. To some degree, Khodabakhshian et al. (2018a) have sketched similar behaviour of concrete mixes with MS and silica fume. They stated that additional or enhanced pozzolanic reactions lead to pore refinement and not reduction in total porosity, which implies that ultimate water absorption might be same for mixes with different compressive strengths also.



**Fig. 4.27: Variation of capillary water absorption of mortar mixes with increase in percentage of MS for series D**

#### **4.4.3 Scanning electron microscopy**

To confirm the formation of CSH and CASH detected using FTIR and TGA, scanning electron microscopy (SEM) was also used. SEM with chemical mapping was carried out for mixes ASF0 (Fig. 4.28) and ASC30 (Fig. 4.29), which helped detect the presence of a dense gismondine zeolite. Tang et al. (2016) have postulated that this zeolite is formed due to the reaction between fly ash and CSH, CAH or Ca(OH)<sub>2</sub>. For ASC30, in addition to the formation of gismondine, magnesium ions appear to be spread across the entire microstructure. This can be because of dissolution of dolomite aggregate in the alkaline environment of the cement hydration products.

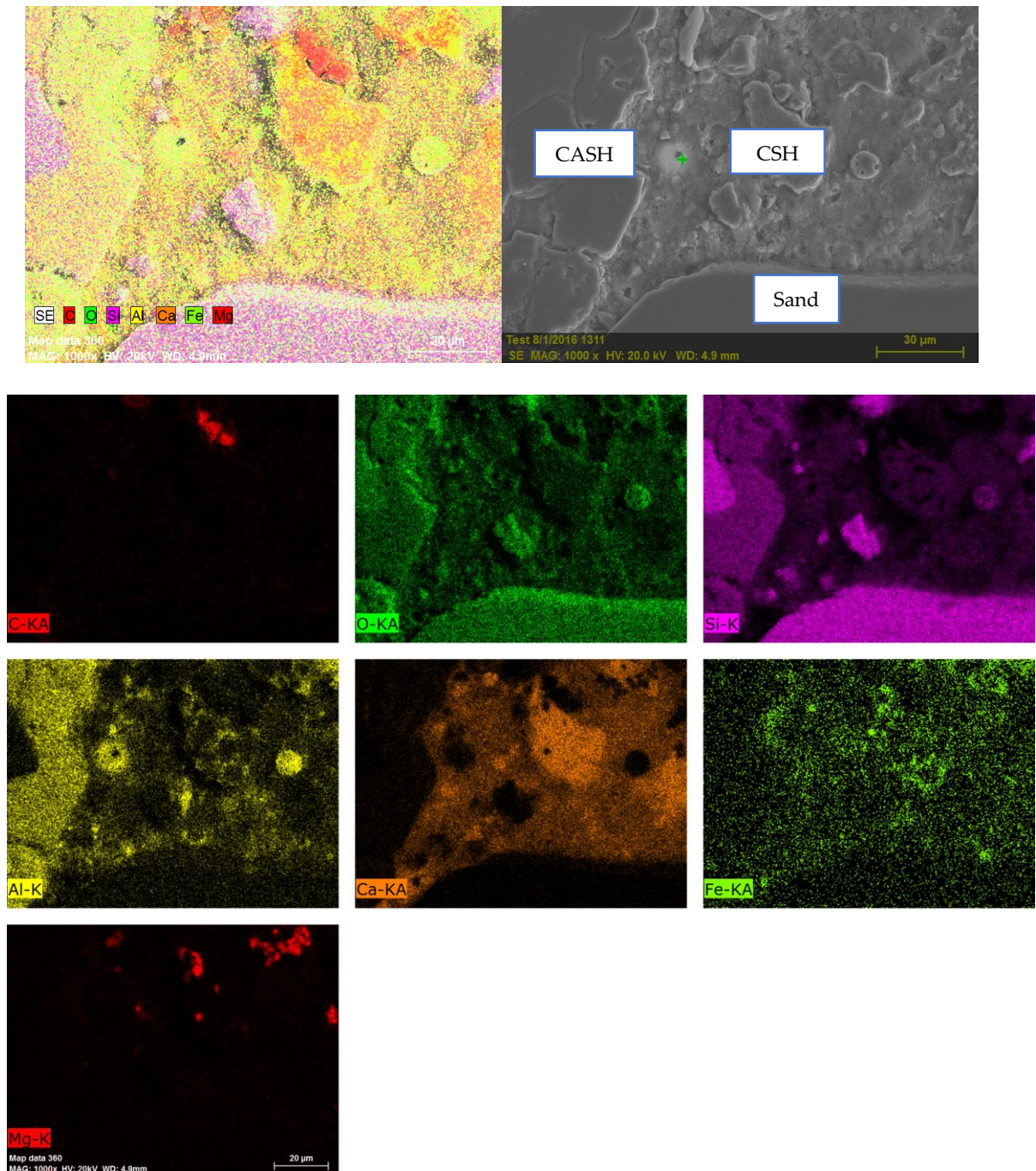


Fig. 4.28: Elemental mapping of mortar mix ASF0

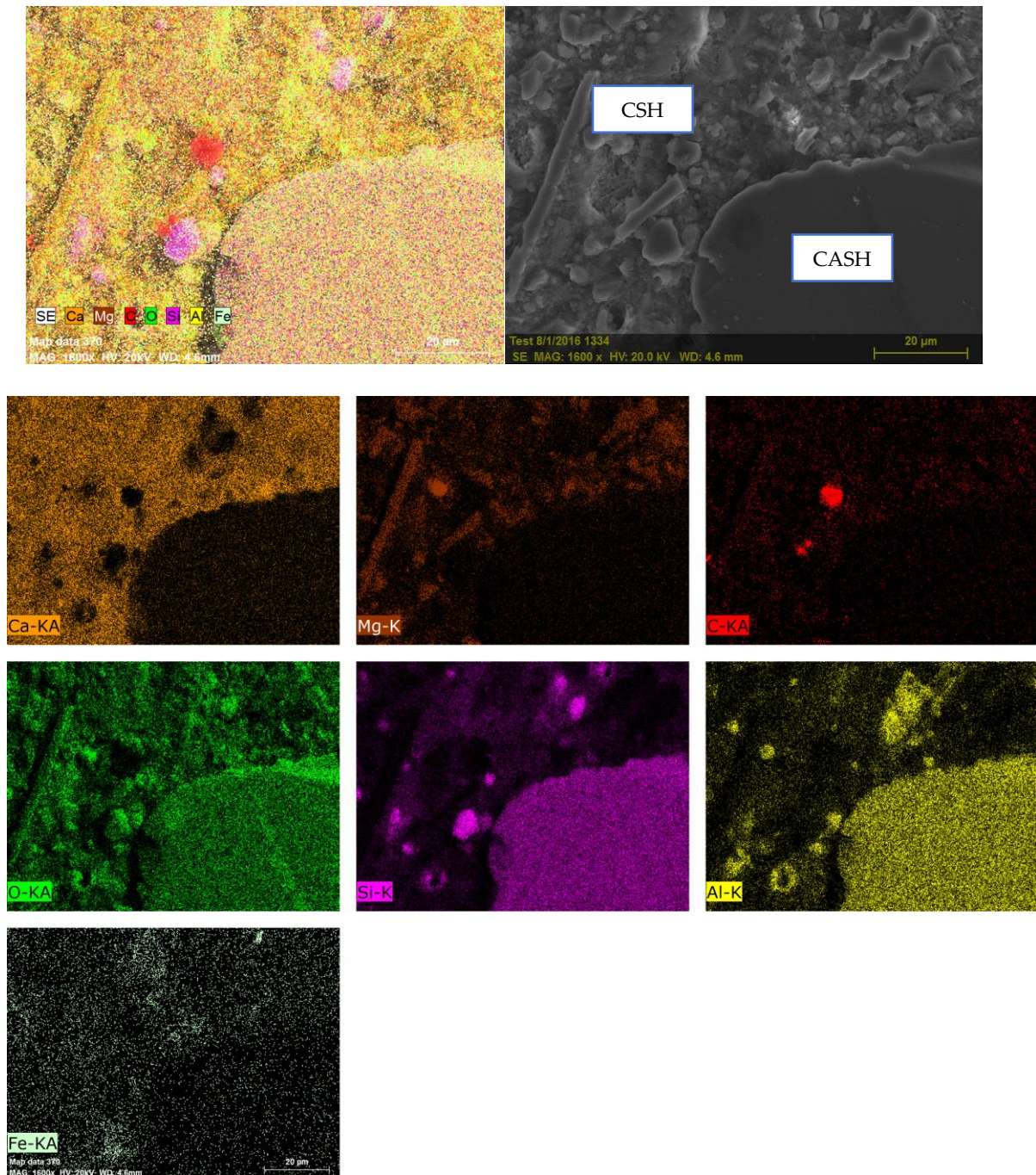


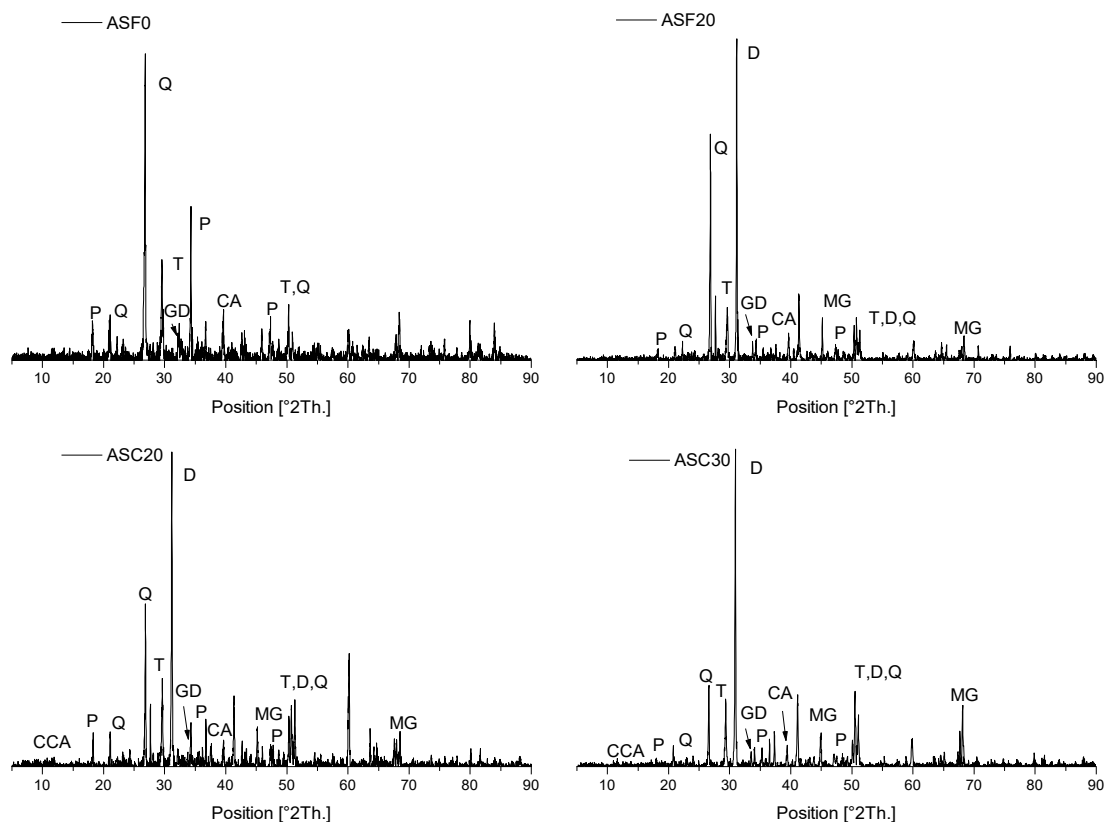
Fig. 4.29: Elemental mapping of mortar mix ASC30

#### 4.4.4 X-ray Diffraction Analysis and Fourier transform infrared spectroscopy

X-ray diffraction analysis was carried out to identify the mineral compounds that could not be traced using FTIR, SEM – EDAX and TGA methods. The XRD patterns for the four mixes ASF0, ASF20, ASC20 and ASC30 are shown in Fig. 4.30. From the XRD plots the following points can be noted. Firstly, the major peaks of CSH occur at  $29.36^\circ$  and  $50.08^\circ$ . Gismondine (CASH) can be detected by the presence of a peak at  $33.24^\circ$ . Major



peaks of quartz from river sand can be assigned to  $21.09^\circ$  and  $26.8^\circ$ . Calcium aluminate hydrate (CAH – katoite) was identified by the peak at an angle of  $39.58^\circ$ . Presence of Portlandite can be identified by the peaks at  $18.26^\circ$ ,  $34^\circ$  and  $47.14^\circ$  as listed by Tang et al. (2016). From the intensity of these peaks it can be seen that, portlandite content appears to be less in mixes with MS when compared to the control mortar. This is an indication that secondary pozzolanic reaction has taken place to a better extent, thereby consuming the portlandite for the formation of gismondine.



CCA – Calcium mono-carboaluminate; P – Portlandite; GD – CASH; Q – Quartz; T – CSH; D – Dolomite; CA – Calcium aluminate hydrate; MG – Mg-Si-Al complex

**Fig. 4.30: X-Ray diffractograms of mixes ASF0, ASF20, ASC20 and ASC30**

In addition to the above compounds, mixes with MS were detected to have additional minerals in their mortar matrix. With regard to formation of calcium carbo-aluminates, peaks at a diffraction angle of  $11.67^\circ$  were noticed for mixes ASC20 and ASC30, which is indicative of the formation of calcium monocarbo-aluminate. Luz and Pandolfelli (2012) studied the effect of inclusion of calcium carbonate on the hydration of calcium aluminate cements and detected a peak at the same angle of diffraction. The presence of the complex involving Mg-Al-Si was noticed in the form of the mineral

magnesiostauroelite (Barthelmy, 2003) which had characteristic peaks at angles around  $45^\circ$ ,  $67.6^\circ$  and  $37.5^\circ$ . Apart from the higher quantity of hydration products (as noticed with the help of FTIR and TGA) these two additional compounds can be the reason behind the improved mechanical performance of mixes with MS.

The FTIR plots of ASF0 and ASF20 were already discussed in section 4.1.9. For the remaining two mixes ASC20 and ASC30 the FTIR plot is given in Fig. 4.31. Similar differences are noted for these two mixes also. According to Chukanov (2014), the peak  $1010\text{ cm}^{-1}$  for ASF0 is due to the polymerization of Si-O-Si and Si-O-Al (asymmetric stretching vibration) to form CSH and CASH. This is reduced to  $1006\text{ cm}^{-1}$  and  $1004\text{ cm}^{-1}$  for ASC20 and ASC30 respectively indicating substitution of Si by Al ions.

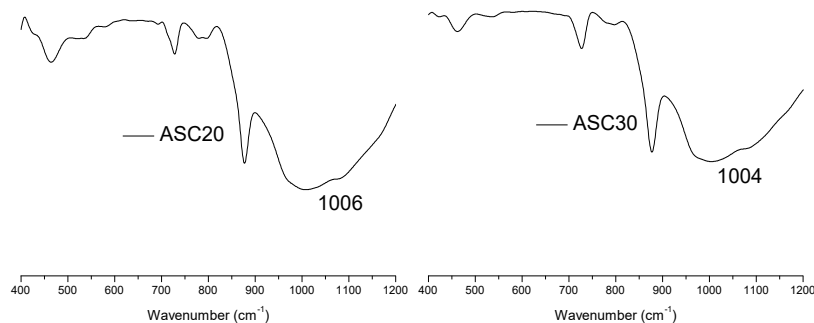


Fig. 4.31: FTIR spectrum of two mixes ASC20 and ASC30

## 4.5 Performance Evaluation of Mortar Mixes when Exposed to Aggressive Environments:

The following section presents the results of tests performed on mortars samples after exposing them to different aggressive environments. The results obtained from the mechanical and physical tests have been supplemented with data obtained from microstructural studies wherever necessary.

### 4.5.1 Salt crystallization

The variation of weight of mortar mixes after 15 cycles of salt crystallization is shown in Fig. 4.32 for series A and D. At the end of the cycles, mixes from the series A have undergone the least weight change. The marginal increase in weight is due to accumulation of sodium sulphate crystals in the pore network. There is no noteworthy change in appearance also (Fig. 4.33 a)) However significant weight loss was noted for the mixes DSF20 and DSC30 of series D. The salt formation has developed internal tensile

stresses, which has led to the rupture resulting in loss of material. This might be because these mixes have the highest water absorption capacity in their series (Table 4.3). For the other two mixes, the loss in mortar material is not greater than the accumulation of salt inside. The appearance has changed for all the four mixes of this series, significantly for mixes with MS (Fig. 4.33 b)), with DSF20 showing maximum damage and DSF0 showing the least.

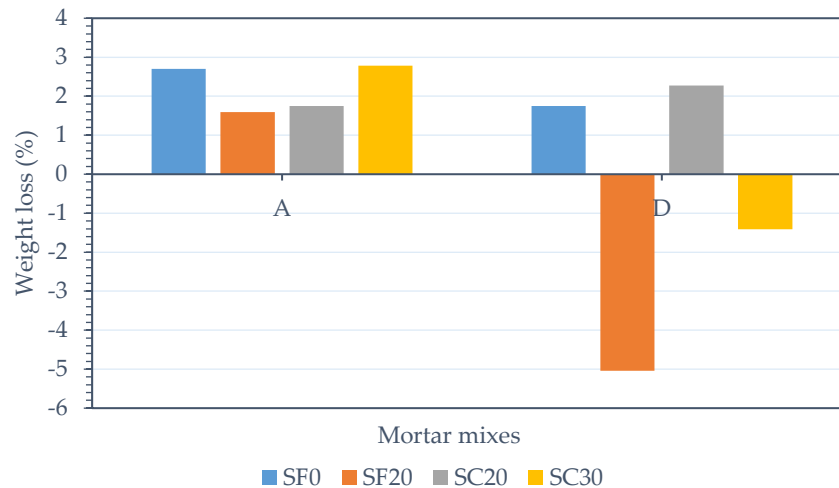


**Fig. 4.32: Change in weight of samples when subjected to cycles of salt crystallization**

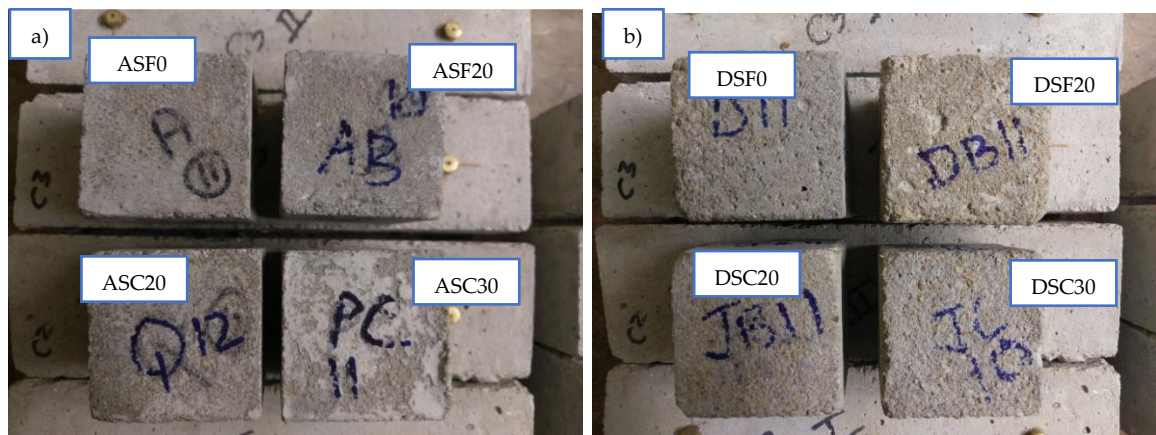


**Fig. 4.33: Appearance of samples of series a) A and b) D when subjected to cycles of salt crystallization**

Water absorption capacity of the mortar mixes after the salt crystallization cycles is shown in Fig. 4.34 for series A and D. The benefit the mixes ASF20 and ASC20 had of absorbing lesser water is lost after the salt crystallization test. This is indicative of the fact that these mixes have lost their water tightness. In case of series D, mixes with MS did not

sustain the internal stresses developed when they were being evaluated for capillary water action, such that they cracked and collapsed after 4 hours of exposure duration.

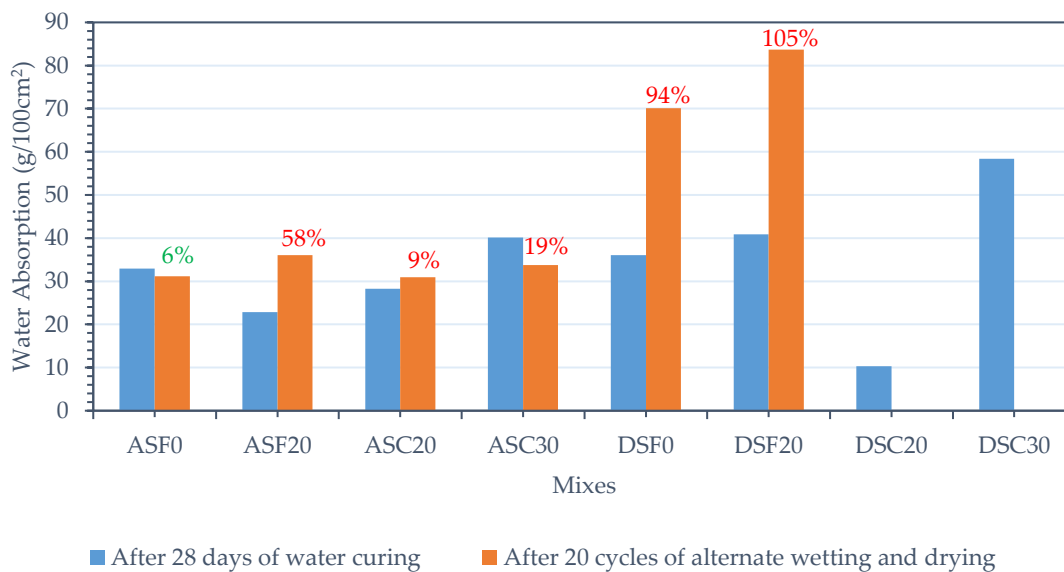


**Fig. 4.34: Variation of capillary water absorption after the salt crystallization cycles for series A**

Such a rupture is due to the expansion of thenardite crystals and thereby converting into mirabilite on absorbing water which impart these internal tensile stresses. Mixes with MS are also stiffer (as indicated by the dynamic modulus of elasticity shown in Table 4.3) than mortar made with only river sand. With such increased stiffness, the capacity to undergo elastic deformation is reduced and when the tensile stresses developed are more than tensile capacity, rupture occurs. Clearly in the series D, MS addition had led to loss of weight by excessive rupture of material during the cycles or immediately after it due to the above reasons.

From the analysis of variation in compressive strength after conducting the salt crystallization tests (Fig. 4.35), mix ASF20 had undergone greatest change in compressive strength. It has increased by 33%, whereas the other three mixes have undergone a change in resistance to the tune of 17% to 23% for series A. The increase in mechanical performance for series A is primarily due to the filling of pores by the absorbed salt i.e. crystallized salt is not in sufficient quantity to impart internal stresses for rupture. For series D, mixes with combination of sand with MS had no residual compressive strength at all, while the other sole mix DSF0 showed a gain of 1.6%.

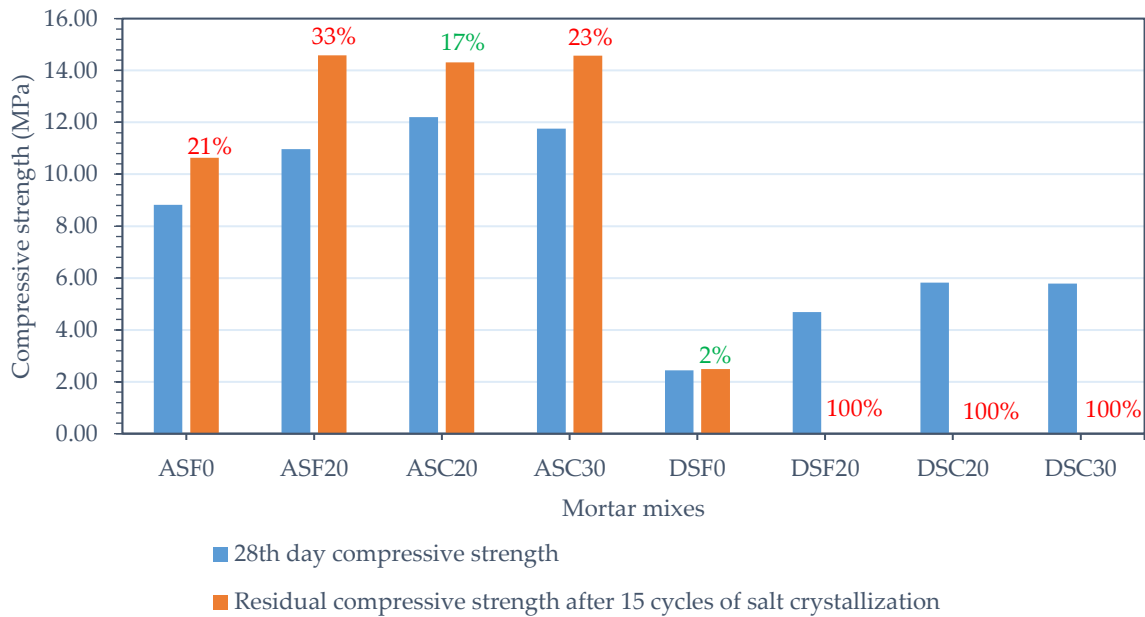


**Fig. 4.35: Compressive strength of mortar mixes when subjected to cycles of salt crystallization**

On examining the SEM images (Fig 4.36 a), b), c) and d)) of samples after the salt crystallization showed the microstructure has changed from being compact to cloudy for all the four mixes. This appearance is similar to the damage caused by sodium sulphate solution to mortars tested by Aye et al. (2010). There was no significant difference in the damage caused by the crystallization among the four mixes, indicating salt crystallization is not as severe for rich mixes with MS than on lean mixes. The presence of both elongated thenardite (Fig. 4.36 f)) and prismatic glauberite (Fig. 4.36 e)) crystals were also detected.

The FTIR spectra (Fig. 4.37) of the mixes after salt crystallization showed a reduction in wavenumber at around  $1010\text{ cm}^{-1}$ . For all the four mixes this band drops to around  $990\text{ cm}^{-1}$ . This might be because of continuous hydration of cement clinker on continuous exposure to water. But however due to the growth of sodium sulphate crystals inside the mortar matrix has led to the decline of mechanical performance. These crystals can be identified by the creation of the bands at  $620\text{ cm}^{-1}$  and  $1102\text{ cm}^{-1}$  in all the four mixes shown in the same figure.

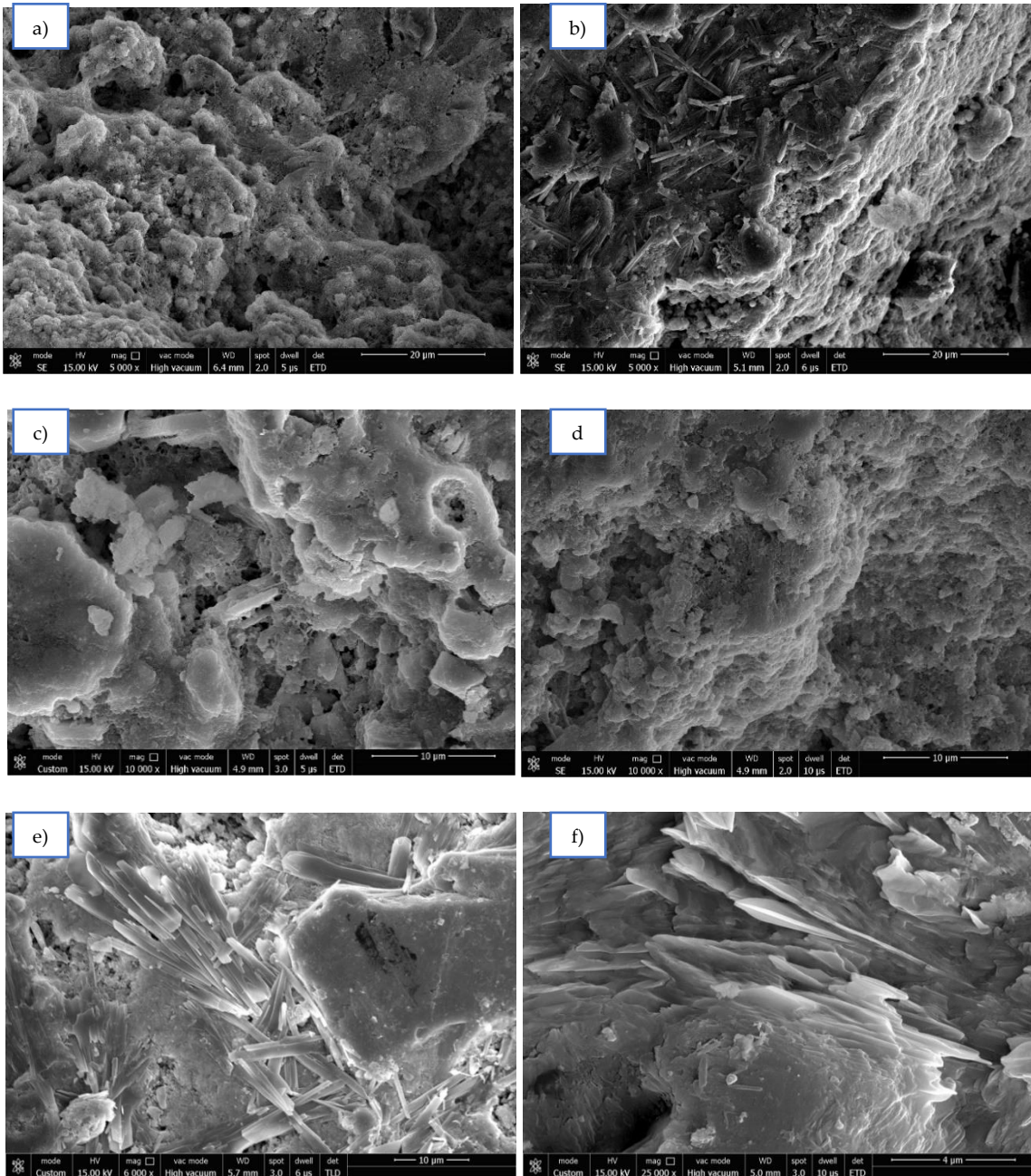


**Fig. 4.36: Scanning electron micrographs of a) ASF0, b) ASF20, c) ASC20 and d) ASC30 after salt crystallization cycles, e) glauberite and f) thenardite crystals**

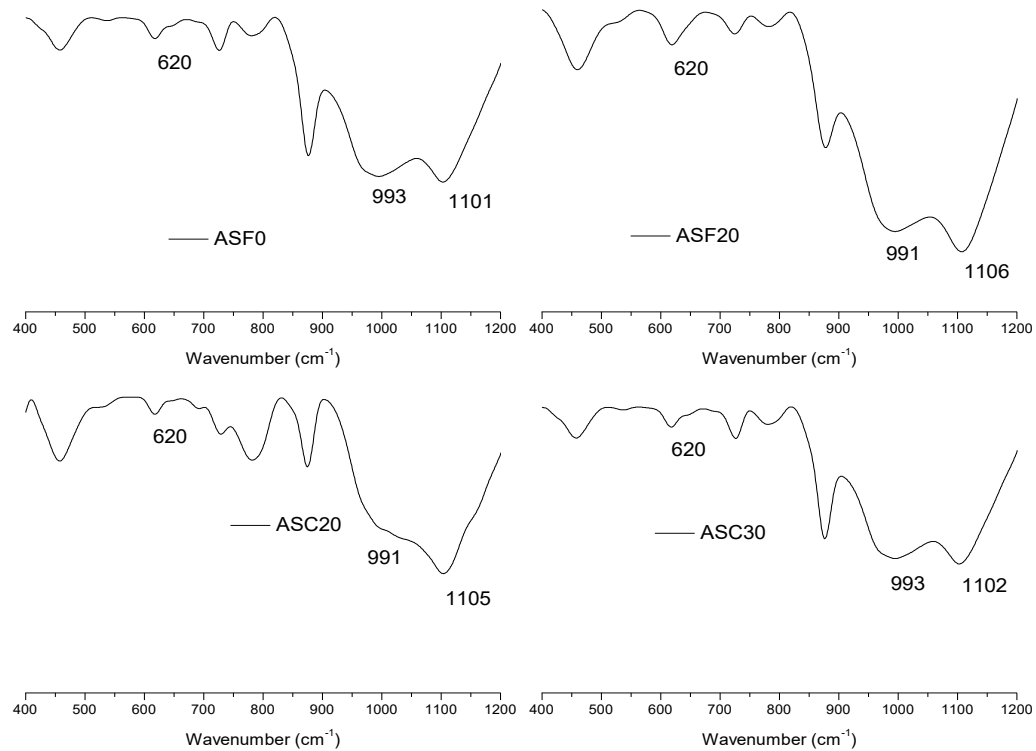


**Fig. 4.37: FTIR spectra of mortar mixes after salt crystallization cycles**

#### 4.5.2 Wet – dry cycles

Mortar samples were exposed to 20 cycles of alternate wetting and drying. Each cycle consisted of soaking the samples in water for six hours and then followed by drying in an oven for 18 hours. After completion of the cycles, change in performance of the mortar mixes was gauged in terms of appearance, compressive strength, water absorption and loss of weight. Results of this test are discussed below.

Change in weight of samples subjected to alternate cycles of wetting and drying are given in Fig. 4.38 for series A (1:3) and D (1:6). Weight loss at the end of the test was most significant for ASF20 at 7.7% whereas for other mixes ASF0, ASC20 and ASC30 it was 5.7%, 6.1% and 6% respectively. For series D, the control mortar showed the most significant damage, recording a loss of weight by around 6.4% whereas mix DSC20 showed the least variation at 4.6%. These variations of weight loss among all mixes of both the series can be considered insignificant.

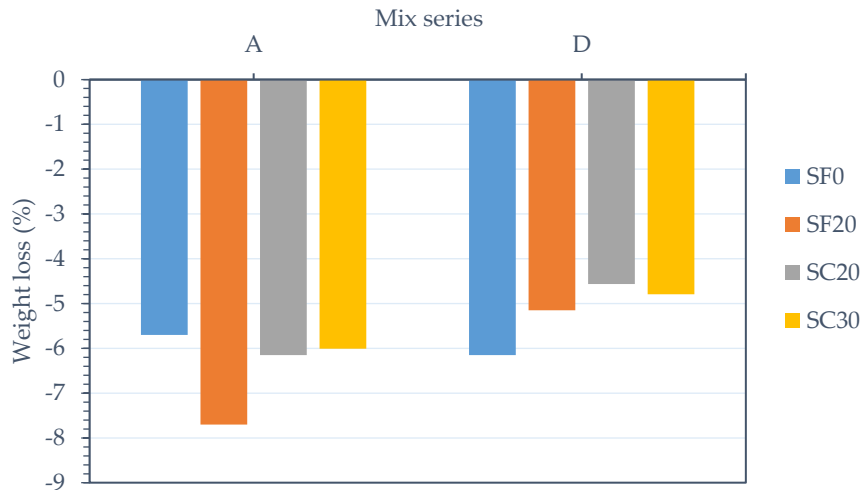


Fig. 4.38: Change in weight of samples when subjected to wet – dry cycles

The appearance of mortar samples of series A and D after the wetting and drying cycles is shown in Fig. 4.39 a) and b) respectively. Here for series A, the samples showed no or very minimal hair line cracking. For series D, DSF0 and DSF20 showed slight chipping of surface layers. DSC20 and DSC30 exhibited no significant change.

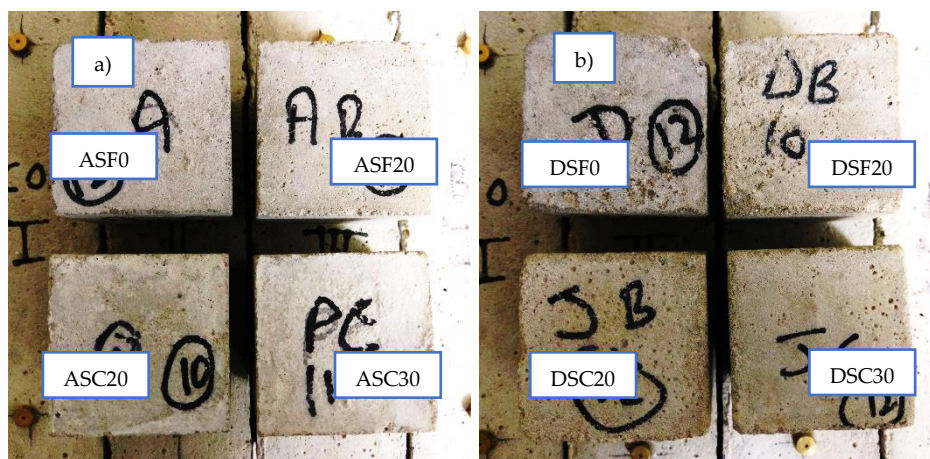
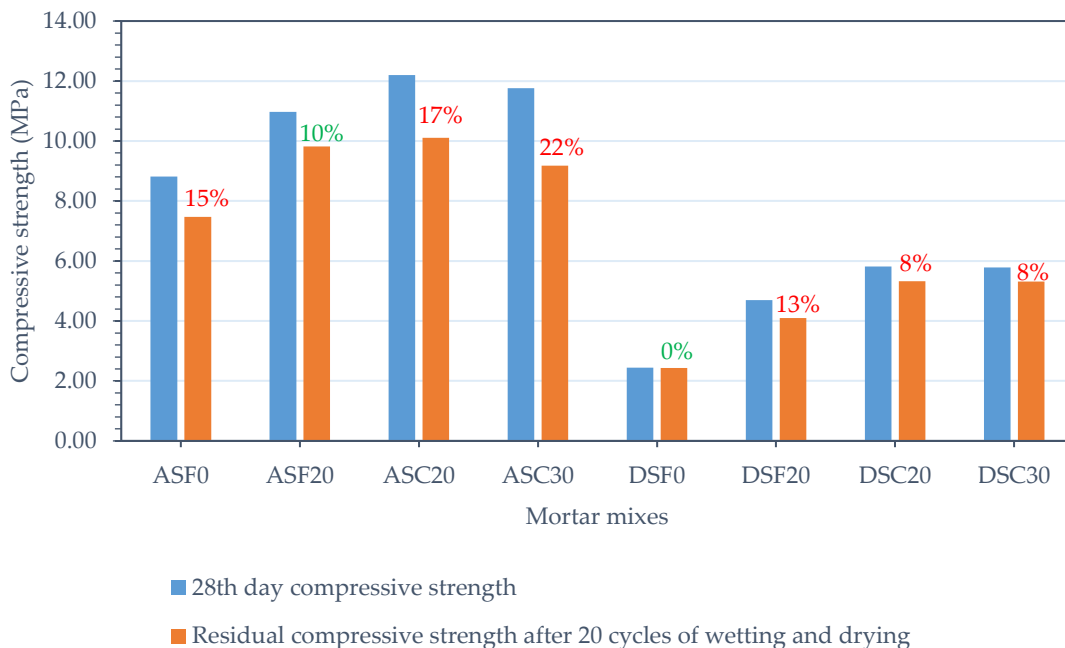


Fig. 4.39: Appearance of samples of series a) A and b) D when subjected to wet – dry cycles

With regard to compressive resistance (Fig. 4.40) ASF20 displayed the least decline in performance (10%), whereas the other three mixes showed a fall in performance ranging between 12% to 22%. For series D, control mix virtually did not undergo any change in this parameter. But mixes DSC30 and DSF20 had lost strength by 8%, while mix DSC20 showed a fall of 13%. From the above variations it can be said that, mixes with highest initial porosity (as shown in Table 4.3) have shown the highest decline in compressive strength. The fall in performance is because of the mortars cracking up on cycles of heating and cooling in water, due to the increase in tensile stresses. This allows more water to



penetrate deeper and aggravate the damage further. However for all the mixes with MS, the residual compressive strength is still greater than the corresponding control mixes.



**Fig. 4.40: Compressive strength of mortar mixes when subjected to wet – dry cycles**

The extent of water absorbed by capillary action after alternate wetting and drying cycles by the mixes is shown in Fig. 4.41 for series A and D. For mix ASF0 of series A, no change in this parameter was noted. But for mixes with MS, for both the series, water absorption capacity had significantly gone up. Maximum variation was seen for mixes (ASF20 and DSC30) which had the least initial porosity in their corresponding series. As seen in the results of salt crystallization tests, these drastic reductions in performance can be related to the high stiffness values of the mortar mixes with MS.

From the micrographs as shown in Fig. 4.42 for series A, there was considerable damage to microstructure to the mixes ASC20 and ASC30. The control mortar without any MS showed very negligible damage. The initial water tightness of ASF0 and better elastic deformation characteristics when compared to stiffer MS incorporated mortars might have reduced its susceptibility to damage as experienced by the other three mixes.

The FTIR plot of these mixes is shown in Fig. 4.43. The band at  $1000\text{ cm}^{-1}$  has reduced to a lower wavenumber as seen in salt crystallization tests.



■ After 28 days of water curing    ■ After 20 cycles of alternate wetting and drying

**Fig. 4.41: Variation of capillary water absorption after wetting and drying cycles**

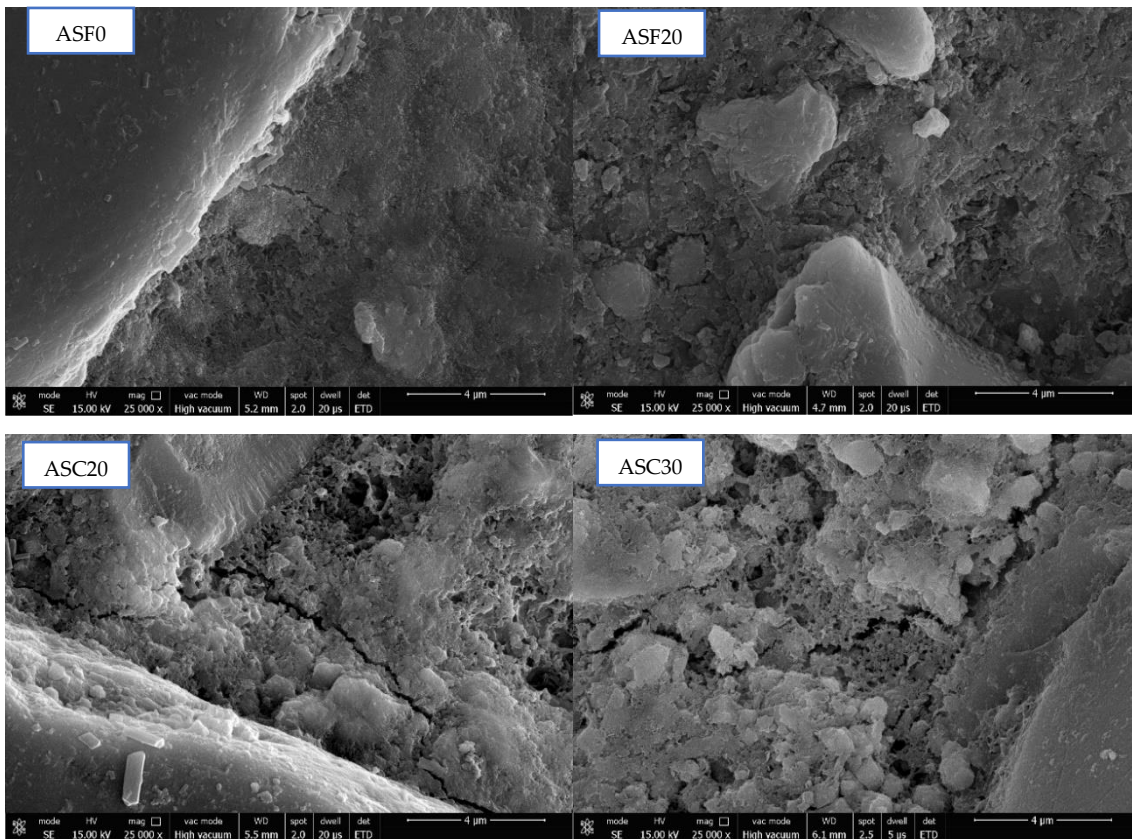


**Fig. 4.42: Scanning electron micrographs of mixes of series A after wet – dry cycles**

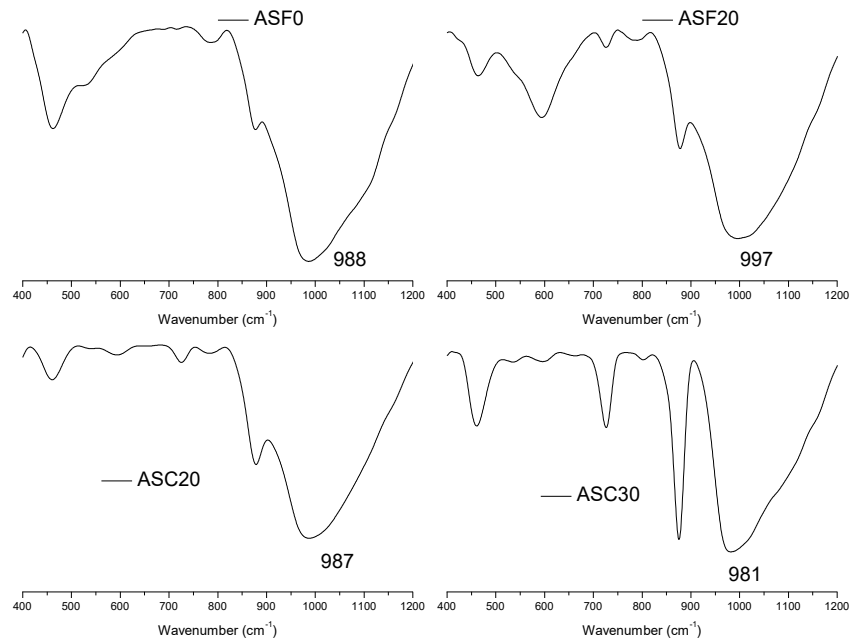


**Fig. 4.43: FTIR spectra of mortar mixes of series A after wet – dry cycles**

### **4.5.3 Rapid freezing and thawing:**

Mortar samples were subjected to 20, 50 and 100 cycles of rapid freezing and thawing. Each cycle constituted of 6 hours during which, samples were frozen to  $-18^{\circ}\text{C}$  and then thawed to  $4^{\circ}\text{C}$  in succession. Change in performance of these mortar mixes was assessed in terms of appearance, change in length and weight and compressive strength. The results of the above test are discussed below.

The change in compressive strength of mixes of series A, when subjected to 20, 50 and 100 cycles of rapid freezing and thawing is shown in Fig. 4.44. From this figure, it can be seen that resistance to compression of mix ASF0 remained predominantly unchanged (4%) until the end of the test regime. But however mixes ASF20 and ASC20 showed reduction in strength by 18% and 24% respectively after 100 cycles. This reduction in performance might be due the increased stiffness of these mixes by 18% and 24% respectively when compared to ASF0. Their tensile strength capacity is also slightly less than that of control mortars as seen in section 4.2.1. These two mixes had also undergone the highest permanent deformation, measured in the form of length change on mortar bars as shown in Fig. 4.45. The loss in weight (Fig. 4.46) of these mixes is also about 1% higher than that of control mortar.

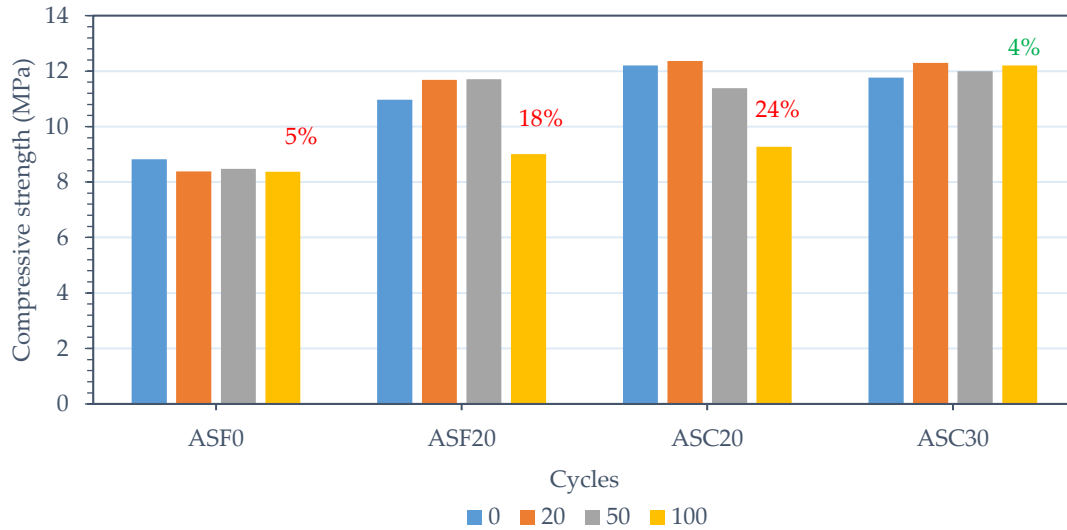


**Fig. 4.44: Variation of compressive strength of mortar mixes of series A after rapid freezing and thawing**

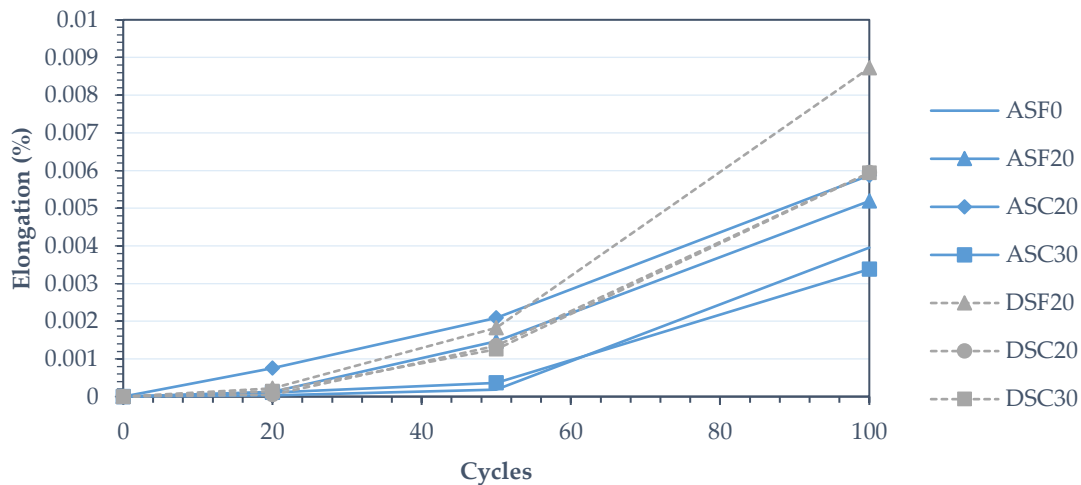


**Fig. 4.45: Change in length undergone by mixes after rapid freezing and thawing**

However for mix ASC30 no significant change after the completion of 100 cycles as seen in Fig. 4.44. The deviation in performance of this mix when compared to the other two mixes with MS can be because of increased porosity. As seen from earlier sections (Table 4.3), mix ASC30 had the highest porosity at 21% when compared to the 18% of ASF0. This excess porosity seems to provide an extra cushion for the freezing water and hence reduces the tensile stresses developed internally. The other two mixes, ASF20 and ASC20 had porosity of 17% and 19% respectively. Apart from this, mix ASC30 is the least stiff mix with MS (as mentioned in table 4.3).



**Fig. 4.46: Extent of weight loss suffered by mortar mixes of series A after rapid freezing and thawing**

The appearance of the mortar mixes after 100 cycles of rapid freezing and thawing is shown in Fig. 4.47. Mortars with maximum marble content in their corresponding series appear to have suffered maximum surface scaling due to pop-outs. Such a surface disintegration is a consequence of greater water absorption capacity of MS which results in more water freezing in its pores, leading to failure. These pop-outs have led to highest loss in weight of mix ASC30 at 13%. Bogas et al. (2015) had also encountered similar disintegration of mortar samples made with recycled aggregates when they were subjected to rapid freezing and thawing.



**Fig. 4.47: Change in appearance of mortar mixes of series a) A and b) D after rapid freezing and thawing**

As seen in Fig. 4.48, for series D also, the mix with the highest MS content, DSC30 has recorded the highest loss of weight of about 21% at the end of 100 cycles when compared to weight loss (12%) of the control mix. From visual inspection (Fig. 4.47) this mix can be clearly delineated from the other three mixes of the series D due to excessive pop outs. This weight loss has significantly affected the residual compressive strength of mix DSC30 which has shown a fall of 25% as seen in Fig. 4.49. DSF0, DSF20 and DSC20 have shown a fall of 18%, 21% and 41% respectively. As in the case of series A, this fall in compressive strength of the mixes with MS can be directly related to their initial void content and stiffness as shown in Table 4.3.

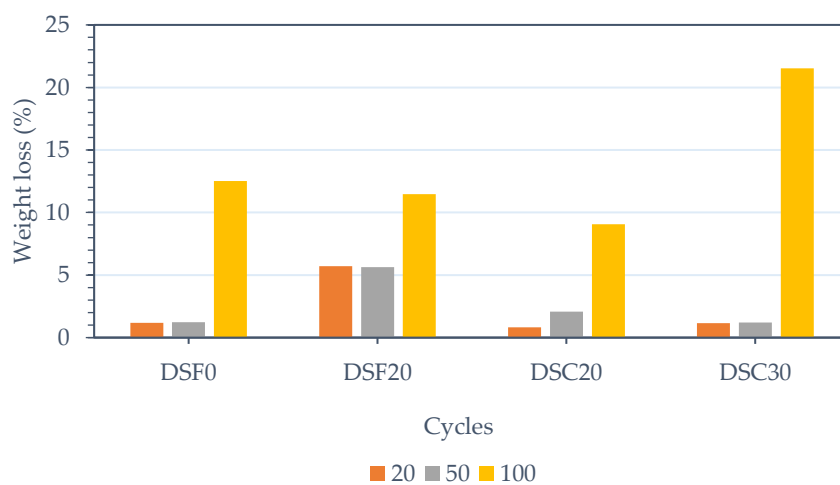


**Fig. 4.48: Extent of weight loss suffered by mortar mixes of series D after rapid freezing and thawing**

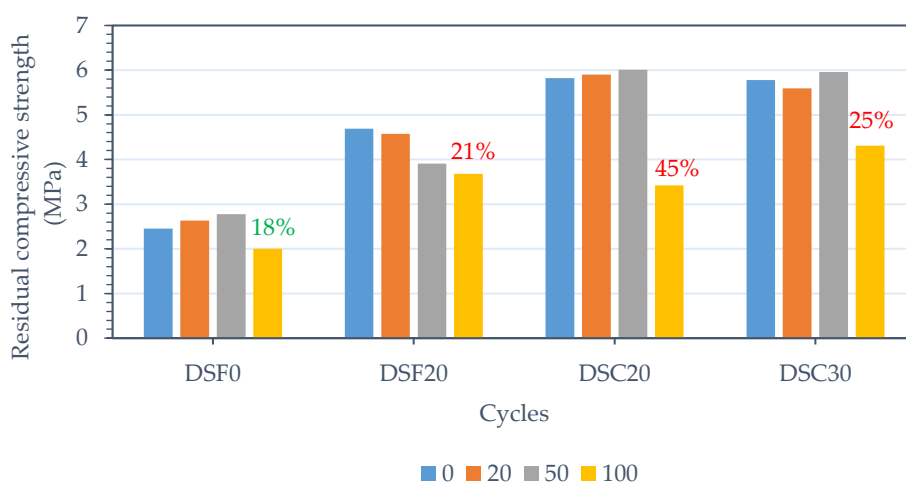


**Fig. 4.49: Change in compressive strength of mortar mixes of series D after rapid freezing and thawing**

The FTIR plot of the four mixes of series A is shown in Fig. 4.50. The band that represents the polymerization of Si-O-Si/Si-O-Al chain which initially was seen around  $1010\text{ cm}^{-1}$  has reduced to around  $991\text{ cm}^{-1}$  for mixes ASF0, ASF20 and ASC20 and to  $998\text{ cm}^{-1}$  for mix ASC30. A similar pattern in variation of FTIR spectrum was obtained after performing salt crystallization and wet - dry cycles.

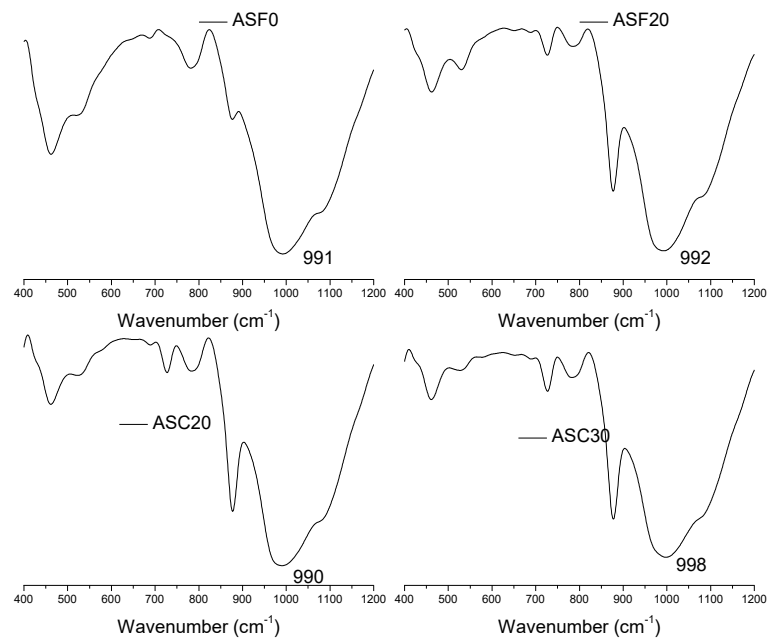


**Fig. 4.50: FTIR spectra of mortar mixes of series A after rapid freezing and thawing**

Keleştemur et al., (2014b) have also evaluated marble dust incorporated cemented mortars' resistance to freeze and thaw. Because marble dust was finer than the sand it was used to replace, resulted in reduction of porosity. Hence these mixes performed adversely after 30 cycles of rapid and freezing and thawing.

#### **4.5.4 Exposure to fire:**

Before exposing to fire, all the samples were oven dried at a temperature of  $60^{\circ}\text{C}$  for 48 hours. The test specimens were then subjected to standard fire in a furnace. The temperature of exposure was in the range of  $200^{\circ}\text{C}$  to  $800^{\circ}\text{C}$ . The rate of increase in temperature of fire in this furnace followed the standard fire curve as given in ISO 834. The change in compressive strength and loss of weight of the samples when subjected to the above temperature ranges is detailed in the following paragraphs.

The variation of compressive strength of mortars of series A when subjected to the action of fire is shown in Fig. 4.51. From this figure it can be seen that, when the samples

were heated to a temperature of 200°C, compressive strength increased by 46% to 97% in comparison to results of specimens at room temperature. Presence of free water in moist samples creates a disjoining pressure which reduces the van der Waals' forces of attraction between CSH. Hence on drying or heating, this free water is released which leads to the improvement in performance as noticed here (P. Kumar and Monteiro, 2015).

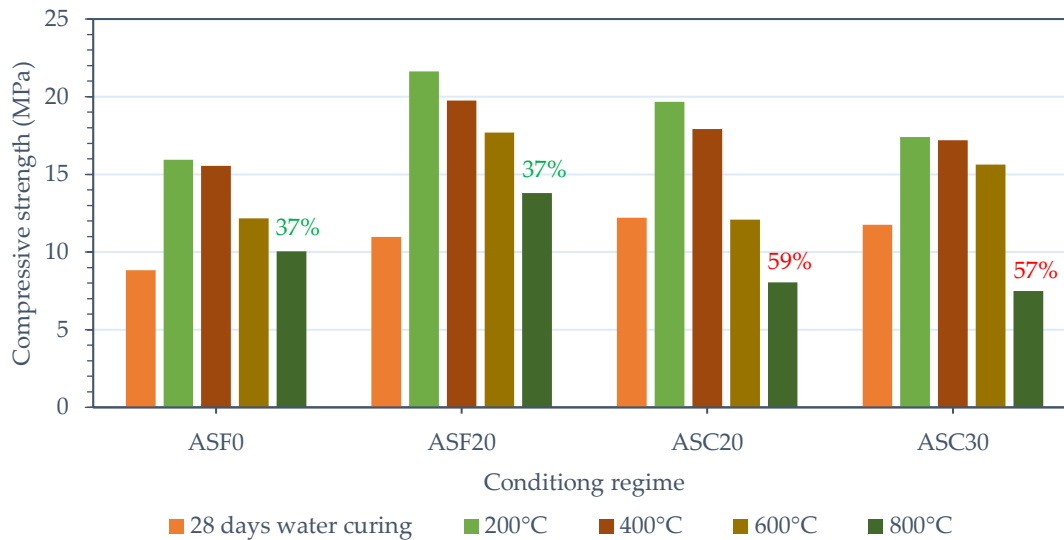


**Fig. 4.51: Change in compressive strength of mortar mixes of series A after exposure to fire**

After 5 minutes of exposure to fire when the temperature had risen to 400°C, there was slight fall in compressive strength of mixes ASF0 and ASC30 as seen in Fig. 4.51. But for the mixes (ASF20 and ASC20) with the highest stiffness, the reduction in strength is around 8.5% to 9%. It is around this temperature where 70% of the water which is present in the interlayers of CSH or chemically combined, is lost on heating. This further increases the van der Waal's forces of attraction between the CSH layers (Lu et al., 2017). But however, if the rate of heating is sufficiently high, then the generated water vapour creates an internal pore pressure. When this pore pressure exceeds the tensile capacity, the mortar matrix starts failing as explained by Ma et al. (2015) in their extensive review on performance of concrete when exposed to elevated temperature. This along with the partial thermal disintegration of CSH, calcium aluminate hydrates and calcium carbo-aluminates led to the reduction in compressive strength for these mixes.

Significant difference in compressive resistance was noticed when the mortar mixes were exposed at 600°C to fire within 10 – 15 minutes. The variation ranges from 10% to 39% from the peak strength (measured on heating up to 200°C). Maximum variation was



noted for ASC20, while the least for ASC30. It is around this temperature (573°C), quartz mineral in silica based river sand, undergoes a reversible transformation from  $\alpha$  to  $\beta$  form. This transformation is accompanied by 0.85% increase in volume of the aggregates, whereas the carbonate aggregates are stable up to this temperature (P. Kumar and Monteiro, 2015). From the mass loss curve shown in Fig. 4.52, the extent of loss in weight around 500°C to 600°C in FS appears to be more when compared to CS by 1%. This extra mass loss has helped mixes with FS to cope better with the volume change associated with quartz inversion than mixes with CS. Hence among the mixes with 20% MS, mix ASC20 had undergone the most significant reduction in strength at 39%, whereas the compressive strength of ASF20 had reduced by only 18%.

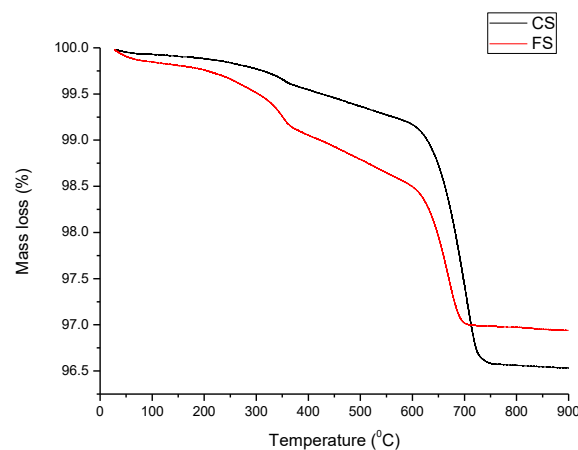
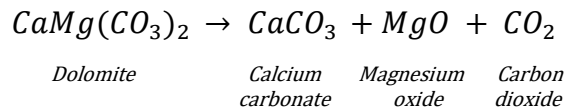
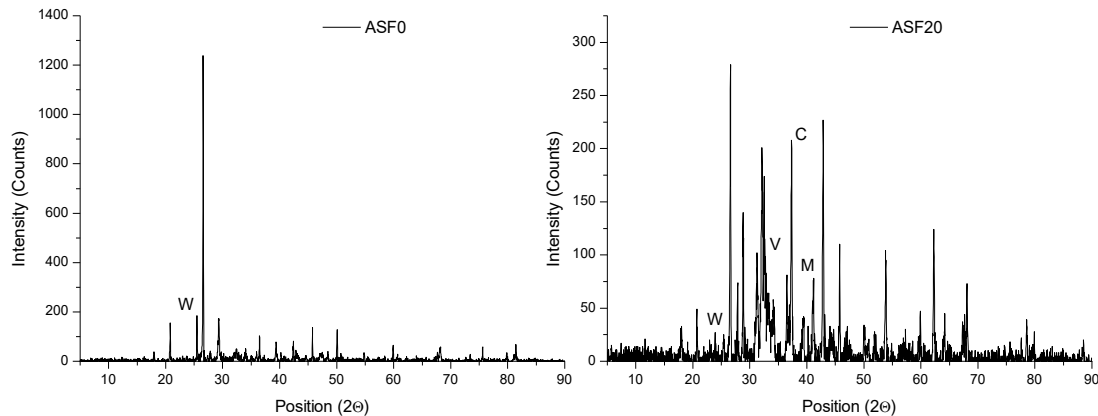


**Fig. 4.52: Mass loss pattern when CS and FS are heated up to 900°C**

When the exposure is further prolonged, temperature was further increased to 800°C and the reduction in compressive strength was still higher. Maximum loss was recorded for mix ASC20 at 59%, whereas mixes ASF0 and ASF20 recorded a fall in performance of about 37%. The residual compressive strength of these two mixes was still higher than that of their corresponding 28<sup>th</sup> day compressive strength. The sharp fall in compressive resistance of mixes is because of three factors. According to Földvári (2011), CSH dehydrates to form wollastonite whose presence was confirmed by the peak at 25.48° as shown in X-ray diffractogram in Fig. 4.53. With regard to sand, Horszczaruk *et al.* (2017) pointed out that difference in thermal expansion between the cement paste and aggregate, ruptures the ITZ. Whereas dolomite aggregate undergoes decarbonation which increases the porosity of the mortar matrix. Netinger *et al.* (2013) also encountered a similar increase in porosity of their concrete samples at a temperature of 700°C. This decarbonation reaction is given by the equation:



Presence of calcium carbonate (vaterite) and magnesium oxide in ASF20 was confirmed by the occurrence of peaks at 32.12° and 42.87° respectively (Fig 4.53)



W – Wollastonite; V – Calcium carbonate; C – Calcium oxide; M – Magnesium oxide

**Fig. 4.53: X-ray diffraction pattern of ASF0 and ASF20 after exposure to fire at 800°C**

The extent of weight loss experienced by the same series of mortars when subjected to the action of fire is shown in Fig. 4.54. Around 200°C there was no perceivable weight loss in any mix. The specimens were oven dried at 60°C before subjecting to fire. Hence the weight loss indicating the evaporation of free water was not recorded here. After 5 minutes of exposure to fire when the temperature had raised to 400°C, mixes with the highest water content (w/c, as shown in section 4.2) ASF0 and ASC30 had recorded 1.7% and 1.4% weight loss, respectively. Whereas the other two mixes ASF20 and ASC20 which have the least w/c ratio and porosity had shown to lose 0.3% and 0.4% of their weight around this temperature.

When the temperature had risen to 600°C, the weight loss was significantly higher around 3.2% to 3.8% for mixes with CS. Whereas mixes ASF0 and ASF20 have recorded a loss in weight of about 2.9% and 1.2% respectively. This weight loss is due to the expansion of quartz aggregate when it undergoes transformation from  $\alpha$  to  $\beta$  form. After 30 minutes, when the temperature had risen to 800°C, mixes with MS had recorded the maximum weight loss. The predominant reason for this is due to decarbonation of dolomite aggregate which decomposes to release carbon di-oxide as mentioned above.

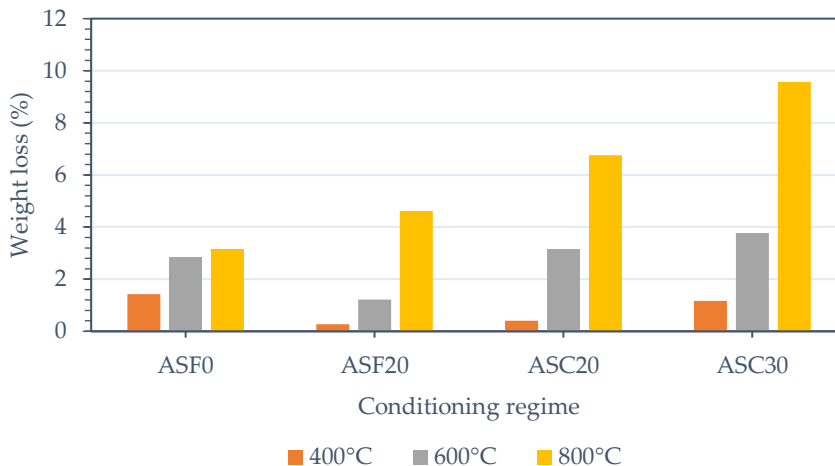


**Fig. 4.54: Extent of weight loss suffered by mortar mixes of series A after exposure to fire**

The variation of compressive strength of series D, when they were subjected to the action of fire is given in Fig. 4.55. From this figure it can be seen that the change in compressive strength is similar to that of noticed for series A. Maximum compressive strength was attained after heating the samples to 200°C, after which there was a gradual fall in performance. When the temperature had risen to 600°C, the fall in compressive resistance of the mix DSF20 was the least at 34%, whereas the other three mixes had recorded a decline of 41% to 49%. This shows that inclusion on MS had reduced the extent of expansion caused by the transformation of the quartz river sand (FS) from  $\alpha$  to  $\beta$  form.

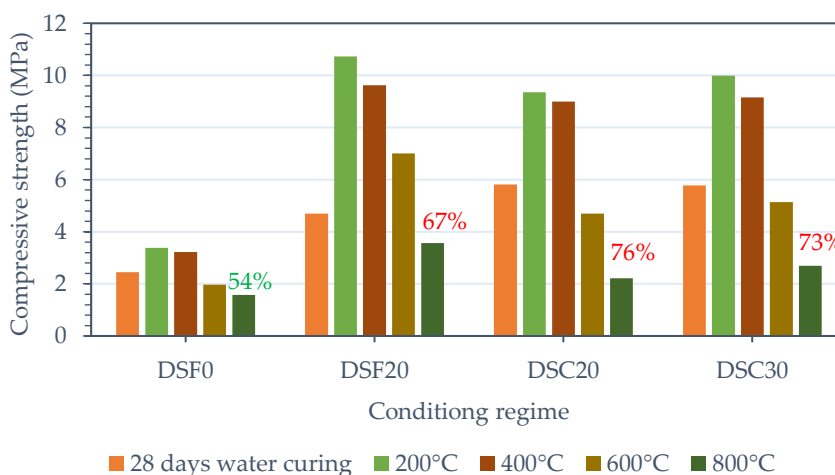


**Fig. 4.55: Change in compressive strength of mortar mixes of series D after exposure to fire**

Also, when compared to series A, the fall in compressive strength of series D was greater for all the four mixes. This can be because of the aggregate content which was two times more than that of the quantity used in mixes of series A. At the end of the testing

regime no mixes retained their initial capacity, however mix DSF20 has highest resistance to compression at 3.57 MPa. The extent of loss in weight experienced by mixes is shown in Fig. 4.56. From this figure we can see that the variation of this physical property for series D is similar to that of the variation of series A.

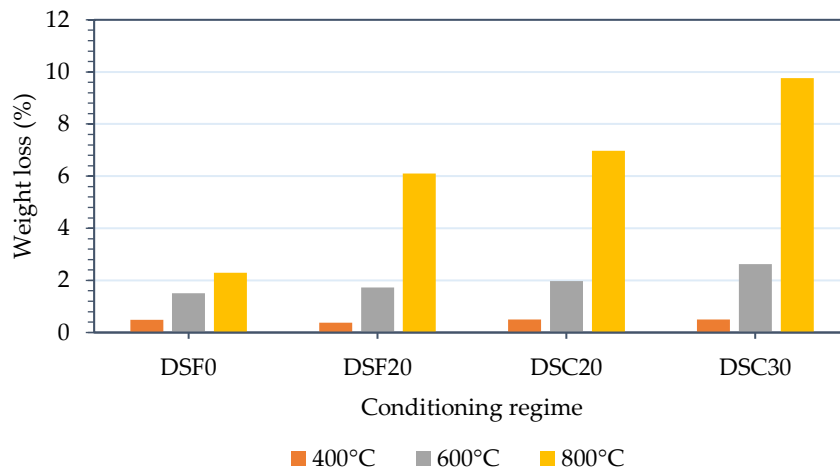
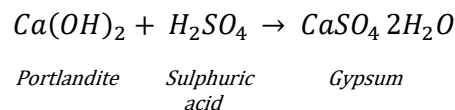
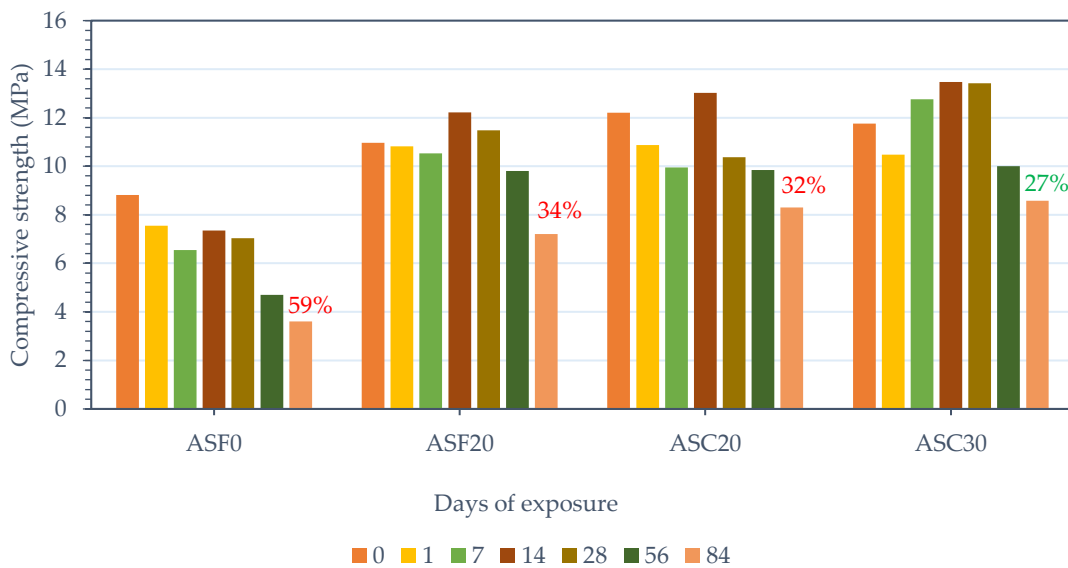


Fig. 4.56: Extent of weight loss suffered by mortar mixes of series D after exposure to fire

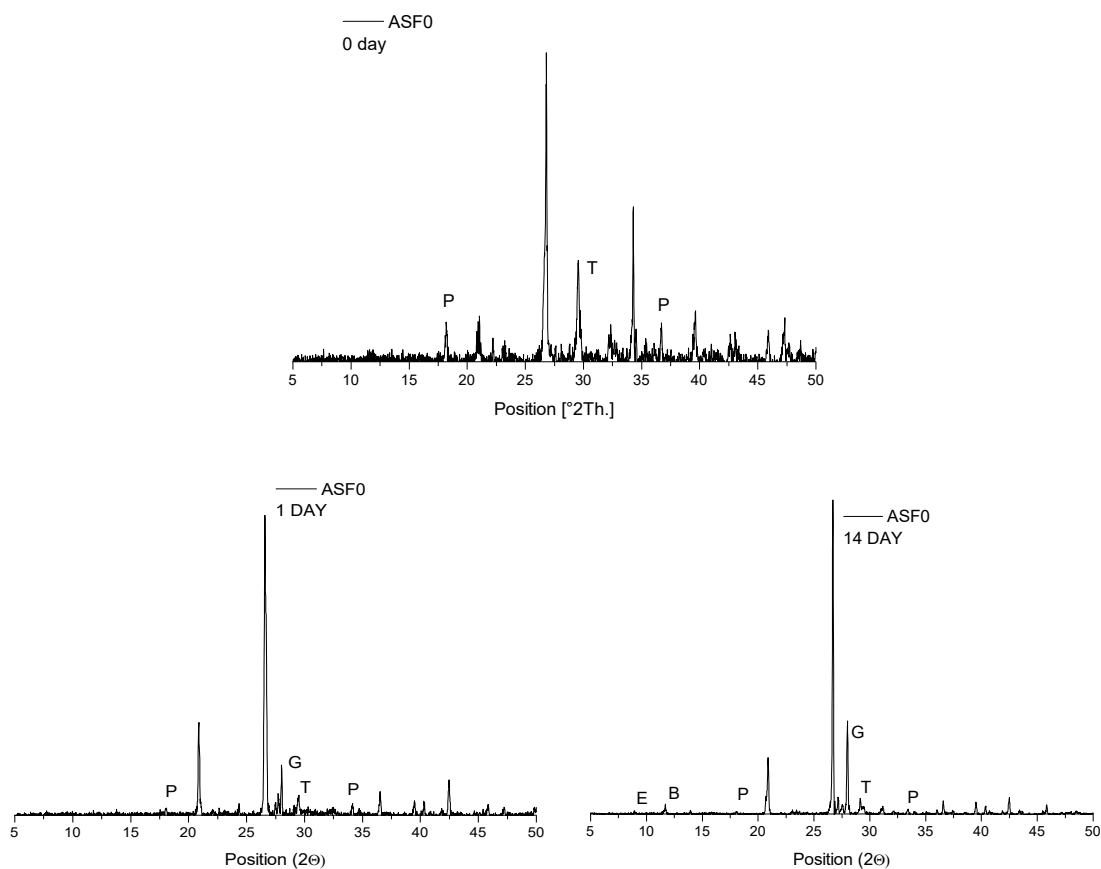
#### 4.5.5 Acid attack:

Effect on compressive strength of mortars of series A when exposed to sulphuric acid for 1, 7, 14, 28, 56 and 84 days is graphically represented in Fig. 4.57. From this figure it can be seen that, the variation in compressive strength of all the mortar mixes follows a similar pattern. Initially, when exposed to the acidic medium there was gradual fall in performance between 1 to 7 days of exposure. For the mix ASF0, this might be due to the consumption of Portlandite by sulphuric acid. This is indicated by the fall in intensity of XRD peaks at diffraction angles of 18.26°, 34° and 47.14° (Fig. 4.58). This consumption of portlandite resulted in loss in weight of the specimens after 7 days of exposure as seen in Fig. 4.59. The chemical reaction occurring can be written as





**Fig. 4.57: Compressive strength of mortar mixes of series A when subjected to an acidic medium**



G – Gypsum; P – Portlandite; E – Ettringite; B – Basanite; T – CSH

**Fig. 4.58: X-Ray diffractograms of mix ASF0 after 0,1 and 14 days of exposure to acid attack**

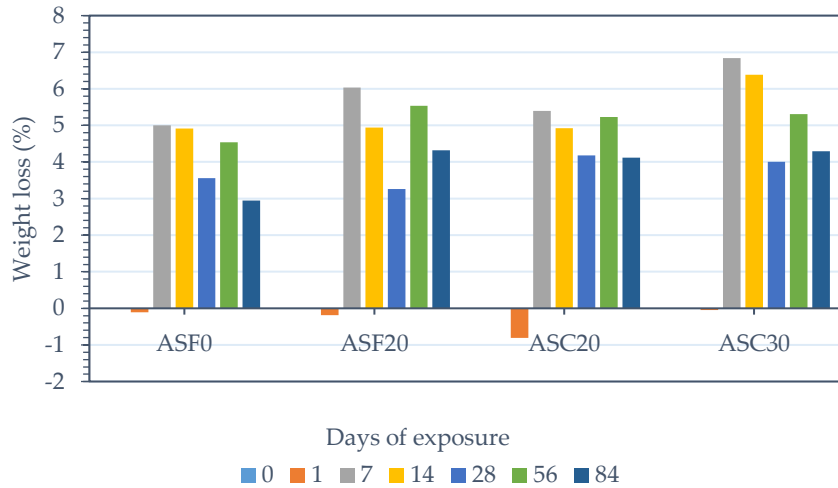
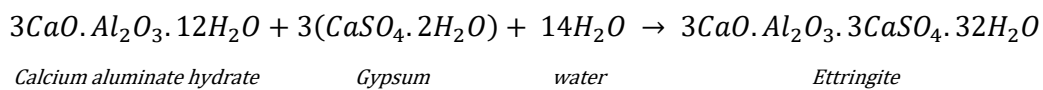
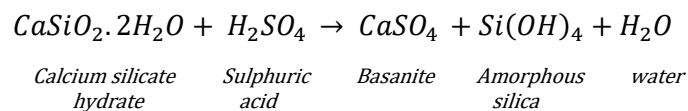


**Fig. 4.59: Weight loss of mortar mixes of series A when subjected to an acidic medium**

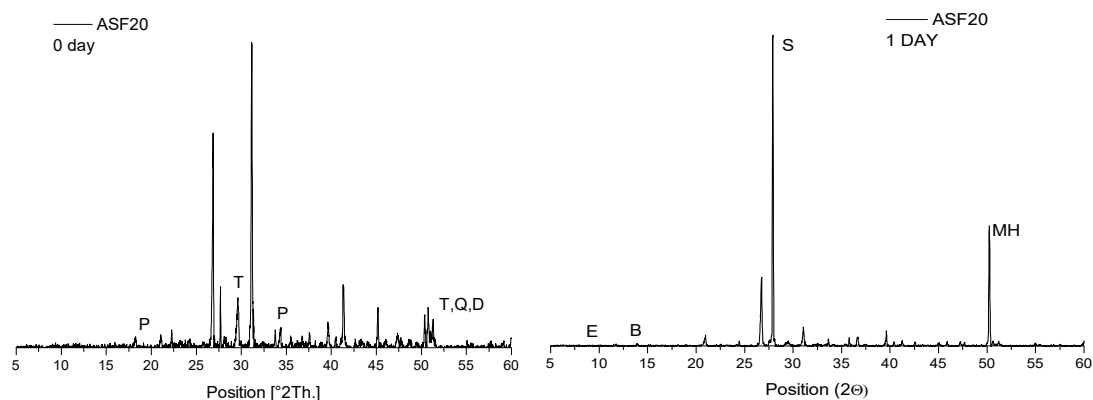
The consumed portlandite has been converted into gypsum as indicated by the peak at  $28^\circ$  (Fig. 4.58) that becomes more intense with period of exposure. This also helps in filling the pores, which has resulted in increase in compressive strength after 14 days of exposure as noticed in Fig. 4.57. The peaks representing portlandite completely diminished after 14 days of exposure. The intensity of gypsum continued to rise and the presence of ettringite ( $8.99^\circ$ ) along with basanite ( $13.94^\circ$ ) were detected as shown in Fig. 4.58. This implies that by this stage, portlandite was exhausted and consumption of CSH and CAH/CASH had resulted in formation of basanite and ettringite as seen in following equations:



On continued exposure beyond 14 days, loss of weight was detected which implies leaching out of these sulphate compounds. Compressive strength was also seen to fall after 14 days which reached a minimum value at the end of the test period. The compressive strength of ASF0 had reduced from 8.82 MPa to 3.61 MPa on 84<sup>th</sup> day of exposure.

For mixes with MS, on initial exposure to the acidic medium, there is a gradual fall in performance, which is similar to that of control mortar. However on studying the microstructure, the decomposition seems to happen through another mechanism. As mentioned earlier in section 4.2.4., due to accelerated hydration, portlandite is available at

an earlier stage for fly ash to react with and form CASH. Hence these mixes have low portlandite content. Therefore when they are exposed to an acidic medium, decomposition of CSH and CAH/CASH starts right from the initial days of exposure itself. This leads to the formation of basanite and ettringite along with gypsum at an early age of 1 day as seen in Fig. 4.60. The attack on CSH and CASH can be noticed by the increase in wavenumber around the band  $1000\text{ cm}^{-1}$  which was initially at  $1007\text{ cm}^{-1}$  had moved to  $1017\text{ cm}^{-1}$  (Fig. 4.61). This attack might be the reason for fall in compressive strength up to 1 – 7 days of exposure. The band indicating the presence of Al-O bond has also become prominent. These changes in FTIR spectra are not noticed in ASF0 as presence of sufficient portlandite prevents damage to CSH.



S – Calcium sulphite; P – Portlandite; E – Ettringite; B – Basanite; T – CSH; MH - Brucite

**Fig. 4.60: X-Ray diffractograms of mix ASF20 after 0 and 1 day of exposure to acid attack medium**

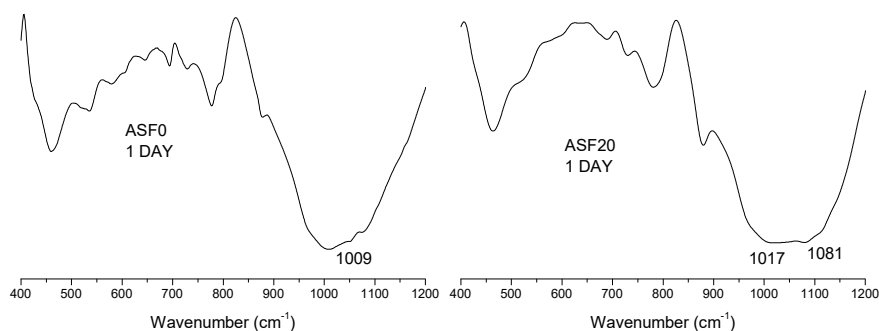
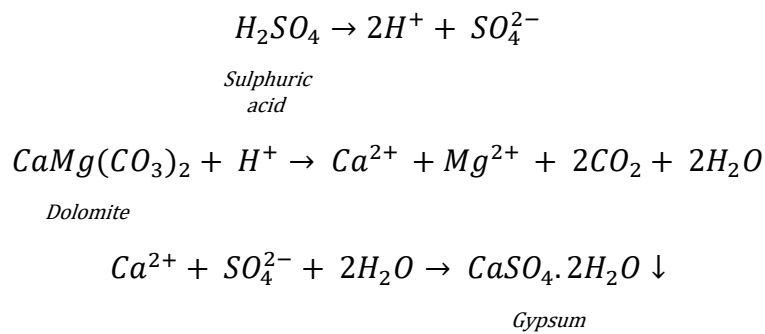


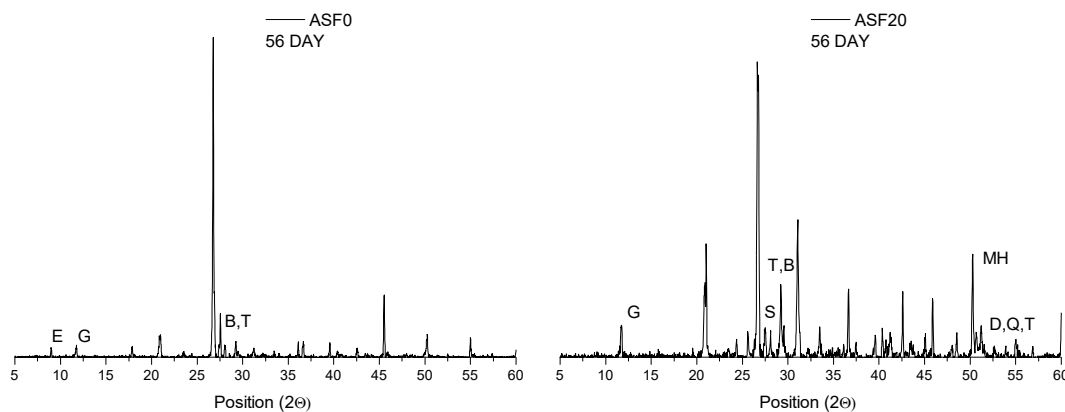
**Fig. 4.61: FTIR spectra of mixes ASF0 and ASF20 after subjecting to an acidic medium for 1 day**

Apart from this, dolomite aggregate also seem to have undergone decomposition. Creation of peak around  $27.89^\circ$  (Fig. 4.62) indicated the formation of calcium sulphite,

which can be an intermediate product of dolomite decomposition on treating to sulphuric acid. Magnesium from dolomite appeared as brucite ( $Mg(OH)_2$ ) having a diffraction angle at  $50.22^\circ$ . On continued exposure of around 14 days, calcium sulphite later converted to gypsum. Around this period, these mixes gain strength by 6 – 14% when compared to their initial capacity as shown in Fig. 4.57. Huang et al. (2018) and Xiao et al. (2018) had outlined the chemical reactions involving sulphuric acid and dolomite marble as follows:



On continued exposure, basanite was only detected again after 56 days along with gypsum at reduced intensity. From this, it can be implied that decomposition of CSH has started again. These reactions are accompanied by fall in compressive strength and fluctuations in weight of the mixes. At the end of the test regime the residual strength of mixes ASF20, ASC20 and ASC30 is of the order 65%, 68% and 72%.



G – Gypsum; P – Portlandite; E – Ettringite; B – Basanite; T – CSH; S – Calcium sulphite; MH – magnesium hydroxide; D – Dolomite; Q – Quartz

**Fig. 4.62: X-ray diffraction pattern of ASF0 and ASF20 after different periods of exposure to acidic medium**

SEM images of the ASF0 and ASF20 mixes are shown in Fig. 4.63. From these images it can be seen that the extent of damage on control mortar mix ASF0 was always severe, right from the initial days of exposure. At 56 days the damage was extensive with



most of the CSH destroyed in mix ASF0 but ASF20 still looked robust. No formation of calcium sulphate could be detected in ASF20, whereas calcium sulphate was present as scales in the mortar matrix of ASF0.

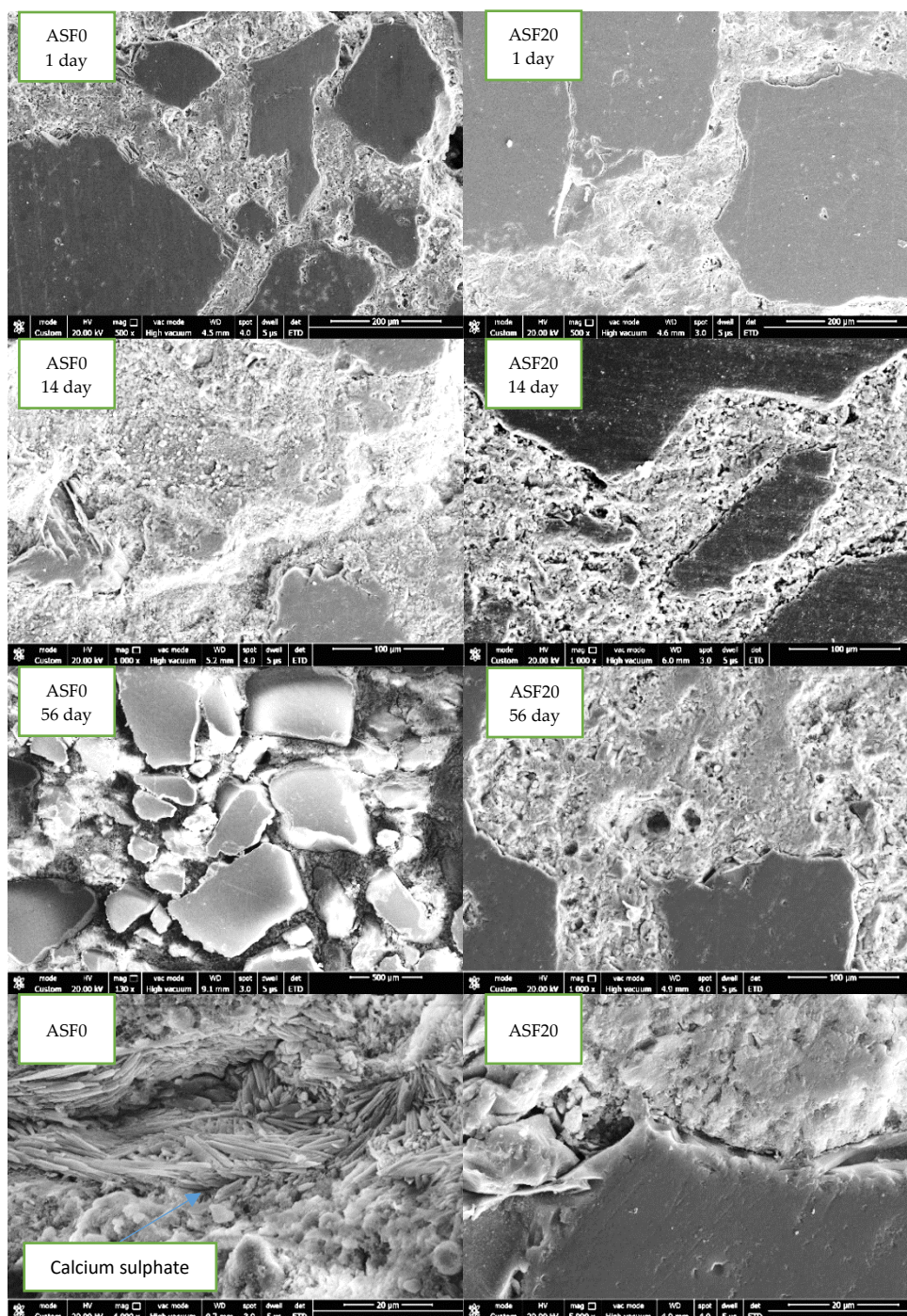


**Fig. 4.63: Scanning electron micrographs of ASF0 and ASF20 after exposure to different periods of acidic environment**

The variation in performance of series D can be considered analogous to series A. As seen from Fig. 4.64, at the end of the test period, mix DSF0 had no residual strength, whereas mixes DSF20, DSC20 and DSC30 could resist 13%, 51% and 33% of their initial

capacity of compressive strength. This pattern of residual strength follows the pattern of initial porosity of these mixes with MS (Table 4.3), i.e. mix with the lowest initial porosity has the highest residual strength.

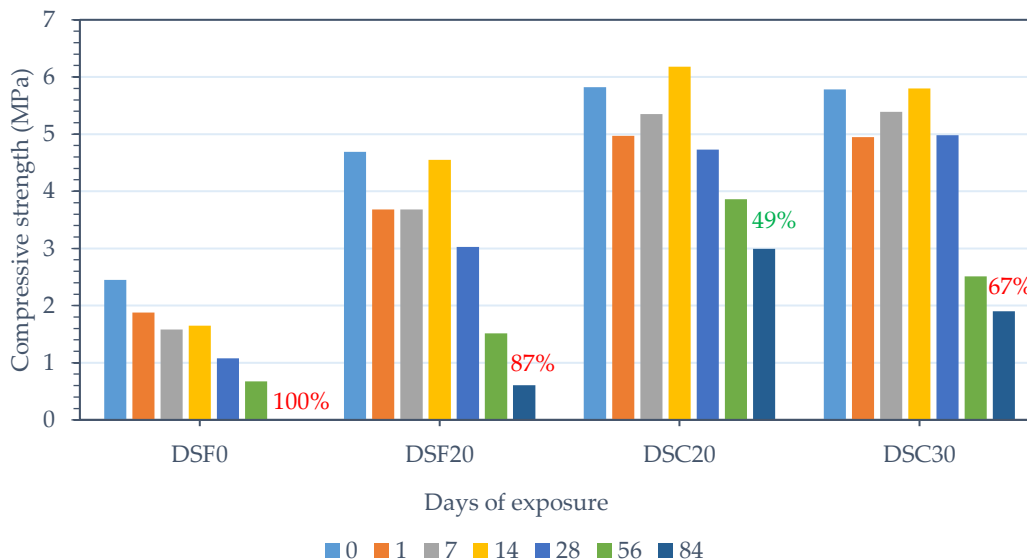


**Fig. 4.64: Compressive strength of mortar mixes of series D when subjected to an acidic medium**

The weight loss pattern shown in Fig. 4.65 shows that weight loss starts only after 7 days of exposure and was more in case of mixes which contain MS. The appearance of these mixes is shown in Fig. 4.66. Based on this figure, the reduction in compressive strength must have been taken due to lack of adhesion rather than expansion and cracking. Also, mix ASF0 appeared to have undergone damage slightly more than the other mixes of this series A, whereas DSF0 had undergone the most distressing change.

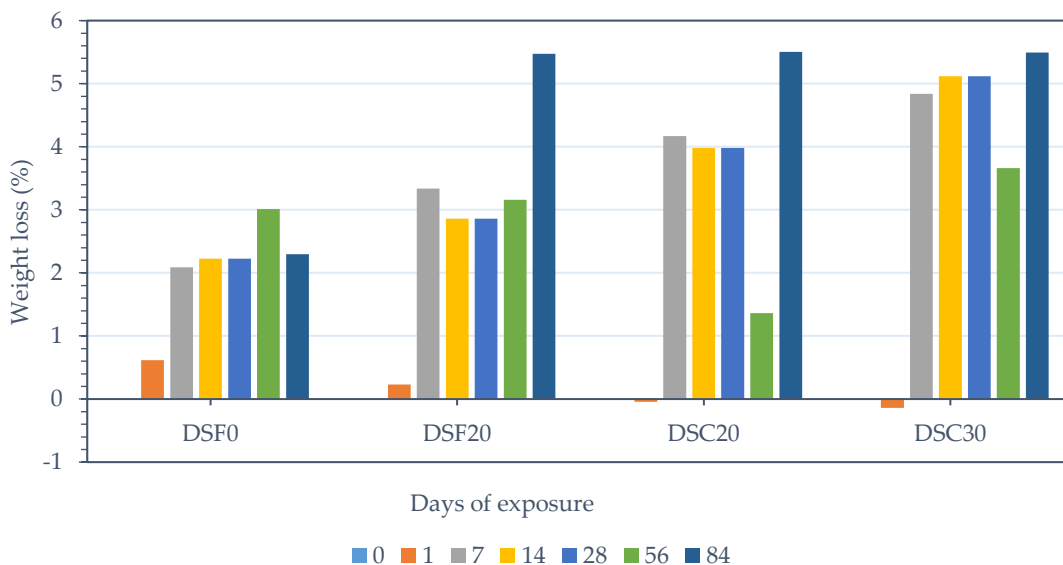


Fig. 4.65: Weight loss of mortar mixes of series D when subjected to an acidic medium

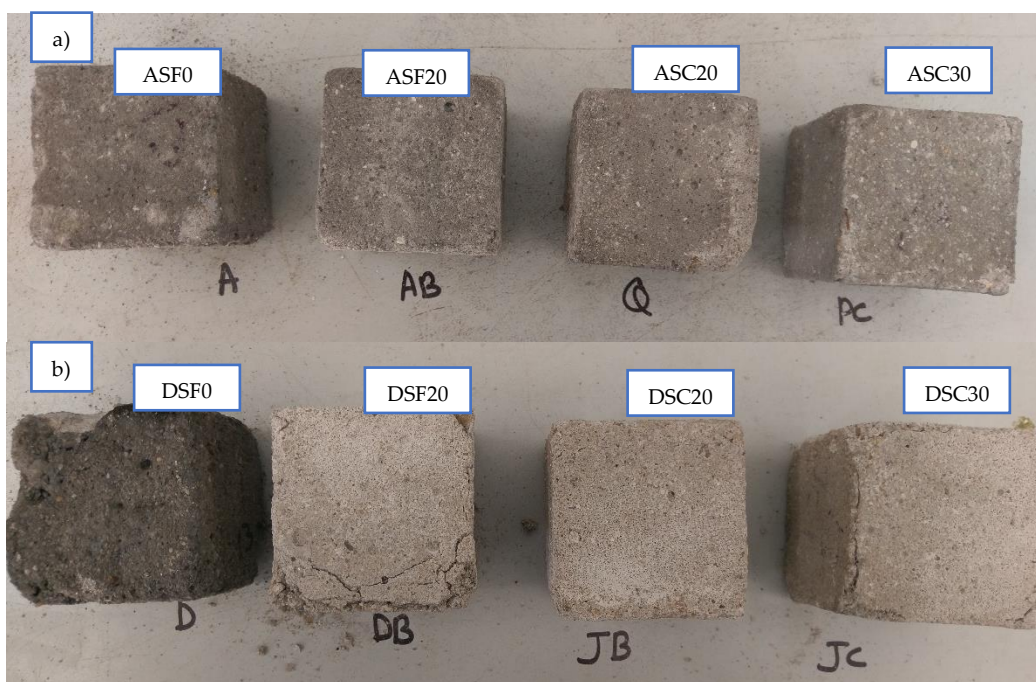


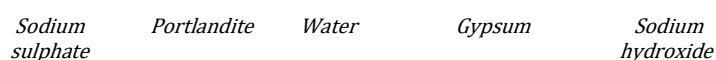
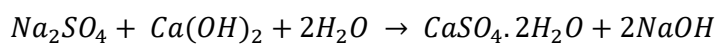
Fig. 4.66: Appearance of mortar mixes of series a) A and b) D when subjected to an acidic medium for 84 days

Evaluation of dolomitic marble based mortars, when they are exposed to an acidic medium has not been reported elsewhere. The positive results presented above are despite the fact that marble waste are acid soluble in nature. Hence it can be concluded that, presence of an acid neutralizing aggregate in the form dolomite marble has provided a buffer to reduce risk of CSH and CASH disintegration. Therefore at a substitution level of 20% – 30% of sand by MS, acid resistance of mortars improve as compared to control mixes.

#### 4.5.6 Sulphate attack:

Mortar mixes were subjected to a 5% sodium sulphate solution and properties like compressive strength, loss in weight and change in length were measured at the end of 28, 84 and 164 days. The variation in compressive strength of mixes of series A (mixes with 1:3 mix proportion) during the testing regime is shown in Fig. 4.67. From this figure it can be seen that, compressive strength increases for all mixes and reached a maximum value after 84 days of exposure. The increase in strength was in the range 23% to 47% for mixes with MS, whereas for the control mix ASF0 it was increased by 68%.

It is understood that when cement composites come in to contact with a sodium sulphate solution, portlandite is transformed in to gypsum. The chemical reaction given by P. Kumar and Monteiro (2015) is



Gypsum thus formed, reacts with calcium aluminate hydrates to form ettringite, whose chemical reaction was mentioned in section 4.5.5. The presence of these minerals is confirmed by using XRD as shown in Fig. 4.68.

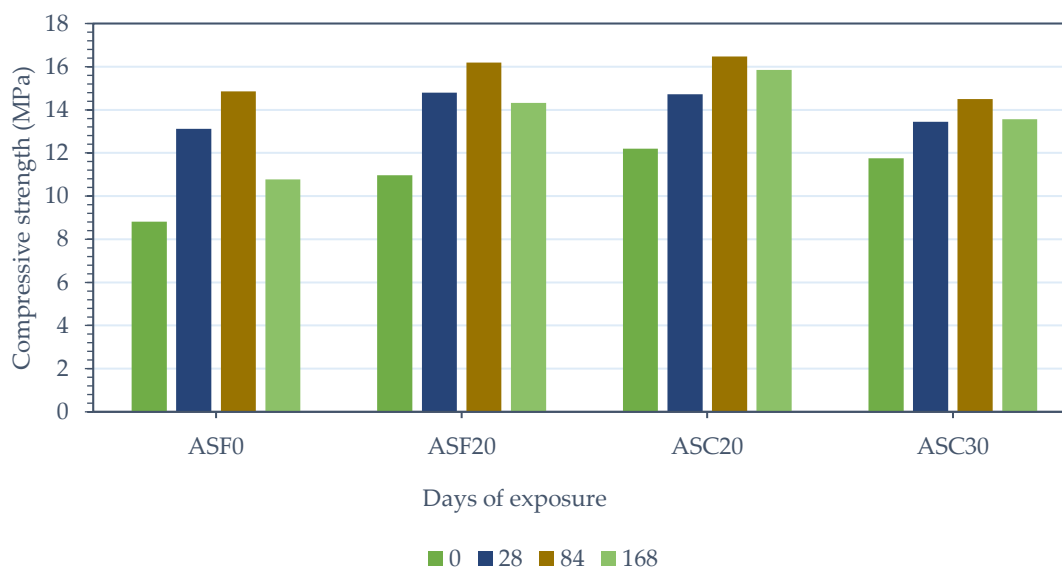
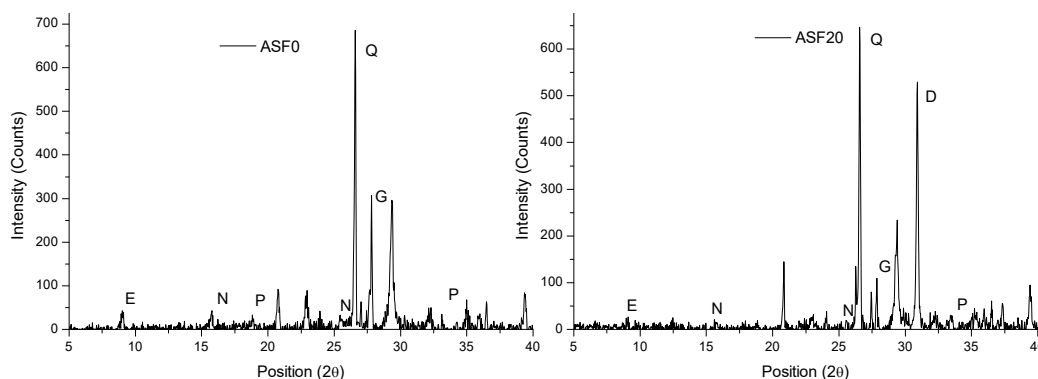


Fig. 4.67: Compressive strength of mortar mixes of series A when subjected to sulphate attack

The peaks detected at angles  $27.58^\circ$  and  $8.96^\circ$  are due to the presence of gypsum and ettringite respectively. These minerals (gypsum and ettringite) are pore filling in nature, hence increase in compressive strength was noticed as mentioned earlier.



G – Gypsum; P - Portlandite; E – Ettringite; N – Sodium aluminate gel; Q – Quartz; D - Dolomite

**Fig. 4.68: X-ray diffraction pattern of ASF0 and ASF20 after exposure to sulphate attack for 164 days**

As seen in Fig. 4.67, mixes with MS show relatively reduced strength gain when compared to the control mortar during the same exposure period. This better resistance of mixes with MS to sulphate attack can be because of two reasons. Portlandite and calcium aluminate hydrates are the most susceptible constituents of cement hydration products to undergo damage when subjected to attack from sulphate reagents. The advantage derived from accelerated hydration which led to quicker consumption of portlandite during hydration (as shown in section 4.4.4) might have reduced the chances of formation of gypsum. This along with the formation of calcium carbo-aluminates from calcium aluminate hydrates (as shown in section 4.4.4) has toned down the damage experienced by these mixes due to reduced formation of ettringite also. This can be confirmed by the X – ray diffraction peaks shown in Fig. 4.68. The peaks representing the formation of ettringite and gypsum are feeble in mix ASF20 when compared to the peaks shown in ASF0.

Neville (2004) pointed out that formation of gypsum and ettringite are known to cause expansion of the mortar matrix. This expansive nature of gypsum and ettringite is confirmed by the increase in length of mortar specimens as shown in Fig. 4.69. It can be seen that, up to 84 days of exposure, the control mix has expanded 52% more than ASF20. Among the mixes with MS, mixes (ASF20 and ASC20) which have the least initial porosity (as mentioned in Table 4.3) have undergone the least expansion.

According to P. Kumar and Monteiro (2015), due to the formation of gypsum and ettringite, expansion is also accompanied by reduction in cohesion. This results in loss of weight of the specimens as shown in Fig. 4.70. As seen in this figure, no definite pattern

can be drawn between individual mixes with respect to the changes noted in weight loss. This can be because deterioration of samples proceeds by accumulation of salts and simultaneous removal of soluble compounds.

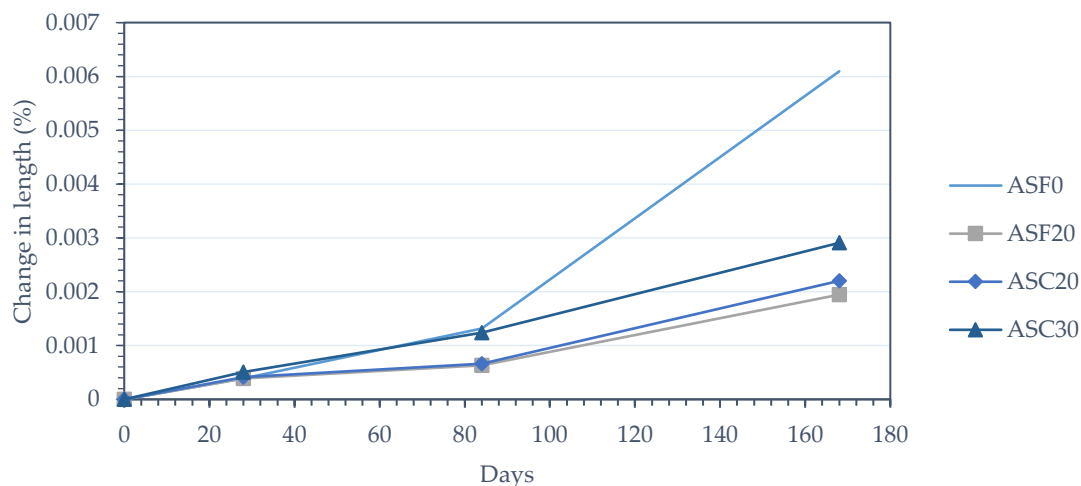


**Fig. 4.69: Change in length of specimens of series A due to sulphate attack**

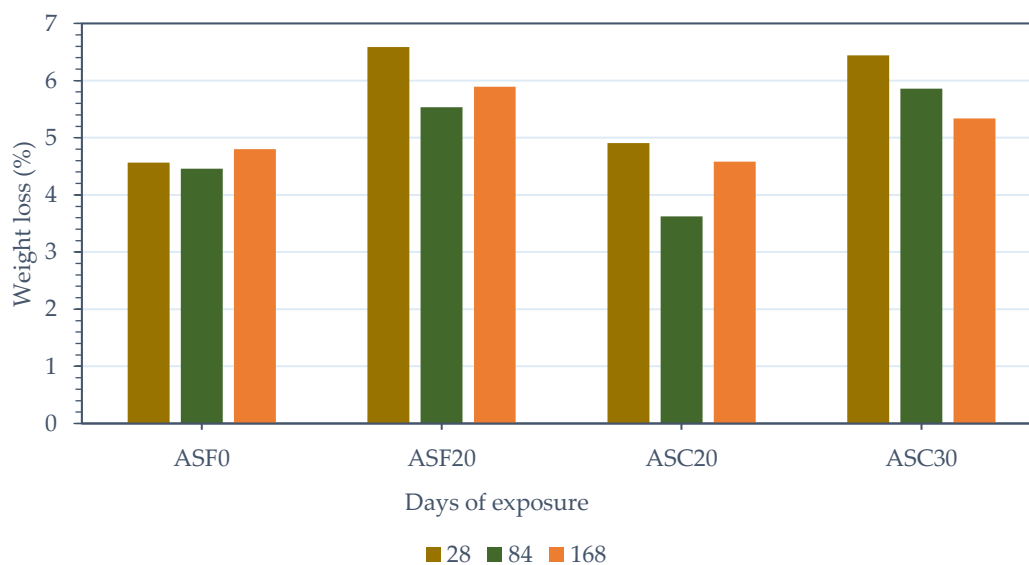


**Fig. 4.70: Weight loss of mortar mixes of series A when subjected to sulphate attack**

As the exposure prolonged, the expansion caused by gypsum and ettringite was so severe that, it resulted in reduction in compressive strength after 84 days of exposure as seen in Fig. 4.67. The fall in strength was more severe in the case of mix ASF0 when exposed for 164 days. For this mix a reduction of 27% from its peak strength (after 84 days of exposure) can be noted. For mixes with MS, it was between 3% to 11%. However, the residual strength of all mixes was still higher than their initial 28<sup>th</sup> day strength. The highest

residual compressive strength recorded is 15.85 MPa for ASC20, while compared to 10.77 MPa of the control mortar.

The severity of the expansive stresses undergone by mix ASF0 which has resulted in its reduction in strength can be noted by the extent of length change shown in Fig. 4.69 after 164 days. From this figure it is very clear that, mix ASF0 has undergone 109% more expansion than ASC30. Among the mixes containing MS, mix ASF20 has undergone the least expansion while ASC20 and ASC30 have expanded 13% and 49% more than ASF20. This variation in performance can be because of the difference in stiffness and porosities of these mixes as shown in Table 4.3.

The formation of calcium sulphate compounds and ettringite is accompanied by formation of sodium hydroxide which helps in maintaining the alkalinity of both systems with and without MS. This reduces the severity of sulphate attack which is not possible in the case when sulphate ions are from an acidic medium as seen in the results mentioned in the previous section. This sodium hydroxide can also act an alkali activator for fly ash which results in the formation of sodium aluminate gel whose traces can be detected by the peak at  $25.59^\circ$  (Fig. 4.68) after 84 days for mixes with and without MS. Nath et al. (2016) observed similar peaks when they used sodium hydroxide as an alkali activator for the preparation of fly ash based geopolymers mortar samples. There is also a better cross linking Si-O-Al chain which has led to the reduction of its associated wavenumber from  $1010\text{ cm}^{-1}$  to  $978\text{ cm}^{-1}$  as shown in Fig. 4.71. This is detected on the first of day of exposure itself and remains identical right till the end. The same figure depicts the presence of gypsum by the bands at around  $605\text{ cm}^{-1}$  and  $1090\text{ cm}^{-1}$  wavenumbers.

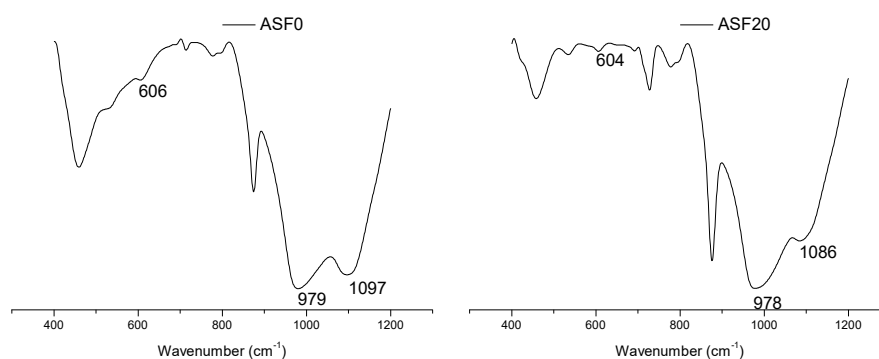


**Fig. 4.71: FTIR spectra of ASF0 and ASF20 after exposure to sulphate attack for 164 days**

Series D can be considered analogous to series A. But, the extent of damage caused to DSF0 was more pronounced than ASF0. From the failure of mix DSF0 as seen in Fig. 4.72, it can be said that rupture has taken place due to expansion and cracking, as in the case of ASF0. The samples of same mixes prepared for measuring length change did not sustain the internal stresses developed beyond 28 days of exposure, hence the results are not shown in Fig. 4.73. There was no residual strength (Fig. 4.74) and specimen crumbled (Fig. 4.75) after 164 days of exposure. For mixes with MS, the strength gain is 40% to 90% of the initial strength at the end of testing as seen in Fig. 4.74. Mix DSC20 which had the least porosity among the mixes with MS, had undergone the least change in length as depicted in Fig. 4.73.

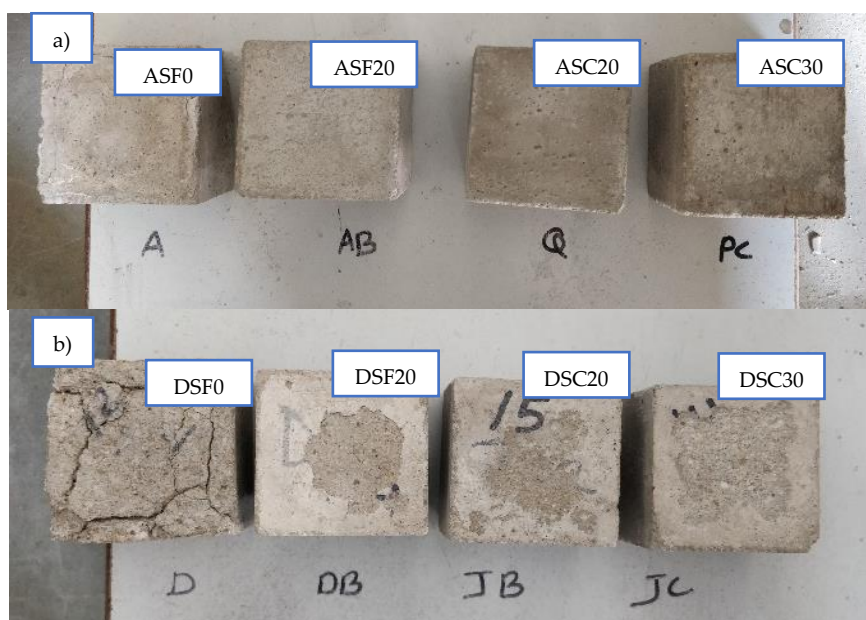


Fig. 4.72: Appearance of mortar mixes of series a) A and b) D when subjected to a sulphate solution for 168 days

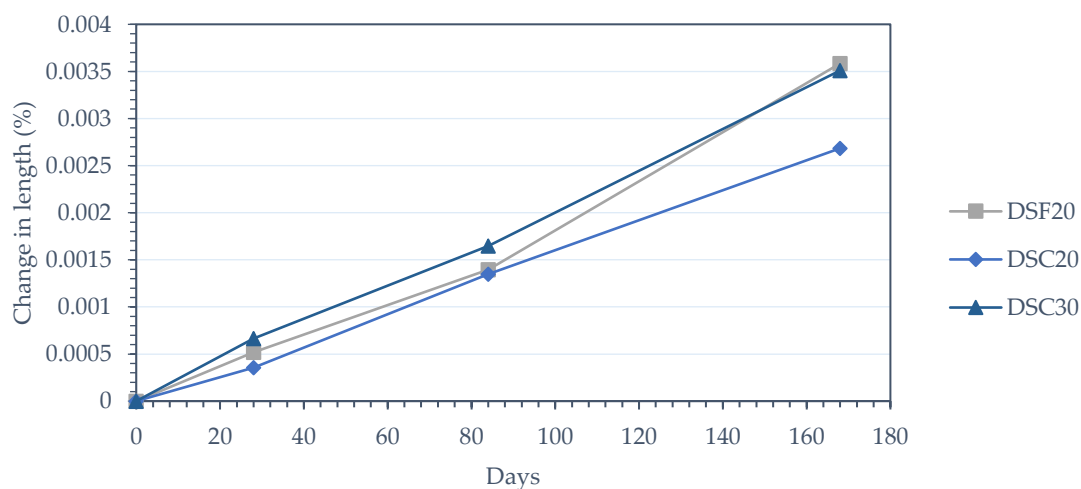


Fig. 4.73: Change in length of specimens of series D due to sulphate attack



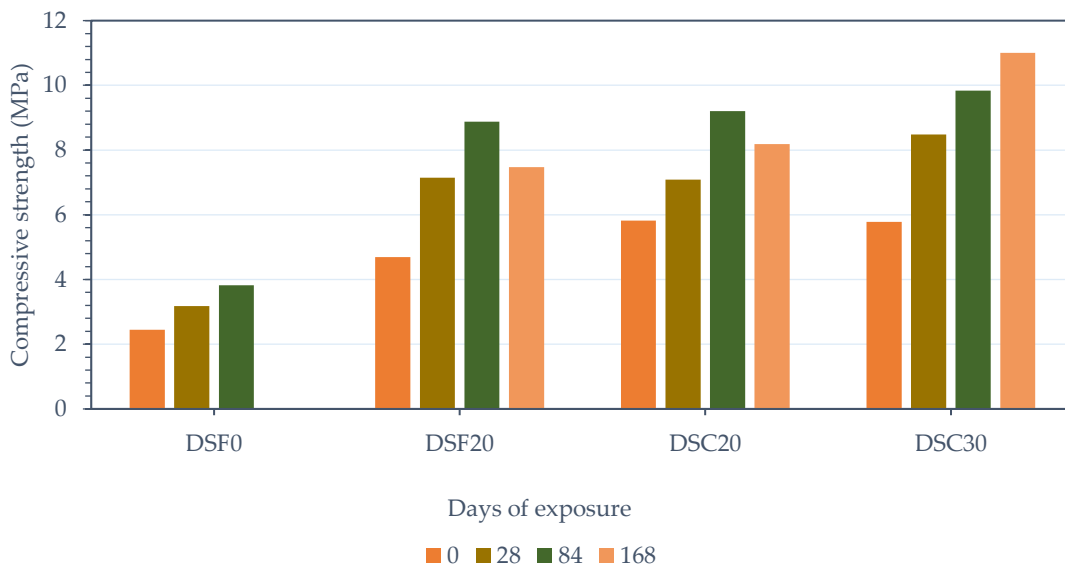


Fig. 4.74: Compressive strength of mortar mixes of series D when subjected to sulphate attack

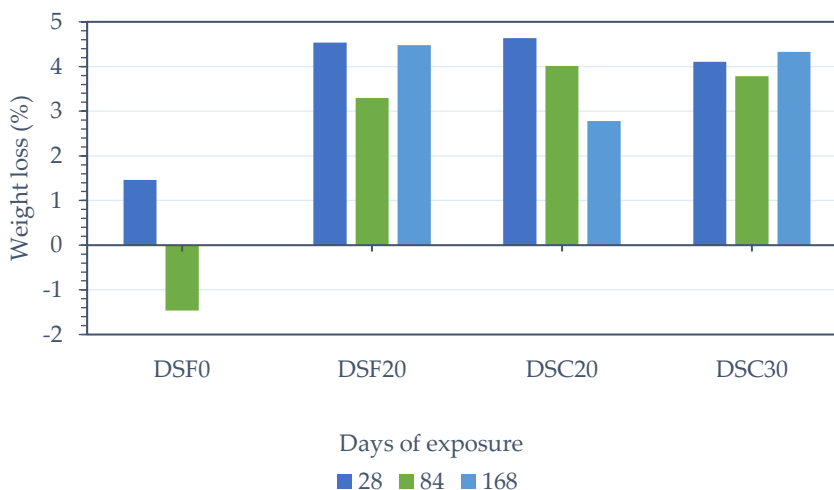


Fig. 4.75: Weight loss of mortar mixes of series D when subjected to sulphate attack

As seen earlier, these results are in line with the outcomes reported by Binici et al. (2007). However, it can be pointed out that, the mechanism by which such an advantage is derived by incorporating MS in cement composites has not been detailed by anyone before. Therefore, this current study has made an attempt to evaluate this reason for the enhanced behaviour of cement composites in the presence of marble waste exposed to sulphate reagents.

#### 4.5.7 Chloride penetration:

Prisms of size 40 x 40 x 160 mm were painted with an epoxy paint on five sides, leaving one of the 40 x 40 mm side uncoated. These prisms were then immersed in a solution of 1% NaCl for 1, 7, 14, 28, 56 and 84 days. The depth of presence of free chloride

was detected by spraying 0.1N AgNO<sub>3</sub> on longitudinally split samples. The distance from the uncoated side at which white AgCl precipitate changes to brown colour of AgNO<sub>3</sub> is noted as depth of penetration of chloride ions. This depth is graphically represented in Fig. 4.76 for all the eight mixes of both series A (1:3) and D (1:6). From this figure it can be seen that with inclusion of MS the depth up to which free chloride ions were present had reduced for both the series. This reduction is significant for series D and which ranged from 29% (DSC30) to 44% (DSC20) when compared to the control mortar. Maximum penetration was seen to happen within the first day of exposure itself for all mixes, which seemed to stabilize within 7 to 14 days and 14 to 28 days of exposure for series A and D, respectively. This would mean all or most of the free chloride was chemically bound within these periods of exposure.

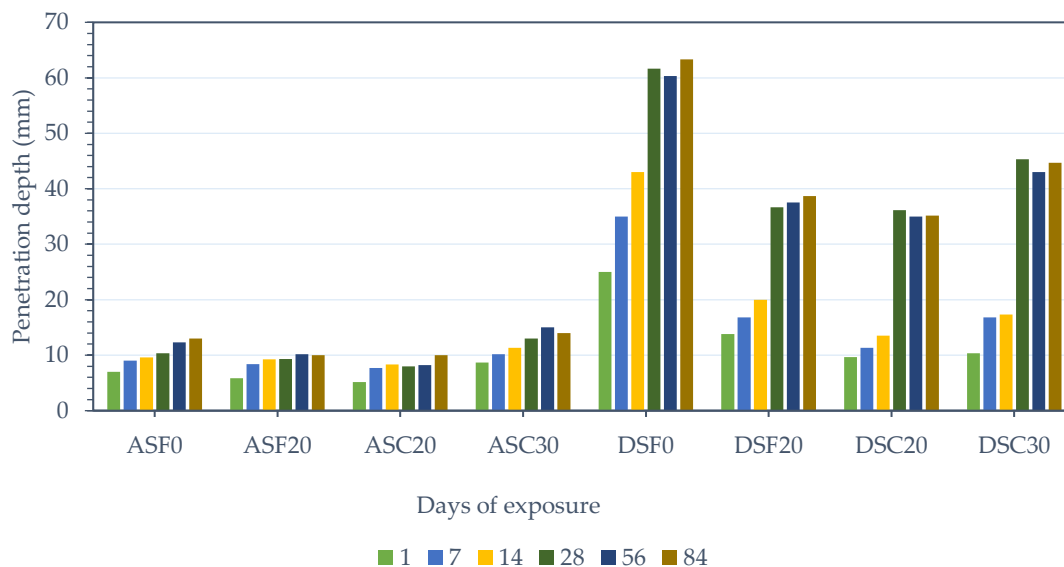
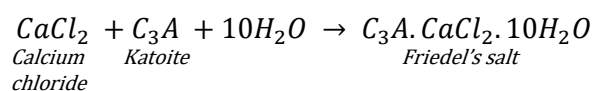
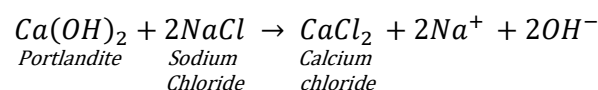
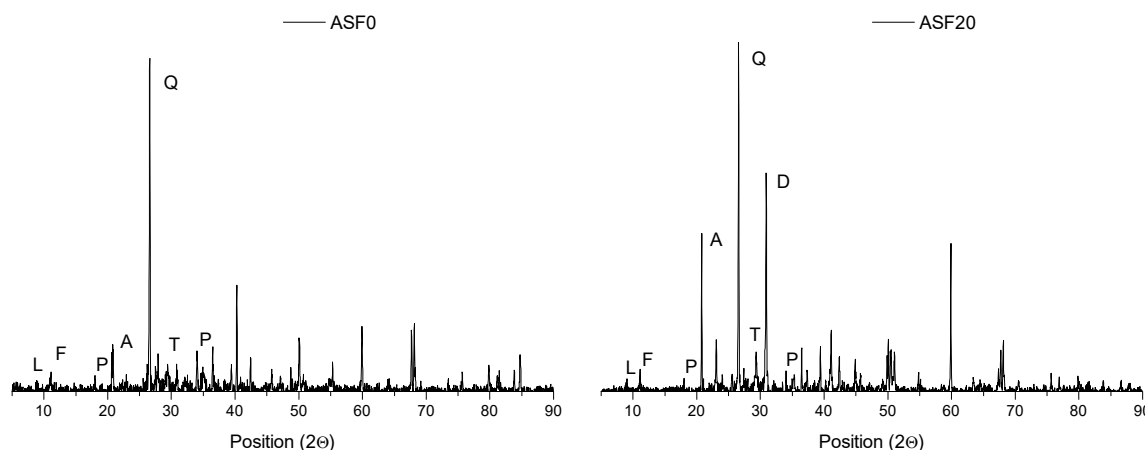


**Fig. 4.76: Position of colour change front of mixes after exposure to sodium chloride**

The binding of chloride ions takes place by consumption of portlandite ( $\text{Ca}(\text{OH})_2$ ) and subsequent formation of calcium chloride ( $\text{CaCl}_2$ ). Calcium chloride further reacts with calcium aluminate hydrate ( $\text{C}_3\text{AH}_6$  - katoite) to form Friedel's salt ( $\text{C}_3\text{A} \cdot \text{CaCl}_2 \cdot 10\text{H}_2\text{O}$ ) as detailed by Yuan et al. (2009). These chemical reactions can be written as:



Presence of Portlandite in mixes ASF0 and ASF20 after 28 days of curing has already been confirmed in the X – ray diffractograms by the occurrence of peaks at  $18^\circ$  and  $34^\circ$  (Fig. 4.30). As seen in Fig. 4.77, the intensity of these peaks has reduced after exposure to sodium chloride for 84 days. From this it can be confirmed that portlandite has been converted into Friedel’s salt. This mineral can be identified by the formation of a peak at  $11.4^\circ$  (Fig. 4.77).



L – Amstallite; P – Portlandite; F – Friedel’s salt; Q – Quartz; T – CSH; D – Dolomite; A - Gibbsite

**Fig. 4.77: X-ray diffraction pattern of ASF0 and ASF20 after 84 days of exposure to sodium chloride**

However for mix ASF20, the initial portlandite content was very much less when compared to ASF0 (refer Fig. 4.30). Hence apart from the formation of Friedel’s salt, the other most significant change noted for this mix is the change in wavenumber associated with Si-O-Si/Si-O-Al polymeric chain which had increased to  $1034\text{ cm}^{-1}$  from  $1007\text{ cm}^{-1}$  as shown in Fig. 4.78 This can be linked to release of Al ions from gismondine (CASH), resulting into the formation of gibbsite ( $\text{Al}(\text{OH})_3$ ). This might be the reason in increase in intensity of the peak at diffraction angle at  $20.78^\circ$  in the X-ray diffractogram (Fig. 4.77) and increase in prominence of the band around  $1080\text{ cm}^{-1}$  in the FTIR spectra (Fig. 4.78). As shown in Fig. 4.77, there is also formation of new peak at  $8.93^\circ$  which is present in both ASF0 and ASF20 mixes and can be associated to a mineral (amstallite) which is similar to gismondine but with the inclusion of chloride ions. Apart from this, chloride ions can also be bound physically by CSH. This binding can be by chemisorption, or can be held in their interlayers or bound intimately in its lattice.

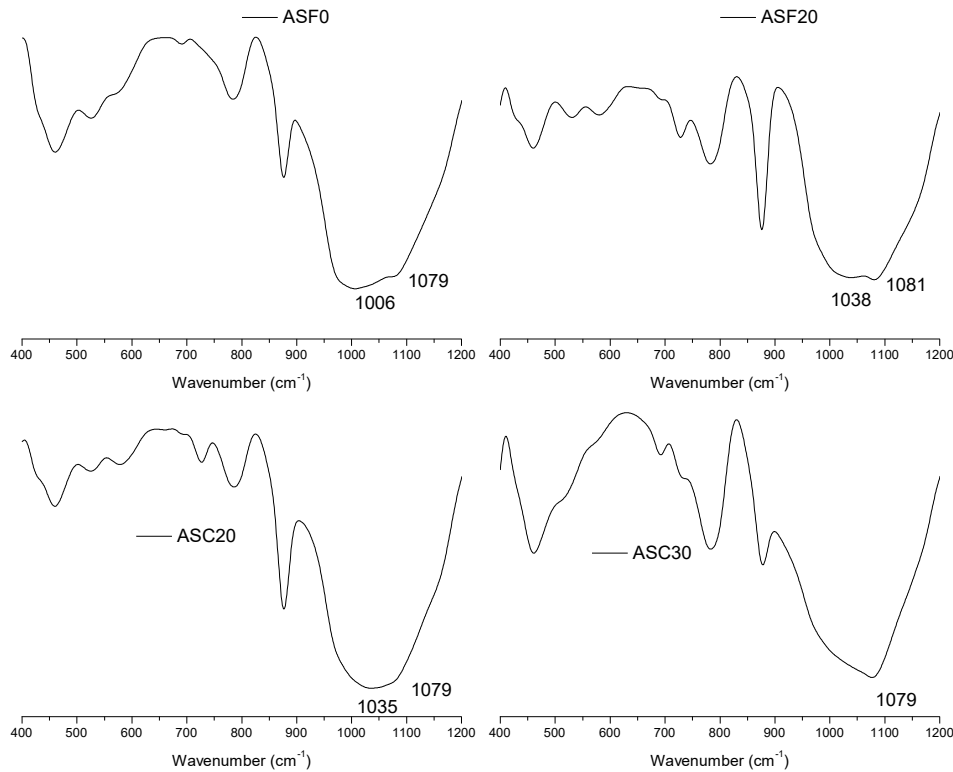


**Fig. 4.78: FTIR spectra of mixes ASF0, ASF20, ASC20 and ASC30 after 84 days of exposure to sodium chloride**

Hence it can be concluded that, in the presence of sufficient portlandite, NaCl reacts with it to form  $\text{CaCl}_2$ , and then Friedel's salt. But with mixes with MS where sufficient portlandite is not available, calcium aluminium silicate hydrate decomposes to gibbsite and amstallite like minerals and binds the free chloride. These mixes have greater amount of gismondine and CSH and therefore greater is the chloride binding capacity hence lesser is the extent of free chloride when compared with mix ASF0. Therefore mixes with MS have greater resistance to chloride ions penetration. With regard to the variation of depth of free chloride ions for series D, it can be considered analogous to series A.

#### **4.5.8 Carbonation:**

For evaluating mortar mixes resistance to carbonation, samples of size 40 x 40 x 160 mm were coated on all sides by epoxy paint, except one of the 40 x 40 mm face. Then these samples were conditioned in a carbonation chamber where the concentration of carbon di-oxide was maintained at 5% with a relative humidity of 50%. Extent of carbonation was measured at the end of 1, 7, 14, 28, 56 and 84 days. At the end of each

exposure period the samples were split open along their longitudinal dimension and sprayed by a suitable phenolphthalein solution. The depth at which the mortar specimens' colour changes to pink is graphically represented in Fig. 4.79. From this figure, as noted in chloride penetration test, there was no perceivable variation in performance of the series A. But for series D there is appreciable change noted when MS was introduced in to the mortars. Greatest reduction in carbonation was seen for mix DSC20 (46%) and the least for DSC30 (13%). This variation among mixes with MS in series D seems to be in line with their void content (Table 4.3).

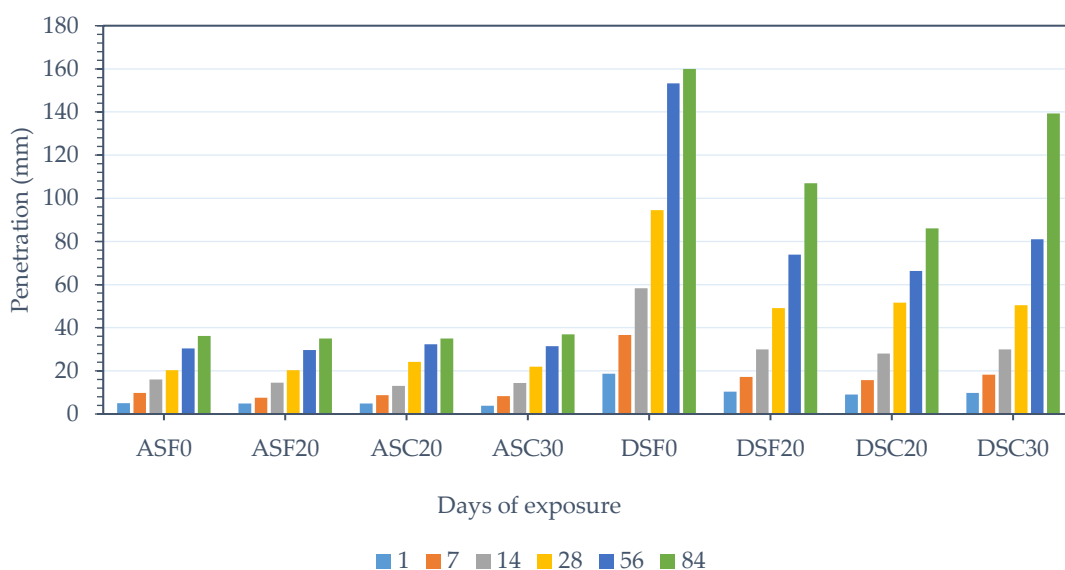
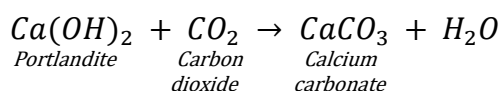
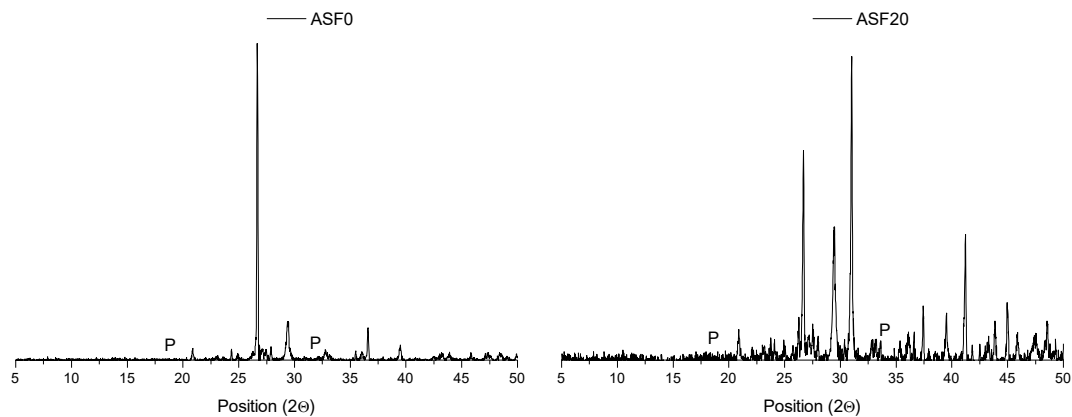
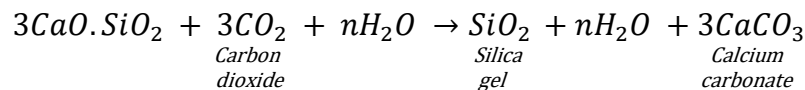


Fig. 4.79: Position of colour change front of mixes after exposure to carbon dioxide

Carbonation occurs by conversion of portlandite into calcium carbonate. This can be noted by the disappearance of the peak at angles of  $18^\circ$  and  $34^\circ$  after 84 days of exposure (Fig. 4.80). The calcium carbonate formed cannot be traced in the X-ray diffractograms because of overlap of peaks among other major minerals. The chemical reaction given by Savija and Lukovic (2016) is



The next significant change occurs is the decalcification of CSH and CASH in which calcium ions are removed from its' interlayers. This leads to the increase in silicate chain length and formation of amorphous silica. According to Savija and Lukovic (2016) the chemical reaction can be given as



P – Portlandite

**Fig. 4.80: X-ray diffraction pattern of ASF0 and ASF20 after 84 days of carbonation**

The increase in chain length is characterized by the shift in wavenumber from 1010  $\text{cm}^{-1}$  to 1055  $\text{cm}^{-1}$  as seen in Fig. 4.81. Using nuclear magnetic resonance (NMR) technique Sevelsted and Skibsted (2015) were able to detect the effect of carbonation on CASH. According to them, CASH too undergoes decalcification where the aluminium ions are also released and get embedded in the amorphous silica phase itself.

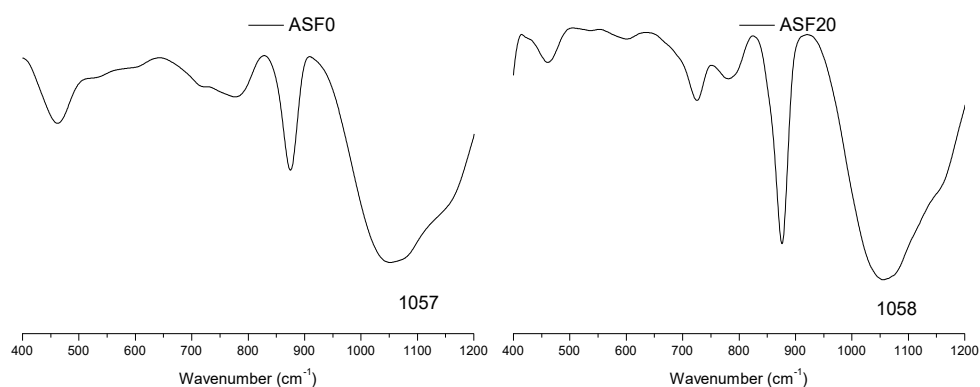


**Fig. 4.81: FTIR spectra of ASF0 and ASF20 after 84 days of carbonation**

Mixes without MS possess more portlandite than the mixes with MS. But however this has not made any significant variation in all the above mentioned changes in the

microstructure for series A. This might be because of the fact mixes with MS have denser impermeable pore space as shown in Table 4.3. On formation of calcite this density further increases which prevents further carbonation. For series D, despite the fact that reduction in pH happens only to a lesser depth, the carbonation shrinkage (Fig. 4.82) seems to be more in mixes with MS than DSF0.

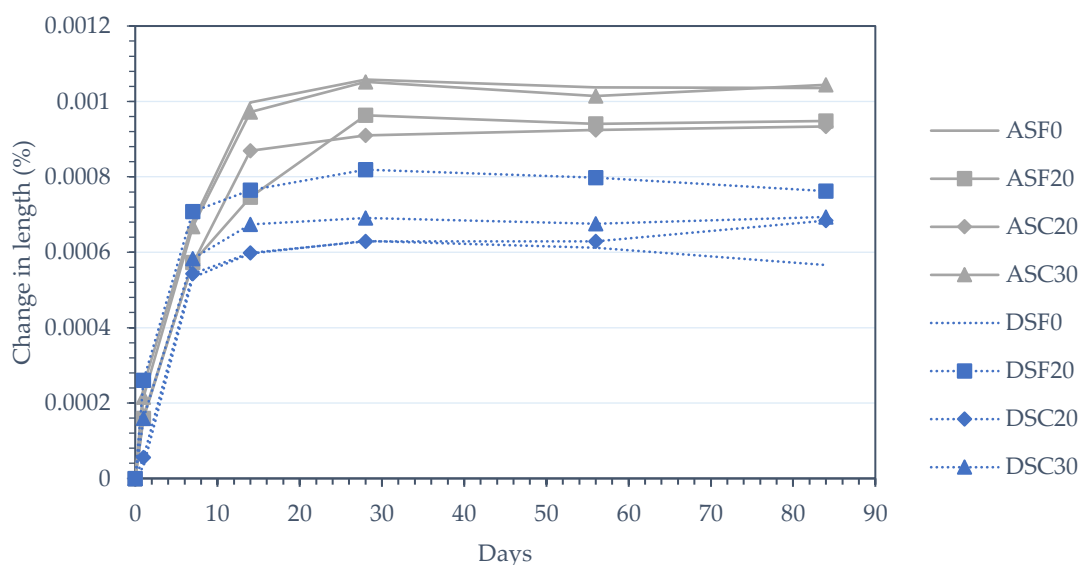


Fig. 4.82: Change in length undergone by mixes after carbonation

Maximum variation can be seen for mix DSF20 which has carbonation shrinkage higher by 35% when compared to DSF0. This shrinkage is a consequence of decalcification of CSH and CASH minerals, which would imply that in the absence of portlandite, CSH and CASH are more vulnerable and hence carbonation shrinkage would be greater than that noticed in mixes without MS.

#### 4.5.9 Alkali carbonate reaction:

To check whether the dolomite aggregate causes any expansion of the mortar specimens due to alkali carbonate reaction, five mortar bars were moist cured for three months. The increase in length of the mortar bars is as shown in Fig. 4.83 for series A (1:3) and D (1:4). The variation in change in length among all the mixes shows that the specimens mixes made with dolomite aggregate do not undergo any detrimental volume expansion. For both the series, change in length of mixes with 20% MS is very similar to the mixes made with only river sand. In turn, at 30% replacement, the increase in length of mortar bars is convincingly lesser than the control mixes. For series A and D it is 12% and 33% lesser respectively. A similar trend was observed by Štukovnik et al. (2014), when they

replaced a reactive cherty sand by limestone fines. Increase in length was almost completely prevented on complete substitution. Prinčič et al. (2013) also observed that the length change undergone by mortar prisms with limestone and dolostone aggregates was the same over a three month period. Hence it can be concluded that as conventionally understood, alkali carbonate reaction which involves dedolomitization of dolomite aggregate is not accompanied by increase in volume of the cement paste.

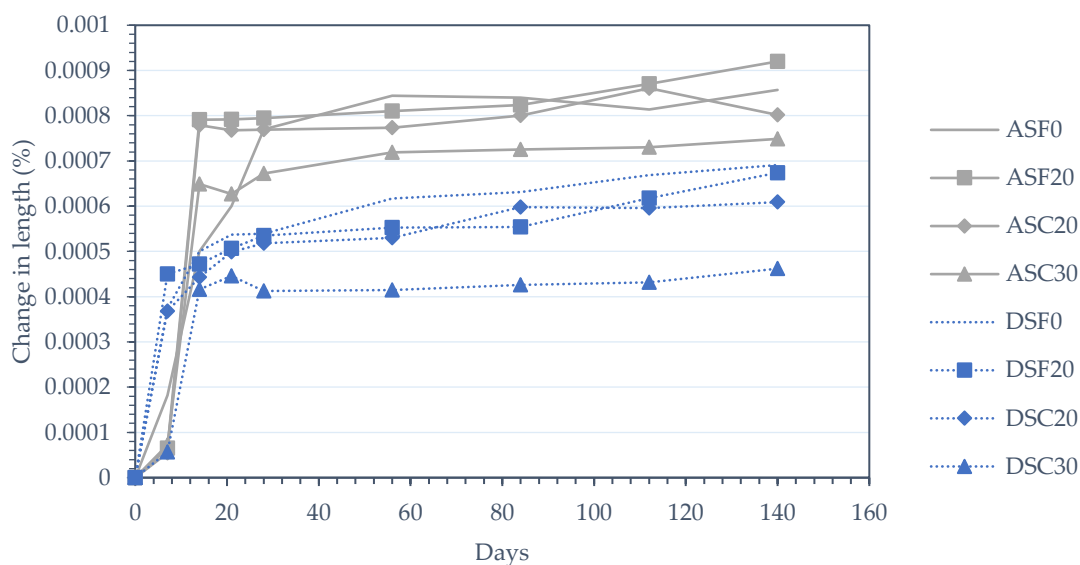


**Fig. 4.83: Change in length of specimens due to alkali aggregate reaction**

Also, the dolomite aggregate used here can be said to be not potentially deleteriously reactive since the expansion of the mortar bars is lesser than 0.015% at the end of three month test period as per ASTM C 1105 (2008).

#### 4.6 Consolidated evaluation

The normalized form of three indices, viz., mechanical, environmental and economical have been graphically indicated in the Fig. 4.84. From this figure we can see that in terms of environmental performance, mixes made with MS are very similar to the control mortar for series A. For series D, the advantage is little higher, largely due to the reduction in water requirement for the production of these mixes with MS. Economic evaluation shows that there is a minimal advantage in cost due to reduced water consumption in production of mortars. However this is negated by the cost involved in processing MS altogether even at substitution of 20% for rich mixes with coarse sand. For the lean mix there is no variation at all.



Performance evaluation of mixes with regard to mechanical and durability constrains shows that mixes of proportion 1:3 (series A) show substantial improvement irrespective of sand grading on inclusion of MS. For a mix proportion of 1:6, a coarser sand grading is best suited for combining with MS. For the mix containing 80% coarse sand and 20% MS, (mix DSC20) most significant improvement is noticed in properties like adhesive and tensile bond strengths when compared to the mix containing 80% fine sand and 20% MS (mix DSF20) as seen from the earlier sections (Table 4.3). DSC20 has reduced shrinkage also. This particular mix has the least porosity which enables it to absorb the less water and hence improves resistance against sulphate and acid attack and chloride ion penetration. Hence all these advantages has resulted in enhancement in overall performance of mix as seen in Fig. 4.84 when compared to the other two mixes with MS of series D (1:6). Performance dips when the substitution is greater than 20% for both mix proportions.

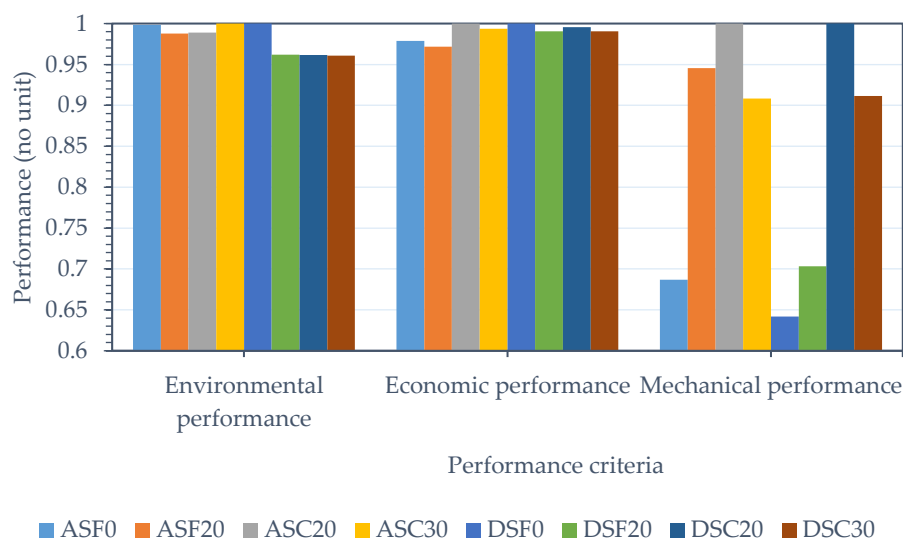


**Fig. 4.84: Performance evaluation of mortar mixes**

On consolidating all the three performance criterion (Fig. 4.85), it can be seen that MS incorporation in mortar mixes is best suited when combined with a relatively coarser river sand at a substitution level of 20%. The lean mix proportion of 1:6 seems to benefit more than the rich mix. Mainly due to the reduction in mechanical performance and slight increase in cost, the consolidated performance sees a dip when the substitution is increased to 30%.

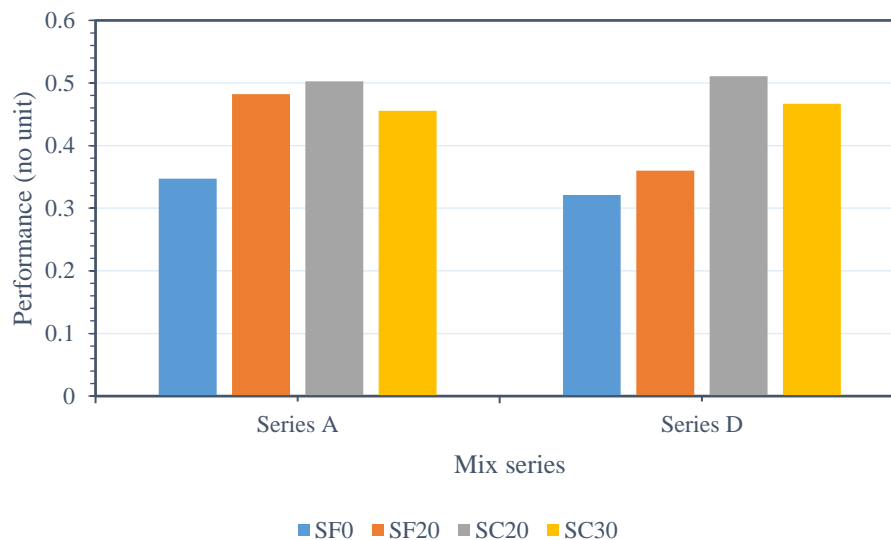


**Fig. 4.85: Consolidated performance evaluation of mortar mixes**

Hence it can be concluded that, at 20% substitution maximum benefits can be derived in terms of mechanical, environmental and economic parameters. When a coarser sand is used for lean mix proportion (series D), significant gain in performance can be achieved as compared to mixes prepared with fine sand as noticed in Fig. 4.85.

## CHAPTER 5

### CONCLUSIONS

This study is a comprehensive evaluation of marble powder (dried marble slurry) as a substitute for fine aggregate for the production of cement mortars of four different mix proportions of 1:3, 1:4, 1:5 and 1:6. An attempt has also been made to improve the extent of utilization by using coarse river sand. Apart from the basic parameters, crucial properties like tensile bond strength between mortars and masonry, drying shrinkage, resistance to acid attack, wet – dry cycles and salt crystallization have been evaluated for the first time. The properties of mortars have also been consolidated based on their physical, mechanical, durability, economic and environmental performance. The major findings from the study are drawn below:

1. Due to marble powder's thixotropic property and fineness, its volumetric substitution by 20% in place of river sand reduces the water requirement of all mix proportions.
2. Compressive resistance of mixes with 20% dried marble powder in place of fine aggregate have shown maximum strength when compared to corresponding control mortars. This improvement is basically due to reduced water content required in these mixes.
3. Mixes containing marble powder up to 60% volume as fine aggregate have compressive strength comparable with control mortars. This can be attributed to the capability of marble powder to accelerate the hydration of tricalcium silicate ( $C_3S$ ). Tricalcium aluminate ( $C_3A$ ) also hydrates to form calcium carbo-aluminates which densify the microstructure, which was supported by the SEM, TGA and FTIR techniques.
4. Mortar mixes containing 20% - 30% of fine aggregate as MS, undergo same amount of drying shrinkage as that observed in control mixes.
5. With regard to adhesive and tensile bond strengths, best results can be derived when fine/coarse river sand is replaced by 20% marble powder for 1:3 and 1:4 mix proportions and 40% for 1:5 and 1:6 mix proportions. At these substitution levels, the replacement of sand by MS and reduction in water content help in improving

the strength of hydration product developed at the interface of mortar and bricks.

6. Dynamic modulus of elasticity has a peak value at 20% substitution of river sand by marble powder for all mortars irrespective of sand grading. Such mixes have marginal variation in water absorption and porosities values when compared to their control counterparts.

The dominating characteristics that limit the usage of marble incorporated mortars and renderings to 20% - 30% substitution are their water requirement to achieve necessary workability, water absorption capacity and drying shrinkage. For rich mixes (1:3 and 1:4), in addition to the above parameters, tensile bond and adhesive strength also restrict the utilization to the same extent. Therefore, further studies on durability were limited to substitution levels of 20% - 30% in 1:3 and 1:6 mix proportions only.

7. Since the mixes with MS are more stiff than conventional mortars, inclusion of MS proves to be detrimental when they were subjected to salt crystallization. However, mortars with mix proportion 1:3 with up to 30% marble powder have a similar strength gain pattern when compared to that of control mortars.
8. When mortar mixes are subjected to wet – dry cycles, the residual compressive strength of rich mixes with marble powder is higher by 23% to 35% when compared to the corresponding control mortars. In case of lean mixes with MS, it is higher by at least 1.7 to 2.2 times when compared to the mix with only river sand at the end of the test period.
9. Mortar mixes produced by replacing 20% of fine aggregate with marble powder undergo same extent of weight loss when compared to control mortars when subjected to rapid freezing and thawing. Their residual strength is also comparable at the end of the test regime.
10. Replacement of quartz river sand by MS reduces the damage caused by the inversion of quartz from  $\alpha$  to  $\beta$  form. Hence, mortar mixes with marble powder reduce the susceptibility of drop in compressive strength after exposure to standard fire at a temperature of 600°C in a specially fabricated set up at MNIT, Jaipur. Above 800°C, mixes with fine sand and 20% marble powder have compressive strength at par with control mortars.
11. Dried marble powder's acid neutralization capacity proves very beneficial in

reducing the vulnerability of mortar mixes when exposed to a sulphuric acid medium. The residual compressive strength of mixes with marble powder was higher than conventional mortars at the end of 84 days test period. This was quite in contrast to the general belief that utilization of acid soluble MS may lead to reduced resistance to an attack from acidic agents.

12. Mixes with marble powder have lesser portlandite and calcium aluminate hydrate content. Reduction of these two minerals reduces the vulnerability to attack from sulphate reagents. Hence rich mixes with dried marble powder have residual compressive strength higher by 26% to 47% when compared to the conventional mortars at the end of 168 days of test period. This advantage is more significant in case of lean mix, where the control mortar had no residual strength at all.
13. With regard to the ability to bind chloride ions, no change was noticed in performance for the rich mix with incorporation of marble powder. For the lean mix there was significant improvement (35% – 45%) in chemical and physical binding of chloride ions due to enhanced hydration when MS was used for partial replacement of fine aggregate.
14. Lean mixes with MS show significant reduction in carbonation by 15% to 46% when compared to the control mortar. However due to unavailability of portlandite leads decalcification of CSH/CASH and hence carbonation shrinkage is higher by 34%. Hence such mixes can be used in non – industrial zones only. For the rich mixes with MS, carbonation resistance and carbonation shrinkage are comparable to the control mortar.
15. When tested for alkali carbonate reactivity, the length change of specimens is within the specified limits of 0.015% for all the mixes with marble powder as per ASTM C 1105.
16. On consolidating all the evaluating parameters, it can be concluded that 20% substitution of fine aggregate by marble powder can be considered ideal for all mix proportions. Environmental performance of lean mixes with MS is appreciably higher than the control mortar. These mixes can be produced at the same cost of conventional mortars.

Based on the properties on the mortars with MS summarized above, it can be concluded that such mortars can find the following areas of utilization:

1. Irrespective of the sand grading, cement – sand – marble powder (CSM) based mortars can be used for all interior plastering and masonry work of buildings. If the exterior surfaces are not exposed to any aggressive environment these mortars can also be used for exterior elements.
2. CSM mortars will have better service life when compared to conventional mortars when used for the construction of foundations of masonry buildings in soils contaminated by sulphate agents.
3. As seen from the results of mortars subjected to acid attack, the extent of acid soluble marble waste seems to be within the threshold limits for the CSM mortars. In turn, the residual performance of mortars with marble waste is higher than conventional mortars even in a recharged acidic medium. Therefore they can be used as a lining for pipes which carry sewage and acidic industrial waste water.
4. Based on the results obtained from chloride ion penetration tests, CSM mortars can also be used along with metal lath for stucco and rendering purposes without the concern of corrosion.
5. The water absorption capacity of CSM mortars is also comparable to conventional mortars. Hence they can be used in the construction of canal lining made with masonry.

Limitations of mortars with marble powder are

1. When there is susceptibility of high thermal gradient between external and interior surfaces of a dwelling with attack salt contaminated water or when there is high temperature variation during the day and night, MS has to be used only with a rich mix proportion.
2. If there is susceptibility of exposure to sub-zero temperatures followed by thawing CSM mortars are to be avoided.

Based on the aggressiveness of the environment, utilization of such mortars should be limited as given in the following table.

Table 5.1: Extent of utilization of CSM mortars based on durability criteria

<b>Durability Criteria</b>	<b>Plastering</b>	<b>Masonry</b>
<b>Salt crystallization, wet – dry cycles and carbonation</b>	1:3	1:3
<b>Sulphate and acid attack and corrosion</b>	1:3 and 1:6	1:3 and 1:6
<b>Freezing and thawing</b>	Not permissible	Not permissible

### *Scope for future work*

1. Production of geopolymer concretes involves using alkaline solutions for the activation of slags. As dolomitic marble is also unstable in an alkaline environment. The effect on incorporating dolomitic marble on modification of strength development of such concretes can be evaluated.
2. Cement binders containing slags and pozzolanas have reduced rate of strength gain when compared to OPC. Dolomitic marble powder has the ability to accelerate the hydration of tri-calcium silicate. Hence marble powder can be used to accelerate the primary hydration reaction of composite cement binders and reduce the above disadvantage.
3. On hydration, tricalcium aluminate forms metastable hydrates which later get converted to stable minerals. However formation of the final tri-calcium aluminate hydrate from the other metastable hydrates is accompanied by increase in porosity and fall in strength. Dolomitic marble powder can prevent the reduction in strength by the formation of calcium carbo-aluminates instead of tri – calcium aluminate. Hence a study can be taken up to evaluate the possibility of such a change.
4. Due to the ability of marble powder to improve cohesivity, its effect on segregation resistance of harsh lean mixes can be evaluated.
5. Marble powder along with quarry sand can be tested as a potential replacement for entire river sand for the production of mortars. Marble mining waste of proper particle size distribution can also be used along with marble powder.
6. A proper three phase mix proportion of cement – sand – marble powder can be derived such that it can be easily be replicated on field. These proportions should be equivalent to mix proportions 1:3, 1:4, 1:5 and 1:6 with 20% of fine aggregate as marble waste.

7. Since inclusion of marble waste is accompanied by improvement in compressive strength, trials can be carried out where cement quantity is reduced so that the required performance is achieved with optimum cement content.

Hence, based on the learnings from the current study, it can be concluded that marble waste when used in appropriate size and quantity can have appreciable effect on the behaviour of cement composites. Incorporation of such industrial by products for the production of construction materials will also reduce dependency on natural resources.



## REFERENCES

- Acchar, W., Vieira, F.A., Hotza, D., 2006. Effect of marble and granite sludge in clay materials. *Mater. Sci. Eng. A* 419, 306–309. <https://doi.org/10.1016/j.msea.2006.01.021>
- Acchar, W., Vieira, F.A., Segadães, A.M., 2006. Using ornamental stone cutting rejects as raw materials for red clay ceramic products: Properties and microstructure development. *Mater. Sci. Eng. A* 435–436, 606–610. <https://doi.org/10.1016/j.msea.2006.07.091>
- Agarwal, S.K., Gulati, D., 2006. Utilization of industrial wastes and unprocessed micro-fillers for making cost effective mortars. *Constr. Build. Mater.* 20, 999–1004. <https://doi.org/10.1016/j.conbuildmat.2005.06.009>
- Akbulut, H., Gürer, C., 2007. Use of aggregates produced from marble quarry waste in asphalt pavements. *Build. Environ.* 42, 1921–1930. <https://doi.org/10.1016/j.buildenv.2006.03.012>
- Akhtar, A., Sarmah, A.K., 2018. Construction and demolition waste generation and properties of recycled aggregate concrete: A global perspective. *J. Clean. Prod.* 186, 262–281. <https://doi.org/10.1016/j.jclepro.2018.03.085>
- Akinwumi, I.I., Booth, C.A., 2015. Experimental insights of using waste marble fines to modify the geotechnical properties of a lateritic soil. *J. Environ. Eng. Landsc. Manag.* 23, 121–128. <https://doi.org/10.3846/16486897.2014.1002843>
- Aliabdo, A.A., Abd Elmoaty, A.E.M., Auda, E.M., 2014. Re-use of waste marble dust in the production of cement and concrete. *Constr. Build. Mater.* 50, 28–41. <https://doi.org/10.1016/j.conbuildmat.2013.09.005>
- Alyamac, K.E., Aydin, A.B., 2015. Concrete properties containing fine aggregate marble powder. *KSCE J. Civ. Eng.* 19, 2208–2216. <https://doi.org/10.1007/s12205-015-0327-y>
- Alyamaç, K.E., Ince, R., 2009. A preliminary concrete mix design for SCC with marble powders. *Constr. Build. Mater.* 23, 1201–1210. <https://doi.org/10.1016/j.conbuildmat.2008.08.012>
- André, A., de Brito, J., Rosa, A., Pedro, D., 2014. Durability performance of concrete incorporating coarse aggregates from marble industry waste. *J. Clean. Prod.* 65, 389–396. <https://doi.org/10.1016/j.jclepro.2013.09.037>
- Antiohos, S., Tsimas, S., 2004. Activation of fly ash cementitious systems in the presence of quicklime Part I. Compressive strength and pozzolanic reaction rate. *Cem. Concr. Res.* 34, 769–779. <https://doi.org/10.1016/j.cemconres.2003.08.008>
- Ashish, D.K., 2018. Feasibility of waste marble powder in concrete as partial substitution of cement and sand amalgam for sustainable growth. *J. Build. Eng.* 15, 236–242. <https://doi.org/10.1016/j.jobe.2017.11.024>
- ASTM C 1105, 2008. Standard Test Method for Length Change of Concrete Due to Alkali-Carbonate Rock Reaction, Annual Book of ASTM Standards. ASTM International (Pennsylvania, USA). <https://doi.org/10.1520/C1105-08A.2>
- ASTM C 1148, 2002. Standard Test Method for Measuring the Drying Shrinkage of Masonry Mortar. Annual Book of ASTM Standards (Pennsylvania, USA). <https://doi.org/10.1520/C1148-92AR08.2>
- ASTM C 1403, 2006. Standard Test Method for Rate of Water Absorption of Masonry Mortars. Annual Book of ASTM Standards (Pennsylvania, USA). <https://doi.org/10.1520/C1403-15.2>
- ASTM C 185, 2002. Standard Test Method for Air Content of Hydraulic Cement Mortar. Annual Book of ASTM Standards (Pennsylvania, USA). <https://doi.org/10.1520/C0185-08.2>

ASTM C 267, 2001. Standard Test Methods for Chemical Resistance of Mortars, Grouts, and Monolithic Surfacing and Polymer Concretes. Annual Book of ASTM Standards (Pennsylvania, USA).

ASTM C 307, 2003. Standard Test Method for Tensile Strength of Chemical - Resistant Mortar, Grouts, and Monolithic Surfacing. ASTM International (Pennsylvania, USA).

ASTM C 348, 2002. Standard Test Method for Flexural Strength of Hydraulic-cement Mortars. Annual Book of ASTM Standards (Pennsylvania, USA).

ASTM C 642, 2006. Standard Test Method for Density, Absorption, and Voids in Hardened Concrete. Annual Book of ASTM Standards (Pennsylvania, USA). <https://doi.org/10.1520/C0642-13.5>.

ASTM C 666, 2003. Standard Test Method for Resistance of Concrete to Rapid Freezing and Thawing. ASTM International. ASTM International (Pennsylvania, USA). <https://doi.org/10.1520/C0666>

ASTM C 952, 2002. Standard Test Method for Bond Strength of Mortar to Masonry Units. ASTM International (Pennsylvania, USA).

ASTM C1012/C1012M-15, 2015. Standard test method for length change of hydraulic-cement mortars exposed to a sulfate solution, ASTM International, West Conshohocken, PA. <https://doi.org/10.1520/C1012>

Aye, T., Oguchi, C.T., Takaya, Y., 2010. Evaluation of sulfate resistance of Portland and high alumina cement mortars using hardness test. *Constr. Build. Mater.* 24, 1020–1026. <https://doi.org/10.1016/j.conbuildmat.2009.11.016>

Bacarji, E., Toledo Filho, R.D., Koenders, E.A.B., Figueiredo, E.P., Lopes, J.L.M.P., 2013. Sustainability perspective of marble and granite residues as concrete fillers. *Constr. Build. Mater.* 45, 1–10. <https://doi.org/10.1016/j.conbuildmat.2013.03.032>

Barthelmy, D., 2003. Mineralogy Database [WWW Document]. URL <http://webmineral.com/data/Magnesiostauroilite.shtml#.WqyonefhU2w> (accessed 3.17.18).

Behera, M., Bhattacharyya, S.K., Minocha, A.K., Deoliya, R., Maiti, S., 2014. Recycled aggregate from C&D waste & its use in concrete - A breakthrough towards sustainability in construction sector: A review. *Constr. Build. Mater.* 68, 501–516. <https://doi.org/10.1016/j.conbuildmat.2014.07.003>

Beyene, M., Snyder, A., Lee, R.J., Blaszkiewicz, M., 2013. Alkali Silica Reaction (ASR) as a root cause of distress in a concrete made from Alkali Carbonate Reaction (ACR) potentially susceptible aggregates. *Cem. Concr. Res.* 51, 85–95. <https://doi.org/10.1016/j.cemconres.2013.04.014>

Bilgin, N., Yeprem, H. a., Arslan, S., Bilgin, a., Günay, E., Maroglu, M., 2012. Use of waste marble powder in brick industry. *Constr. Build. Mater.* 29, 449–457. <https://doi.org/10.1016/j.conbuildmat.2011.10.011>

Bilir, T., Gencel, O., Topcu, I.B., 2015. Properties of mortars with fly ash as fine aggregate. *Constr. Build. Mater.* 93, 782–789. <https://doi.org/10.1016/j.conbuildmat.2015.05.095>

Binici, H., Kaplan, H., Yilmaz, S., 2007. Influence of marble and limestone dusts as additives on some mechanical properties of concrete. *Sci. Res. Essays* 2, 372–379.

Binici, H., Shah, T., Aksogan, O., Kaplan, H., 2008. Durability of concrete made with granite and marble as recycle aggregates. *J. Mater. Process. Technol.* 208, 299–308. <https://doi.org/10.1016/j.jmatprotec.2007.12.120>

Bisht, K., Ramana, P.V., 2017. Evaluation of mechanical and durability properties of crumb rubber concrete. *Constr. Build. Mater.* 155, 811–817. <https://doi.org/10.1016/j.conbuildmat.2017.08.131>

- Bogas, J.A., de Brito, J., Ramos, D., 2015. Freeze-thaw resistance of concrete produced with fine recycled concrete aggregates. *J. Clean. Prod.* 1–13. <https://doi.org/10.1016/j.jclepro.2015.12.065>
- BS EN 1015, 2000. Methods of test for mortar for masonry - Part 12: Determination of adhesive strength of hardened rendering and plastering mortars on substrates. British Standards Institution.
- BS EN 12370, 1999. Natural stone test methods - Determination of resistance to salt crystallisation. British Standards Institution.
- BS EN 14066, 2013. Natural stone Test methods Part 6 : Determination of resistance to ageing by thermal shock. British Standards Institution.
- Buyuksagis, I.S., Uygunoglu, T., Tatar, E., 2017. Investigation on the usage of waste marble powder in cement-based adhesive mortar. *Constr. Build. Mater.* 154, 734–742. <https://doi.org/10.1016/j.conbuildmat.2017.08.014>
- Carlson, E.T., Berman, H.A., 1960. Some observations on the calcium aluminate carbonate hydrates. *J. Res. Natl. Bur. Stand. Sect. A Phys. Chem.* 64A, 333. <https://doi.org/10.6028/jres.064A.032>
- Chandra, S., Kumar, P., Feyissa, B.A., 2002. Use of Marble Dust in Road Construction. *Road Mater. Pavement Des.* 3, 317–330. <https://doi.org/10.1080/14680629.2002.9689928>
- Chawla, A., Kabeer, K.I.S.A., Vyas, A.K., 2018. Evaluation of strength and durability of lean concrete mixes containing marble waste as fine aggregate. *Eur. J. Environ. Civ. Engi* 1–16. <https://doi.org/https://doi.org/10.1080/19648189.2018.1471009>
- Chukanov, N. V., 2014. Infrared spectra of minerals and reference samples data, Infrared spectra of mineral species: Extended library. Springer. <https://doi.org/10.1007/978-94-007-7128-4>
- Çınar, M.E., Kar, F., 2018. Characterization of composite produced from waste PET and marble dust. *Constr. Build. Mater.* 163, 734–741. <https://doi.org/10.1016/j.conbuildmat.2017.12.155>
- Corinaldesi, V., Moriconi, G., Naik, T.R., 2010. Characterization of marble powder for its use in mortar and concrete. *Constr. Build. Mater.* 24, 113–117. <https://doi.org/10.1016/j.conbuildmat.2009.08.013>
- Demirel, B., 2010. The effect of the using waste marble dust as fine sand on the mechanical properties of the concrete. *Int. J. Phys. Sci.* 5, 1372–1380. <https://doi.org/10.1016/j.envint.2006.11.003>
- Dong, L., Wang, Y., Scipioni, A., Park, H.-S., Ren, J., 2017. Recent progress on innovative urban infrastructures system towards sustainable resource management. *Resour. Conserv. Recycl.* <https://doi.org/10.1016/j.resconrec.2017.02.020>
- Eliche-Quesada, D., Corpas-Iglesias, F.A., Pérez-Villarejo, L., Iglesias-Godino, F.J., 2012. Recycling of sawdust, spent earth from oil filtration, compost and marble residues for brick manufacturing. *Constr. Build. Mater.* 34, 275–284. <https://doi.org/10.1016/j.conbuildmat.2012.02.079>
- Ercikdi, B., Külekci, G., Yılmaz, T., 2015. Utilization of granulated marble wastes and waste bricks as mineral admixture in cemented paste backfill of sulphide-rich tailings. *Constr. Build. Mater.* 93, 573–583. <https://doi.org/10.1016/j.conbuildmat.2015.06.042>
- Ergün, A., 2011. Effects of the usage of diatomite and waste marble powder as partial replacement of cement on the mechanical properties of concrete. *Constr. Build. Mater.* 25, 806–812. <https://doi.org/10.1016/j.conbuildmat.2010.07.002>
- Farinha, C., De Brito, J., Veiga, R., 2012. Incorporation of fine concrete aggregates in mortars. *Constr. Build. Mater.* 36, 960–968. <https://doi.org/10.1016/j.conbuildmat.2012.06.031>

- Fernández-caliani, J.C., Barba-brioso, C., 2010. Metal immobilization in hazardous contaminated minesoils after marble slurry waste application . A field assessment at the Tharsis mining district ( Spain ) 181, 817–826. <https://doi.org/10.1016/j.jhazmat.2010.05.087>
- Fiksel, J., Lal, R., 2018. Transforming waste into resources for the Indian economy. *Environ. Dev.* 0–1. <https://doi.org/10.1016/j.envdev.2018.02.002>
- Földvári, M., 2011. Handbook of the thermogravimetric system of minerals and its use in geological practice, *Central European Geology*. <https://doi.org/10.1556/CEuGeol.56.2013.4.6>
- Gameiro, F., De Brito, J., Correia da Silva, D., 2014. Durability performance of structural concrete containing fine aggregates from waste generated by marble quarrying industry. *Eng. Struct.* 59, 654–662. <https://doi.org/10.1016/j.engstruct.2013.11.026>
- Gartner, E., Hirao, H., 2015. A review of alternative approaches to the reduction of CO<sub>2</sub> emissions associated with the manufacture of the binder phase in concrete. *Cem. Concr. Res.* 78, 126–142. <https://doi.org/10.1016/j.cemconres.2015.04.012>
- Gartner, E.M., MacPhee, D.E., 2011. A physico-chemical basis for novel cementitious binders. *Cem. Concr. Res.* 41, 736–749. <https://doi.org/10.1016/j.cemconres.2011.03.006>
- Gencel, O., Ozel, C., Koksall, F., Erdogmus, E., Martínez-Barrera, G., Brostow, W., 2012. Properties of concrete paving blocks made with waste marble. *J. Clean. Prod.* 21, 62–70. <https://doi.org/10.1016/j.jclepro.2011.08.023>
- Gurbuz, A., 2015. Marble powder to stabilise clayey soils in sub-bases for road construction. *Road Mater. Pavement Des.* 16, 481–492. <https://doi.org/10.1080/14680629.2015.1020845>
- Haach, V.G., Vasconcelos, G., Loureno, P.B., 2011. Influence of aggregates grading and water/cement ratio in workability and hardened properties of mortars. *Constr. Build. Mater.* 25, 2980–2987. <https://doi.org/10.1016/j.conbuildmat.2010.11.011>
- Hameed, M.S., Sekar, A.S.S., Balamurugan, L., Saraswathy, V., 2012. Self-compacting concrete using marble sludge powder and crushed rock dust. *KSCE J. Civ. Eng.* 16, 980–988. <https://doi.org/10.1007/s12205-012-1171-y>
- Hebhoub, H., Aoun, H., Belachia, M., Houari, H., Ghorbel, E., 2011. Use of waste marble aggregates in concrete. *Constr. Build. Mater.* 25, 1167–1171. <https://doi.org/10.1016/j.conbuildmat.2010.09.037>
- Horszczaruk, E., Sikora, P., Cendrowski, K., Mijowska, E., 2017. The effect of elevated temperature on the properties of cement mortars containing nanosilica and heavyweight aggregates. *Constr. Build. Mater.* 137, 420–431. <https://doi.org/10.1016/j.conbuildmat.2017.02.003>
- Huang, H., Zhang, D., Guo, G., Jiang, Y., Wang, M., Zhang, P., Li, J., 2018. Dolomite application for the removal of nutrients from synthetic swine wastewater by a novel combined electrochemical process. *Chem. Eng. J.* 335, 665–675. <https://doi.org/10.1016/j.cej.2017.11.013>
- Huseien, G.F., Mirza, J., Ismail, M., Ghoshal, S.K., Ariffin, M.A.M., 2016. Effect of metakaolin replaced granulated blast furnace slag on fresh and early strength properties of geopolymer mortar. *Ain Shams Eng. J.* <https://doi.org/10.1016/j.asej.2016.11.011>
- Imamoto, K., Arai, M., 2007. Specific surface area of aggregate and its relation to concrete drying shrinkage. *Mater. Struct.* 41, 323–333. <https://doi.org/10.1617/s11527-007-9245-x>
- Indian Bureau of Mines, 2015. Indian Minerals Yearbook 2014 (Part-III: Mineral Reviews) Marble. Ministry of Mines, Government of India, Nagpur.
- IS 1489, 1991. Portland Pozzolana Cement-Specification Part 1 Fly Ash Based. Bureau of Indian Standards (New Delhi, India).

IS 2116, 1980. Specification for Sand for Masonry Mortars. Bureau of Indian Standards (New Delhi, India).

IS 2250, 1981. Preparation and Use of Masonry Mortar. Bureau of Indian Standards (New Delhi, India).

IS 2720 (Part 5), 1985. Method of test for soils (Part 5) Determination of liquid and plastic limit. Bureau of Indian Standards (New Delhi, India).

IS 383, 2016. Coarse and Fine Aggregate for Concrete - Specification. Bureau of Indian Standards (New Delhi, India).

IS 455, 1989. Portland Slag Cement — Specification. Bureau of Indian Standards (New Delhi, India).

Jiang, Y., Ling, T., Shi, C., Pan, S., 2018. Resources , Conservation & Recycling Characteristics of steel slags and their use in cement and concrete — A review. *Resour. Conserv. Recycl.* 136, 187–197. <https://doi.org/10.1016/j.resconrec.2018.04.023>

Karaşahin, M., Terzi, S., 2007. Evaluation of marble waste dust in the mixture of asphaltic concrete. *Constr. Build. Mater.* 21, 616–620. <https://doi.org/10.1016/j.conbuildmat.2005.12.001>

Keleştemur, O., Arıcı, E., Yıldız, S., Gökçer, B., 2014a. Performance evaluation of cement mortars containing marble dust and glass fiber exposed to high temperature by using Taguchi method. *Constr. Build. Mater.* 60, 17–24. <https://doi.org/10.1016/j.conbuildmat.2014.02.061>

Keleştemur, O., Yildiz, S., Gökçer, B., Arici, E., 2014b. Statistical analysis for freeze–thaw resistance of cement mortars containing marble dust and glass fiber. *Mater. Des.* 60, 548–555. <https://doi.org/10.1016/j.matdes.2014.04.013>

Kerkhoff Beatrix, 2002. Effects of Substances on Concrete and Guide to Protective Treatments. Portland Cement Association.

Khan, S., Haq, F., Saeed, K., 2012. Pollution load in industrial effluent and ground water due to marble industries in district Buner, Khyber pakhtunkhwa, Pakistan. *Int. J. Recent Sci. Res.* 3, 366–368.

Khodabakhshian, A., de Brito, J., Ghalehnovi, M., Asadi Shamsabadi, E., 2018a. Mechanical, environmental and economic performance of structural concrete containing silica fume and marble industry waste powder. *Constr. Build. Mater.* 169, 237–251. <https://doi.org/10.1016/j.conbuildmat.2018.02.192>

Khodabakhshian, A., Ghalehnovi, M., de Brito, J., Asadi Shamsabadi, E., 2018b. Durability performance of structural concrete containing silica fume and marble industry waste powder. *J. Clean. Prod.* 170, 42–60. <https://doi.org/https://doi.org/10.1016/j.jclepro.2017.09.116>

Khyaliya, R.K., Kabeer, K.I.S.A., Vyas, A.K., 2017. Evaluation of strength and durability of lean mortar mixes containing marble waste. *Constr. Build. Mater.* 147, 598–607. <https://doi.org/10.1016/j.conbuildmat.2017.04.199>

Kirgiz, M.S., 2016. Advancements in mechanical and physical properties for marble powder-cement composites strengthened by nanostructured graphite particles. *Mech. Mater.* 92, 223–234. <https://doi.org/10.1016/j.mechmat.2015.09.013>

Kirgiz, M.S., 2015. Use of ultrafine marble and brick particles as raw materials in cement manufacturing. *Mater. Struct. Constr.* 48, 2929–2941. <https://doi.org/10.1617/s11527-014-0368-6>

Kirgiz, M.S., 2016a. Strength gain mechanism for green mortar substituted marble powder and brick powder for Portland cement. *Eur. J. Environ. Civ. Eng.* 20, s38–s63. <https://doi.org/10.1080/19648189.2016.1246691>

- Kırgız, M.S., 2016b. Fresh and hardened properties of green binder concrete containing marble powder and brick powder. *Eur. J. Environ. Civ. Eng.* 20, s64–s101. <https://doi.org/10.1080/19648189.2016.1246692>
- Kore, S.D., Vyas, A.K., 2016. Cost Effective Design of Sustainable Concrete Using Marble Waste as Coarse Aggregate. *J. Mater. Eng. Struct.* 3, 167–180.
- Kore Sudarshan, D., Vyas, A.K., 2017. Impact of fire on mechanical properties of concrete containing marble waste. *J. King Saud Univ. - Eng. Sci.* <https://doi.org/10.1016/j.jksues.2017.03.007>
- Kumar, S., Gupta, R.C., Shrivastava, S., 2017. Long term studies on the utilisation of quartz sandstone wastes in cement concrete. *J. Clean. Prod.* 143, 634–642. <https://doi.org/10.1016/j.jclepro.2016.12.062>
- Li, L.G., Huang, Z.H., Tan, Y.P., Kwan, A.K.H., Liu, F., 2018. Use of marble dust as paste replacement for recycling waste and improving durability and dimensional stability of mortar. *Constr. Build. Mater.* 166, 423–432. <https://doi.org/10.1016/j.conbuildmat.2018.01.154>
- Lu, J.X., Zhan, B.J., Duan, Z.H., Poon, C.S., 2017. Improving the performance of architectural mortar containing 100% recycled glass aggregates by using SCMs. *Constr. Build. Mater.* 153, 975–985. <https://doi.org/10.1016/j.conbuildmat.2017.07.118>
- Luz, A.P., Pandolfelli, V.C., 2012. CaCO<sub>3</sub> addition effect on the hydration and mechanical strength evolution of calcium aluminate cement for endodontic applications. *Ceram. Int.* 38, 1417–1425. <https://doi.org/10.1016/j.ceramint.2011.09.021>
- Ma, Q., Guo, R., Zhao, Z., Lin, Z., He, K., 2015. Mechanical properties of concrete at high temperature-A review. *Constr. Build. Mater.* 93, 371–383. <https://doi.org/10.1016/j.conbuildmat.2015.05.131>
- Marras, G., Careddu, N., 2017. Sustainable reuse of marble sludge in tyre mixtures. *Resour. Policy* 0–1. <https://doi.org/10.1016/j.resourpol.2017.11.009>
- Martins, P., De Brito, J., Rosa, A., Pedro, D., 2014. Mechanical performance of concrete with incorporation of coarse waste from the marble industry. *Mater. Res.* 17, 1093–1101. <https://doi.org/10.1590/1516-1439.210413>
- Mashaly, A.O., El-Kaliouby, B.A., Shalaby, B.N., El - Gohary, A.M., Rashwan, M.A., 2015. Effects of marble sludge incorporation on the properties of cement composites and concrete paving blocks. *J. Clean. Prod.* 1–11. <https://doi.org/10.1016/j.jclepro.2015.07.023>
- Melgar-Ramírez, R., González, V., Sánchez, J.A., García, I., 2012. Effects of application of organic and inorganic wastes for restoration of sulphur-mine soil. *Water. Air. Soil Pollut.* 223, 6123–6131. <https://doi.org/10.1007/s11270-012-1345-8>
- Mohan, V.S., Chiranjeevi, P., Dahiya, S., A., N.K., 2018. Waste derived bioeconomy in India: A perspective. *N. Biotechnol.* 40, 60–69. <https://doi.org/10.1016/j.nbt.2017.06.006>
- Molnar, L.M., Manea, D.L., 2016. New types of plastering mortars based on marble powder slime. *Procedia Technol.* 22, 251–258. <https://doi.org/10.1016/j.protcy.2016.01.076>
- Montero, M.A., Jordán, M.M., Almendro-candel, M.B., Sanfeliu, T., Hernández-crespo, M.S., 2009a. Applied Clay Science The use of a calcium carbonate residue from the stone industry in manufacturing of ceramic tile bodies. *Appl. Clay Sci.* 43, 186–189. <https://doi.org/10.1016/j.clay.2008.08.003>
- Montero, M.A., Jordán, M.M., Hernández-crespo, M.S., Sanfeliu, T., 2009b. Applied Clay Science The use of sewage sludge and marble residues in the manufacture of ceramic tile bodies. *Appl. Clay Sci.* 46, 404–408. <https://doi.org/10.1016/j.clay.2009.10.013>

MSME Development Institute, 2009. Status report on commercial Utilization of Marble Slurry in Rajasthan. Government of India, Jaipur.

Munir, M.J., Abbas, S., Nehdi, M.L., Kazmi, S.M.S., Khitab, A., 2018. Development of Eco-Friendly Fired Clay Bricks Incorporating Recycled Marble Powder 30, 1–11. [https://doi.org/10.1061/\(ASCE\)MT.1943-5533.0002259](https://doi.org/10.1061/(ASCE)MT.1943-5533.0002259).

Nath, S.K., Maitra, S., Mukherjee, S., Kumar, S., 2016. Microstructural and morphological evolution of fly ash based geopolymers. *Constr. Build. Mater.* 111, 758–765. <https://doi.org/10.1016/j.conbuildmat.2016.02.106>

Netinger, I., Varevac, D., Bjegović, D., Morić, D., 2013. Effect of high temperature on properties of steel slag aggregate concrete. *Fire Saf. J.* 59, 1–7. <https://doi.org/10.1016/j.firesaf.2013.03.008>

Neville, A., 2004. The confused world of sulfate attack on concrete. *Cem. Concr. Res.* 34, 1275–1296. <https://doi.org/10.1016/j.cemconres.2004.04.004>

NT BUILD 492, 1999. Concrete, mortar and cement-based repair materials: Chloride migration coefficient from non-steady-state migration experiments, Measurement. Nordtest Method. <https://doi.org/UDC 691.32/691.53/691.54>

Ohajinwa, C.M., van Bodegom, P.M., Vijver, M.G., Peijnenburg, W.J.G.M., 2018. Impact of informal electronic waste recycling on metal concentrations in soils and dusts. *Environ. Res.* 164, 385–394. <https://doi.org/10.1016/j.envres.2018.03.002>

Okagbue, C.O., Onyeobi, T.U.S., 1999. Potential of marble dust to stabilise red tropical soils for road construction. *Eng. Geol.* 53, 371–380.

Ortego, A., Valero, A., Valero, A., Iglesias, M., 2018. Downcycling in automobile recycling process: A thermodynamic assessment. *Resour. Conserv. Recycl.* 136, 24–32. <https://doi.org/10.1016/j.resconrec.2018.04.006>

P. Kumar, M., Monteiro, P.J.M., 2015. Concrete Microstructure, Properties, and Materials, Third Edit. ed. McGraw Hill. <https://doi.org/DOI: 10.1036/0071462899>

Pérez-Sirvent, C., García-Lorenzo, M.L., Martínez-Sánchez, M.J., Navarro, M.C., Marimón, J., Bech, J., 2007. Metal-contaminated soil remediation by using sludges of the marble industry: Toxicological evaluation. *Environ. Int.* 33, 502–504. <https://doi.org/10.1016/j.envint.2006.11.003>

Piasta, W., Góra, J., Budzyński, W., 2017. Stress-strain relationships and modulus of elasticity of rocks and of ordinary and high performance concretes. *Constr. Build. Mater.* 153, 728–739. <https://doi.org/10.1016/j.conbuildmat.2017.07.167>

Pozo-Antonio, J.S., 2015. Evolution of mechanical properties and drying shrinkage in lime-based and lime cement-based mortars with pure limestone aggregate. *Constr. Build. Mater.* 77, 472–478. <https://doi.org/10.1016/j.conbuildmat.2014.12.115>

Prinčič, T., Štukovnik, P., Pejovnik, S., De Schutter, G., Bokan Bosiljkov, V., 2013. Observations on dedolomitization of carbonate concrete aggregates, implications for ACR and expansion. *Cem. Concr. Res.* 54, 151–160. <https://doi.org/10.1016/j.cemconres.2013.09.005>

Rai, B., Naushad, K.H., Kumar, A., Rushad, T.S., Duggal, S.K., 2011. Influence of marble powder / granules in concrete mix. *Int. J. Civ. Struct. Eng.* 1, 827–834. <https://doi.org/10.6088/ijcser.00202010070>

Rana, A., Kalla, P., Csetenyi, L.J., 2016. Recycling of dimension limestone industry waste in concrete. *Int. J. Mining, Reclam. Environ.* 0930, 1–20. <https://doi.org/10.1080/17480930.2016.1138571>

Rana, A., Kalla, P., Csetenyi, L.J., 2015. Sustainable use of marble slurry in concrete. *J. Clean. Prod.* 94, 304–311. <https://doi.org/10.1016/j.jclepro.2015.01.053>

- RILEM CPC 18, 1988. Measurement of hardened concrete carbonation depth. *Mater. Struct.* 21.
- Rodrigues, R., de Brito, J., Sardinha, M., 2015. Mechanical properties of structural concrete containing very fine aggregates from marble cutting sludge. *Constr. Build. Mater.* 77, 349–356. <https://doi.org/10.1016/j.conbuildmat.2014.12.104>
- Saboya, F., Xavier, G.C., Alexandre, J., 2007. The use of the powder marble by-product to enhance the properties of brick ceramic. *Constr. Build. Mater.* 21, 1950–1960. <https://doi.org/10.1016/j.conbuildmat.2006.05.029>
- Sadek, D.M., El-Attar, M.M., Ali, H.A., 2015. Reusing of marble and granite powders in self-compacting concrete for sustainable development. *J. Clean. Prod.* <https://doi.org/10.1016/j.jclepro.2016.02.044>
- Şahan Arel, H., 2016. Recyclability of waste marble in concrete production. *J. Clean. Prod.* 131, 179–188. <https://doi.org/10.1016/j.jclepro.2016.05.052>
- Sancak, E., Özkan, Ş., 2015. Sodium Sulphate Effect on Cement Produced with Building Stone Waste. *J. Mater.* 2015, 1–12. <https://doi.org/10.1155/2015/813515>
- Sarkar, R., Das, S.K., Mandal, P.K., Maiti, H.S., 2006. Phase and microstructure evolution during hydrothermal solidification of clay – quartz mixture with marble dust source of reactive lime. *J. Eur. Ceram. Soc.* 26, 297–304. <https://doi.org/10.1016/j.jeurceramsoc.2004.11.006>
- Savija, B., Lukovic, M., 2016. Carbonation of cement paste: Understanding, challenges, and opportunities. *Constr. Build. Mater.* 117, 285–301. <https://doi.org/10.1016/j.conbuildmat.2016.04.138>
- Segada, A.M., Carvalho, M.A., Acchar, W., 2005. Using marble and granite rejects to enhance the processing of clay products. *Appl. Clay Sci.* 30, 42–52. <https://doi.org/10.1016/j.clay.2005.03.004>
- Sevelsted, T.F., Skibsted, J., 2015. Carbonation of C-S-H and C-A-S-H samples studied by  $^{13}\text{C}$ ,  $^{27}\text{Al}$  and  $^{29}\text{Si}$  MAS NMR spectroscopy. *Cem. Concr. Res.* 71, 56–65. <https://doi.org/10.1016/j.cemconres.2015.01.019>
- Siddique, S., Shrivastava, S., Chaudhary, S., Gupta, T., 2018. Strength and impact resistance properties of concrete containing fine bone china ceramic aggregate. *Constr. Build. Mater.* 169, 289–298. <https://doi.org/10.1016/j.conbuildmat.2018.02.213>
- Silva, D., Gameiro, F., Brito, J. De, 2013. Mechanical Properties of Structural Concrete Containing Fine Aggregates from Waste Generated by the Marble Quarrying Industry. *J. Mater. Civ. Eng.* 27, 1239–1247. [https://doi.org/10.1061/\(ASCE\)MT](https://doi.org/10.1061/(ASCE)MT)
- Singh, M., Srivastava, A., Bhunia, D., 2017. An investigation on effect of partial replacement of cement by waste marble slurry. *Constr. Build. Mater.* 134, 471–488. <https://doi.org/10.1016/j.conbuildmat.2016.12.155>
- Singh, S., Nagar, R., Agrawal, V., 2015. Performance of granite cutting waste concrete under adverse exposure conditions. *J. Clean. Prod.* <https://doi.org/10.1016/j.jclepro.2016.04.034>
- Steckel, J.C., Rao, N.D., Jakob, M., 2017. Access to infrastructure services: Global trends and drivers. *Util. Policy.* <https://doi.org/10.1016/j.jup.2017.03.001>
- Štukovnik, P., Prinčič, T., Pejovnik, R.S., Bokan Bosiljkov, V., 2014. Alkali-carbonate reaction in concrete and its implications for a high rate of long-term compressive strength increase. *Constr. Build. Mater.* 50, 699–709. <https://doi.org/10.1016/j.conbuildmat.2013.10.007>
- Sutcu, M., Alptekin, H., Erdogmus, E., Er, Y., Gencel, O., 2015. Characteristics of fired clay bricks with waste marble powder addition as building materials. *Constr. Build. Mater.* 82, 1–8. <https://doi.org/10.1016/j.conbuildmat.2015.02.055>



- Szybilski, M., Nocun-Wczelik, W., 2015. The effect of dolomite additive on cement hydration. *Procedia Eng.* 108, 193–198. <https://doi.org/10.1016/j.proeng.2015.06.136>
- Tang, S.W., Cai, X.H., He, Z., Shao, H.Y., Li, Z.J., Chen, E., 2016. Hydration process of fly ash blended cement pastes by impedance measurement. *Constr. Build. Mater.* 113, 939–950. <https://doi.org/10.1016/j.conbuildmat.2016.03.141>
- Tawfik, M.E., Eskander, S.B., 2006. Polymer Concrete from Marble. <https://doi.org/10.1177/0095244306055569>
- Tekin, I., Yasin Durgun, M., Gencel, O., Bilir, T., Brostow, W., Hagg Lobland, H.E., 2017. Concretes with synthetic aggregates for sustainability. *Constr. Build. Mater.* 133, 425–432. <https://doi.org/10.1016/j.conbuildmat.2016.12.110>
- Tennich, M., Ben Ouezdou, M., Kallel, A., 2017. Behavior of self-compacting concrete made with marble and tile wastes exposed to external sulfate attack. *Constr. Build. Mater.* 135, 335–342. <https://doi.org/10.1016/j.conbuildmat.2016.12.193>
- Tennich, M., Kallel, A., Ben Ouezdou, M., 2015. Incorporation of fillers from marble and tile wastes in the composition of self-compacting concretes. *Constr. Build. Mater.* 91, 65–70. <https://doi.org/10.1016/j.conbuildmat.2015.04.052>
- Toubal Seghir, N., Mellas, M., Sadowski, Ł., Żak, A., 2018. Effects of marble powder on the properties of the air-cured blended cement paste. *J. Clean. Prod.* 183, 858–868. <https://doi.org/10.1016/j.jclepro.2018.01.267>
- Tozsin, G., Ihsan, A., Oztas, T., Kalkan, E., 2014. Using marble wastes as a soil amendment for acidic soil neutralization. *J. Environ. Manage.* 133, 374–377. <https://doi.org/10.1016/j.jenvman.2013.12.022>
- Tozsin, G., Oztas, T., Arol, A.I., Kalkan, E., 2015. Changes in the chemical composition of an acidic soil treated with marble quarry and marble cutting wastes. *Chemosphere* 138, 664–667. <https://doi.org/10.1016/j.chemosphere.2015.07.063>
- Trezza, M., Lavat, A., 2001. Analysis of the system  $3\text{CaO}\cdot\text{Al}_2\text{O}_3\text{--CaSO}_4\cdot 2\text{H}_2\text{O--CaCO}_3\text{--H}_2\text{O}$  by FT-IR spectroscopy. *Cem. Concr. Res.* 31, 869–872. [https://doi.org/10.1016/S0008-8846\(01\)00502-6](https://doi.org/10.1016/S0008-8846(01)00502-6)
- Tripathi, B., Chaudhary, S., 2016. Performance based evaluation of ISF slag as a substitute of natural sand in concrete. *J. Clean. Prod.* 112, 672–683. <https://doi.org/10.1016/j.jclepro.2015.07.120>
- Tripathi, B., Misra, A., Chaudhary, S., 2013. Strength and abrasion characteristics of ISF slag concrete. *J. Mater. Civ. Eng.* 25, 864–870. [https://doi.org/10.1061/\(ASCE\)MT.1943-5533](https://doi.org/10.1061/(ASCE)MT.1943-5533)
- Ural, N., Karakurt, C., Cömert, A.T., 2014. Influence of marble wastes on soil improvement and concrete production. *J. Mater. Cycles Waste Manag.* 16, 500–508. <https://doi.org/10.1007/s10163-013-0200-3>
- Vardhan, K., Goyal, S., Siddique, R., Singh, M., 2015. Mechanical properties and microstructural analysis of cement mortar incorporating marble powder as partial replacement of cement. *Constr. Build. Mater.* 96, 615–621. <https://doi.org/10.1016/j.conbuildmat.2015.08.071>
- Venkatarama Reddy, B. V., Gupta, A., 2008. Influence of sand grading on the characteristics of mortars and soil-cement block masonry. *Constr. Build. Mater.* 22, 1614–1623. <https://doi.org/10.1016/j.conbuildmat.2007.06.014>
- Wang, R., Meyer, C., 2012. Performance of cement mortar made with recycled high impact polystyrene. *Cem. Concr. Compos.* 34, 975–981. <https://doi.org/10.1016/j.cemconcomp.2012.06.014>

Xiao, D., Huang, H., Zhang, P., Gao, Z., Zhao, N., 2018. Utilizing the supernatant of waste sulfuric acid after dolomite neutralization to recover nutrients from swine wastewater. *Chem. Eng. J.* 337, 265–274. <https://doi.org/10.1016/j.cej.2017.12.097>

Yuan, Q., Shi, C., De Schutter, G., Audenaert, K., Deng, D., 2009. Chloride binding of cement-based materials subjected to external chloride environment - A review. *Constr. Build. Mater.* 23, 1–13. <https://doi.org/10.1016/j.conbuildmat.2008.02.004>

Zanuzzi, A., Arocena, J.M., van Mourik, J.M., Faz Cano, A., 2009. Amendments with organic and industrial wastes stimulate soil formation in mine tailings as revealed by micromorphology. *Geoderma* 154, 69–75. <https://doi.org/10.1016/j.geoderma.2009.09.014>

Zornoza, R., Faz, A., Carmona, D.M., Martínez-martínez, S., Acosta, J.A., 2012. Plant Cover and Soil Biochemical Properties in a Mine Tailing Pond Five Years After Application of Marble Wastes and Organic Amendments. *Pedosphere* 22, 22–32. [https://doi.org/10.1016/S1002-0160\(11\)60188-4](https://doi.org/10.1016/S1002-0160(11)60188-4)

## LIST OF PUBLICATIONS

### Journals - Published

1. Kabeer, K.I. Syed Ahmed, and Ashok Kumar Vyas. 2018. "Utilization of Marble Powder as Fine Aggregate in Mortar Mixes." *Construction and Building Materials* 165. Elsevier Ltd: 321–32. <https://doi.org/10.1016/j.conbuildmat.2018.01.061>.
2. Kabeer, K.I.S.A., Vyas, A.K., 2019. "Experimental investigation on utilization of dried marble slurry as fine aggregate in lean masonry mortars." *J. Build. Eng.* <https://doi.org/10.1016/j.jobbe.2019.01.034>



## BIODATA OF THE AUTHOR

1. **Name:** Syed Ahmed Kabeer K. I.
2. **Date of birth:** 12.10.1990
3. **Address:** 3/9, Puram Prakasam Road, Balaji Nagar, Royapettah, Chennai - 600014.  
Email: kabeer1210@gmail.com  
Phone: +91-9003026030
4. **Educational Qualification:**
  1. B.E (Civil Engineering): College of Engineering, Guindy, Chennai.
  2. M.E (Structural Engineering): Thiagarajar College of Engineering, Madurai, Tamil Nadu.